Statistical Analysis and Modeling of the Agreement between the Intrinsic Frequencies Technique and the Established Cardiovascular Monitoring Methods

By

Marianne Razavi

A Dissertation Submitted in Partial Fulfillment of the Requirements for the Degree of Doctor of Philosophy in Biomedical Informatics

Department of Health Informatics

School of Health Related Professions

Rutgers, the State University of New Jersey

May 2016

RUTGERS
School of Health Related Professions

Final Dissertation Defense Approval Form

Statistical Analysis and Modeling of the Agreement Between the Intrinsic Frequencies Technique and the Established Cardiovascular Monitoring Methods

BY

Marianne Razavi

Dissertation Committee:

Syed Haque PhD PhD

Morteza Gharib PhD

Shankar Srinivasan PhD

Frederick Coffman PhD

Approved by the Dissertation Committee:

_____ Date: _____

_____ Date: _____

_____ Date: _____

_____ Date: _____

_____ Date: _____

ABSTRACT

There is an urgent need for a new cardiovascular monitoring technology in order to address the limitations of the traditional devices currently in use and to curb the epidemic of heart diseases. This study was designed to evaluate Intrinsic Frequencies (IFs), a novel and non-invasive cardiovascular assessment approach with the potential of rendering the monitoring process more practical and cost effective. IFs indices are extracted from the "shape" of the arterial pressure waveform via a modified sparse time-frequency method, designed for analyzing signals. Throughout this study, the performance of the IFs technique for the assessment of Left Ventricular Ejection Fraction (LVEF), Cardiac Output (CO) and Pulse Wave Velocity (PWV) was examined. The results generated by the IFs method were compared to the measurements produced by the established monitoring devices.

Observational studies were conducted and through the application of supervised machine learning, numerous statistical models were produced which, displayed the relationships between the IFs technique and the traditional methods, for the evaluation of cardiovascular parameters. Multiple regression analysis was applied in order to "train" the models. The selected models were subsequently "tested" for their accuracy and precision. The limits of agreement between the IFs method and the established techniques were assessed via Bland Altman approach.

There was an overall strong relationship between the IFs technique and the standard monitoring methods for the assessment of LVEF, CO and PWV. The correlation between LVEF_IFs (Model 2-iPhone) and LVEF_MRI was strong ($r=0.79$, $p<0.0001$) and Bland Altman analysis showed a reasonable clinical agreement between the two methods, with a mean bias of 1.76% and unbiased limits of agreement (LA) of +/- 17.44%. Regarding CO estimates, IFs (Model 4) was fitted on the training set only, since an appropriate testing set was unavailable at the time of the study. The results were satisfactory. The CO study revealed a significant correlation between IFs and MRI ($R=0.68$, $p<0.0001$) as well as an adequate agreement, with zero bias and narrow LA (+/- 1.78 L/min). Moreover, the generated percentage error (36%) was close to the clinically acceptable threshold (30%) for CO. In reference to PWV measurements, IFs (Model 7) displayed a moderately strong correlation with Tonometry ($r=0.64$, $p<0.0001$) and Bland Altman analysis showed a negligible bias of -0.022 m/s and LA of +/- 2.37m/s.

The present study was the first to evaluate the performance of the IFs method with regards to the estimation of the major cardiovascular health indices. We demonstrated that there is a significant correlation and agreement between the IFs technique of assessing LVEF, CO, PWV and the established methods of cardiovascular monitoring.

ACKNOWLEDGEMENT

I would like to express my gratitude to my supervisor, Dr. Syed Haque, Professor and Chair of the Department of Health Informatics at Rutgers, whose expertise, understanding, and patience, tremendously enhanced my graduate experience. It has been an honor to be your student. Thank you for supporting and encouraging me since the first day I began my studies in the field of Biomedical Informatics.

My appreciation also extends to my adviser, Dr. Morteza Gharib, Vice Provost and Professor of Aeronotics and Bio-Inspired Engineering at Caltech for offering me this amazing research project within Gharib Research Group. I truly appreciated working with your remarkable team of scientists: Drs. Peyman Tavallali, Niema Pahlevan and Derek Rinderknecht, who made my research enjoyable and enriching. I will forever be thankful to Dr. Peyman Tavallali, who continuously guided me throughout this project. His mathematical insight and knowledge are priceless.

My sincere appreciation is due to Dr. Gwendolyn Mahon, Dean and Professor at Rutgers, School of Health Related Professions, who helped and encouraged me to consider a graduate career in Biomedical Informatics.

I would like to thank Dr. Shankar Srinivasan, my committee member, for his guidance and for being always available to address my concerns. I would also like to express my appreciation to Dr. Shibata for his feedbacks and interesting course lessons. I

would like to take this opportunity to thank Dr. Coffman for serving as a committee member.

Above all, I am indebted to my family, especially my husband, Reza, for always encouraging me to go above and beyond my highest dream. I truly appreciate all your support throughout these past years. You are my best friend, my compass and anchor in life. I also would like to thank my two beautiful daughters and blessings of my life, Roxanna and Sophia, who kindly endured my lengthy study hours and taught me numerous computer tricks in order to accelerate the completion of my thesis. Special thanks to my wonderful parents and brother for their endless love and support throughout my life. This thesis would not have been possible without the support of my family.

TABLE OF CONTENTS

LIST OF TABLES

LIST OF FIGURES

CHAPTER I INTRODUCTION

1.1 Statement of the problem

Cardiovascular system is an amazing "powerplant" that relentlessly pumps blood throughout the entire body, providing cells with nutrient, while eliminating metabolic wastes. This plumbing marvel consists of the heart and blood vessels, such as arteries and veins. Maintaining a healthy cardiovascular system is crucial for our survival but unfortunately heart disease is the main reason for death and serious illness for both men and women.

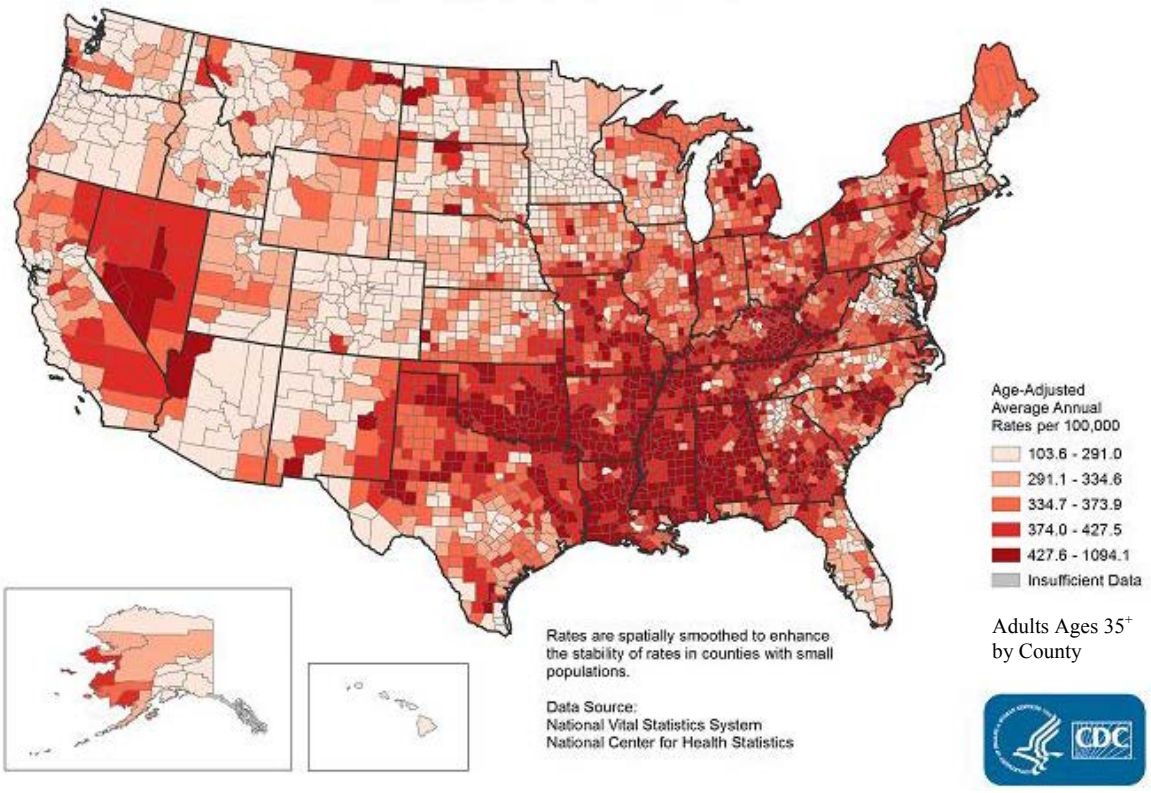

Figure 1: Death rates related to heart disease, 2011-2013[2]

Indeed, "about 600,000 people die of heart disease in the United States every year–that's 1 in every 4 deaths"[1]. It is alarming that about 50% of these heart disease related deaths are due to sudden cardiac arrest, which usually arrives with little or no warning[11]. Moreover, cardiovascular diseases (CDS) involve disability issues and generate high economic costs. Indeed, the total cost related to CDS in the United States was about $444 billion in 2010[13]. As the population ages, these costs are expected to rise significantly. Thus, there is an urgent need to develop practical, efficient and cost-effective cardiovascular monitoring technologies. Traditional devices currently in use, like Echocardiography or Magnetic Resonance Imaging, present numerous limitations, which, contribute to the burden of heart diseases. To address the limitations of the conventional devices, scientists at Caltech have recently introduced Intrinsic Frequencies (IFs), a novel and non-invasive cardiovascular assessment technique that provides estimates of the heart health parameters, such as Left Ventricular Ejection Fraction (LVEF), Cardiac Output (CO) and Pulse Wave Velocity (PWV). Throughout this study, we statistically evaluate the performance of Intrinsic Frequencies (IFs) and analyze the relationship between the IFs method and the established cardiovascular monitoring techniques. If validated, this inexpensive and handy method could render the overall process of cardiovascular monitoring widespread, safe, inexpensive and practical.

1.2 Background

With the rise of morbidity, disability and costs related to CVDs, new or improved technologies are urgently needed in order to safely, reliably and economically monitor

hemodynamic parameters. In this section, we explore hemodynamic indices and their role in cardiovascular health management. We introduce IFs as a new approach to hemodynamic waveform assessment. Then, we discuss the main forms of CVDS and provide an overview of the established monitoring technologies.

1.2.1 Role of Hemodynamic parameters in the assessment of heart health

Hemodynamics correspond to a branch of physiology (described by the heart cycle and pressure waves), which deals with the forces or mechanisms (heart pump) involved in the circulation of blood in the body[23]. Hemodynamic waveforms offer information about the "dynamic" behavior of the heart, the vascular system and their interaction. They provide the "atlas" of a heartbeat, revealing important information about a subject's cardiac health. Before further describing hemodynamic parameters, it is helpful to offer an overview of the cardiac cycle.

1.2.1.1 Foundations of hemodynamics: cardiac cycle and waves

The heart is composed of two separate right and left pumps, each consisting of two chambers, an atrium and a ventricle. The right heart receives blood from the body and pumps blood to the lungs and the left heart collects oxygenated blood from the lungs and pumps the blood back to the body[55]. The cardiac cycle is the cycle of events that take place as the heart contracts. The cycle is composed of two phases: diastole and systole. In general, "diastole" is when heart relaxation occurs (ventricle fills with blood) and "systole" is when heart contraction happens (ventricle empties blood). Each phase may be applied to both sides of the heart, as they both work simultaneously together but

it is easier to describe the process by focusing on one side only. The following events occur on the left side:

- Phase 1: the oxygenated blood from the lungs enters the left atrium (atrial diastole). The left atrium contracts after being depolarized by the "sinoatrial node", a group of cells that depolarizes at regular intervals. The SA node provides an electrical impulse that leads "atrium" to contract and pump blood into the left ventricle (LV) via the mitral valve. Atrial systole occurs. The P wave of an ECG identifies "depolarization". The A wave of the atrial plot shows the atrial contraction. The left ventricle fills with blood (ventricular diastole). The phonocardiogram is silent during this time. The below figure, called Wiggers, illustrates the waves corresponding to a cardiac cycle.

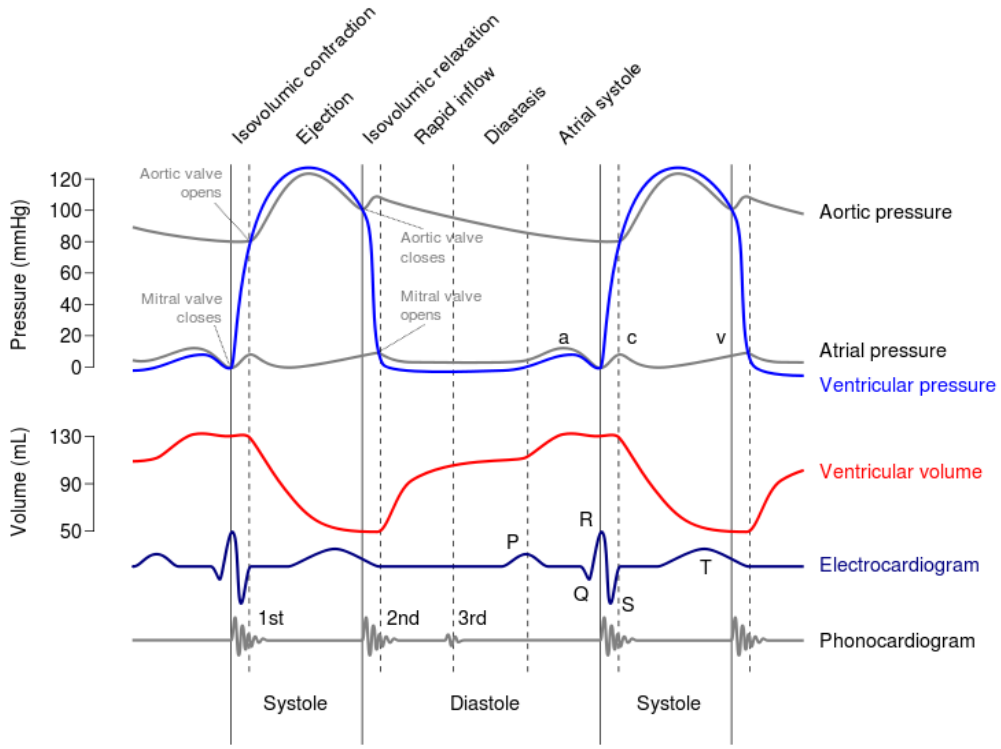

Figure 2: Wiggers Diagram, heart cycle waves [51]

- Phase 2a: the LV contracts after being depolarized by the electrical signals received through "purkinje fibers". The QRS complex is noticed on the ECG during this period (figure 2). The ventricular pressure rises and the mitral valve shuts creating the first heart sound on the phonocardiogram. The mitral valve bulging into the atrium and the related pressure create the rise of the atrial curve (wave c). Although the ventricle is contracting, the volume itself remains unchanged since both the mitral and aortic valves remain shut: ventricular isovolumetric period occurs (IVC). The aortic pressure reaches its minimum pressure (figure 2).

- Phase 2b: the pressure increases in the LV while atrium is relaxing (x-descent on atrial wave curve). Finally, the massive contraction pressure of the LV becomes greater than the aortic pressure, pushing the aortic valve to open and allowing the oxygenated blood flow into the aorta and from there throughout the body: ventricular **ejection** happens. The quantity of blood pumped out with each heart beat is called the "stroke volume" (about 70 ml in a normal subject). The ejection leads to a quick drop in the ventricle volume. As the ventricular muscle stops contracting, both the ventricular and aortic pressures drop too (T wave on ECG), however, the pressure gradually increases in the left atrium as it fills against a closed mitral valve (atrial V wave). When this phase ends, the pressure in the ventricle drops below the aortic pressure and subsequently the aortic valve closes. On the aortic pressure wave, the "Dichrotic Notch" reflects the momentary backflow of blood related to the closing of the aortic valve. The second heart sound can be heard.

- Phase 3: the ventricular pressure continues to drop. Aortic valve remains closed, avoiding the blood to move back into the left ventricle. Thus, iso-volumic relaxation occurs. The ventricular volume is constant and reaches its lowest value. When this phase is over and as soon as the ventricular pressure matches the atrial pressure, the opening of the mitral valve occurs, with atrial emptying blood (y- descent) into the ventricle, which starts filling again. There is a decrease in atrial pressure[18,19,20,21].

All the waves featured in Wiggers diagram are thus known as "hemodynamic" waveforms and the study of their shapes or indices is fundamental in the monitoring of cardiac health.

1.2.1.2 Hemodynamic parameters and normal range of values

Hemodynamic waveforms produce relevant information about the “dynamic” behavior of the heart, the vascular system and their interaction and thus, they can easily reveal cardio vascular problems. A waveform is a graphical interpretation (plot) of a signal in the form of a wave. A signal is any physical phenomenon that carries some information. It varies with one or more independent variable. The input that is used to create a waveform determines its shape[31]. Most often, the information carried by a wave can be represented by a mathematical function of an independent variable[32]. In the field of biology, most waveforms consist of periodical oscillations[31]. The most basic signal is usually a sinusoid signal, which is defined by three characteristics: amplitude, period, frequency and phase. It can be represented by the following equation: $S(t)=A.\sin(2\pi ft+\theta)$. The frequency f of a signal is its number of cycles per second. The amplitude A “is the value of the signal at any point on the wave”. The phase θ “describes the position of

the waveform relative to time zero". It is measured in degrees or radians. For example a phase shift of 360 degree corresponds to a shift of a complete period; a phase shift of 180 degree represents a shift of one-half of a period and a phase shift of 90 degree corresponds to a shift of one-quarter of a period. [33]

A sinus waveform is a very simple type of wave. The Wiggers diagram introduced earlier features more complex signals, such as the aortic, atrial and ventricular pressure waves. Heart monitoring systems evaluate these cardiac signals during each heart cycle. Monitoring these waveforms over time is important as any minor changes in their magnitude or shape can be clinically significant. Collecting "correct" data is also crucial to insure an accurate diagnosis.

The normal ranges for a few hemodynamic indices are: Stroke Volume: 60-100 ml, Ejection Fraction: 0.5-0.7, Cardiac Output 5-6 L/min, Systolic Pressure 100-140 mmHg, Diastolic Pressure 60-90mmHg[139]. The durations of Cardiac phases (with a heart rate of 75bpm) are: Atrial systole 0.11, Isovol. Contraction 0.05, Ejection 0.26 and Isovol. Relaxation 0.08[56].

Any measurements outside of these normal ranges as well as any abnormalities in the shape of the waveforms can raise concern and reveal cardio vascular problems, such as, valve disease, mitral regurgitation, etc. In our study, we focus on the left ventricular ejection fraction (LVEF), Pulse wave velocity (PWV) and cardiac output (CO).

1.2.1.3 Role of LVEF, PWV and CO in the management of heart health

- Left Ventricular Ejection Fraction (LVEF)

LVEF is a measurement of the performance of the left ventricle (it shows if the left ventricle or LV is pumping out blood adequately with each beat). LVEF=% Blood leaving the heart per contraction. As mentioned previously, the usual value is between 50 to 70 percent. LVEF is also represented by the following formula:

LVEF = [Stroke Volume * (EDV-ESV)/EDV]

This parameter can be used as a tool for highlighting diseases such as heart failure (HF) or coronary artery disease. Furthermore, it can reveal any unbalance or improper function between systolic and diastolic dysfunction[25]. A low measurement shows that the heart does not eject an adequate amount of blood throughout the body. For example, a number under 40 may reveal heart failure or cardiomyopathy. The value of the ejection fraction may drop if the heart valves do not work properly, or in the case of hypertension. A value higher than 75 percent may reveal a heart condition such as cardiomyopathy. The following methods usually are used to measure LVEF: Echocardiogram, Cardiac Catheterization, MRI, Nuclear medicine scan and CT scan[63,64].

- Pulse Wave Velocity (PWV)

During systole, the left ventricle contracts and ejects blood into the aorta creating a pressure wave that goes down the vessels and comes back to the heart. PWV represents the velocity or the speed of this pressure wave. This index is very valuable as it can assess the status of the central arteries and thus, reveal arterial stiffness. Usually, as the arteries become old, there is calcium deposition, which, often leads to the increase of arterial stiffness (and consequently to the decrease of wall elasticity of the vessels). A high PWV can reveal heart disease. In general, with normal elasticity of the arteries, the

wave comes to the heart during diastole phase (or late-systole). However, in the case of older subjects, arterial stiffness is more pronounced, thus, the speed of the wave increases and the reflected pressure wave comes back faster to the heart during systole phase (which, is much earlier and can result in high systolic and low diastolic blood pressure). Consequently, "the cardiac ventricular workload increases" leading to ventricular hypertrophy. Furthermore, the coronary blood flow is compromised by the decrease in diastolic blood pressure, which, can lead to an increased risk of myocardial ischemia. Moreover, "increased arterial stiffness is associated with hypertension and is predictive of coronary heart disease, stroke, and cardiovascular mortality" [67,68.]

PWV can be calculated in different sections of the arterial circulation by measuring "two pressure waves at two different sites of the vascular tree"[65,69]. The formula for PWV is the following:

PWV = D (or distance between two waveforms) / T (or waveforms' foot to foot transit time)

The aorta is the main element of the arterial elasticity, therefore, the carotid-femoral PWV offers the easiest noninvasive assessment of regional stiffness[65]. Carotid-femoral pulse PWV represents the portion between the carotid and the femoral arteries. The evaluation PWV (carotid femoral) has been proposed "by the European Society of Hypertension (ESH) and the European Society of Cardiology (ESC) since 2007. PWV is the gold standard to estimate central arterial changes". It is also "a good predictor of increased cardiovascular risk"[68].

- Cardiac Output (CO)

CO is the amount of blood ejected by the ventricle per minute. The related formula is:

CO=Stroke Volume * Heart Rate

A normal adult has values between 4 to 8 liters of blood per minute[70]. Stroke volume represents "the amount of blood ejected from a ventricle in one beat[71]. There are factors that could lead to the change in the individual's functional capacity because of variation in CO, such as "physical exercise of a type or intensity that diminished oxygen supply, ingestion of large meals that place an added workload on the heart, obesity, retention of fluid (edema), hypovolemia or hypervolemia, emotional stress, and smoking"[72]. However, sometimes the variation of CO can lead to CVDs. For example, a decreased cardiac output index can reveal a condition "in which inadequate blood is pumped by the heart to meet the metabolic demands of the body"[72]. The low CO can also be a sign of valvular heart disease or cardiomyopathy[27].

Thus, evaluating hemodynamic indices such as LVEF, PWV and CO is imperative to successfully monitor the cardiac health of a subject. These indices can be used as cardiac biomarkers. Therefore, offering an easy, inexpensive and practical method of monitoring their values can decrease CVDs and morbidity.

1.2.2 Intrinsic frequencies for hemodynamic waveforms assessment

Recently in order to render hemodynamic waveform analysis easier and widespread, Pahlevan et al., mathematically extracted two dominant frequencies or

signals from the arterial pressure waveform. They are referred to as Intrinsic Frequencies ($\omega 1$ and $\omega 2$, or BPM1 and BPM2)[29]. In general and as mentioned earlier, signals are precious since they frequently carry valuable information. However, they usually need to be deciphered. They can embody many different shapes but oscillatory signals are usually the most prevalent in the biomedical realm[30]. Many times a single signal is in reality a composite signal (with multiple sign waves) that is difficult to interpret if left in its present form thus, they are usually decomposed into simpler waves to improve data interpretation. Decomposing a multi-scale signal into the "sparsest" collection of oscillatory signals (or frequencies) and extracting the relevant intrinsic structure beneath, raises the ability to predict outcomes. For example, the arterial wave pressure contains major information about the coupling of heart and vasculature, which, allows making determinations about heart disease conditions. According to Pahlevan et al.it carries information about the dynamics of the left ventricle contraction, arterial system and their related interaction[29]. This delicate balance, linking the heart's pumping features to wave dynamics of the vascular system, can become impaired due to a number of reasons like hypertension, smoking and diabetes. Since the information about these dynamics (including the interaction between LV and arterial tree) is contained in the arterial wave pressure, this signal can efficiently show whether the balance between these mechanisms is impaired, at different ages and for different heart diseases. The monitoring of this wave is crucial as it offers pertinent clinical feedback about the optimum coupling of the left ventricle and arterial network[28,29]. Therefore, prior exploring this waveform, Pahlevan et al., had to break it down into several dominant waves. Indeed, they used a "modified" version of sparse-time frequency (STFR) method to split the arterial

waveform into the "sparsest" decomposition among all the possible decompositions, in order to extract the most relevant intrinsic structure beneath. They analyzed each extracted frequency separately to monitor the performance of the heart [31]. The two dominant frequencies or intrinsic frequencies (ω1 and ω2, or BPM1 and BPM2) were thereby born. A brief explanation of the "modified" STFR algorithm is provided below. It involves 2 steps: first constructing a dictionary "D" of all possible Intrinsic Mode Functions (IMF); then finding the dominant instantaneous signals over this dictionary by solving a minimization problem:

$D=\{a(t)\cos\theta(t): \theta(t)\geq 0, a(t) \text{ is smoother than } \cos\theta(t)\}$

Problem: Minimize: $\|f(t) - a(t)\cos\theta(t)\|_2^{\wedge 2}$; Subject to: $a(t)\cos\theta_i(t) \in D$

This modified version of STFR leads to the IFs algorithm. It allows the extractions of Intrinsic frequencies, which carry the highest energy (or power) among all frequencies in a specific time interval and convey the following information: ω1 or BPM1 represents the "coupled heart + aorta system" (systolic phase) before the aortic valve closure (dicrotic notch) and ω2 or BPM2 highlights the decoupled (diastolic phase) aorta after valve closure. Two auxiliary indices named Cratio and Envratio are simultaneously extracted too.[28,29,30].

The "IFs monitoring technique" per se, consists of a "combination" of main and auxiliary indices, BPM1, BPM2, Cratio, Envratio, as well as a number of heart shape factors, NodeX, NodeY, Decoupling Factor, Duration and also a few physiological variables such as, Age and Weight. The following graph provides details on the

application of this method on a pressure waveform. The main indices BPM1, BPM2 are mathematically extracted.

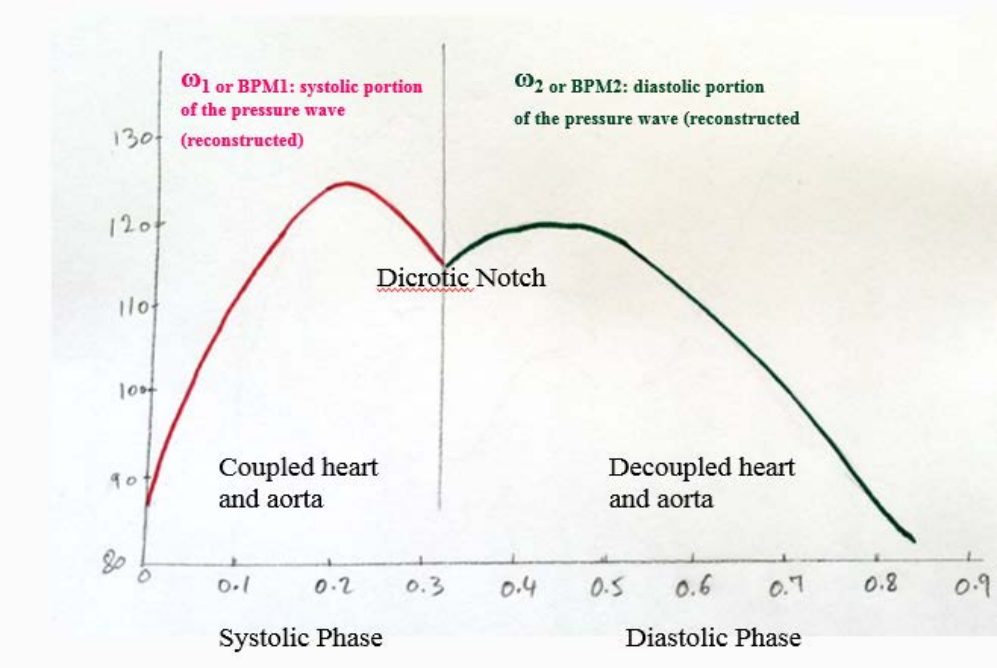

Figure 3: The IF reconstruction of the aortic pressure waveform
Adopted from "a systems approach to hemodynamic waveform analysis with clinical applications"[29]

According to figure 3, the pieces of the "reconstructed waveform" are represented by ω1(BPM1) in red, which shows the coupled heart + aorta (systolic phase) and ω2 (BPM2) in dark green, which, highlights the decoupled aorta (diastolic phase). The first intrinsic frequency or ω1 (BPM1) can be used as "a medical index for heart disease" as it can reflect problems with "the pumping dynamics of the heart" like the heart failure with "LV systolic dysfunction". This condition would generally lead to a high ω1 value. As per Pahlevan et al., all subjects with heart failure conditions showed a ω1 greater than 120 bpm, and on the other hand healthy subjects displayed a ω1 less than 112 bpm. The

second intrinsic frequency or ω2 (BPM2), can be helpful in pinpointing vascular diseases. It shows arterial stiffening and hypertension, and its value decreases with age or heart issues. It can be effectively used as a biomarker for vascular diseases. Since only the shape of the aortic wave is needed (not its magnitude) in order to compute IFs, the related algorithm can be easily embedded within various sensor type devices (like an iPhone) that are handy and inexpensive[28,29,30].

1.2.3 Main types of cardiovascular diseases

- Coronary artery disease: among the leading types of diseases, "coronary artery disease is the most common form of heart disease killing more than 385,000 people annually"[2,3]. It is caused by atherosclerosis, where fatty plaque progressively builds up inside of the blood vessels and ultimately stops the blood's movement, causing stroke. Coronary artery disease can remain silent for years and individuals may not show any signs until an advanced state of the disease.

- Hypertension, or high blood pressure, is another form of heart sickness in which, the pressure in the arteries remains always above the normal values: higher than 140 systolic (the pressure in the heart when it beats or contract) and/or higher than 90 diastolic (the pressure between heartbeats, when the heart muscle refills with blood) [4]. High blood pressure can harden the arteries and ultimately cause heart attack or stroke. Moreover, "high blood pressure was a primary or contributing cause of death for more than 348,000 Americans in 2009—that's nearly 1,000 deaths each day**"**. The related cost is very high too: about $47.5 billion per year [2]. Unfortunately, only 50% of the individuals with high

blood pressure monitor their disorder [2]. Furthermore, "1 in 3 American adults has prehypertension—blood pressure numbers that are higher than normal—but not yet in the high blood pressure range"[2]. Therefore, being able to assess cardio vascular indicators such as Pulse Wave Velocity can become very helpful in blood pressure management. For instance, it was shown that "Pulse Wave Velocity is an Independent Predictor of the Longitudinal Increase in Systolic Blood Pressure and of Incident Hypertension"[133].

- Cardiomyopathy relates to the abnormalities of the heart muscle (or the myocardium) and its inability to contract properly, leading to heart failure and death. There are various types of cardiomyopathy diseases including dilated (a ventricule that is enlarged), hypertrophic (a thick heart muscle), ischemic (related to the narrowing of blood arteries), arrhythmogenic (irregular heartbeats) and restrictive (a stiffness of the heart muscle) [6]. Cardiomyopathy symptoms are often undetected and about 1 of 500 adults may present this condition[7, 8]. Monitoring cardio vascular parameters, such as EF can help in the detection of this condition (for example "a dilated cardiomyopathy is defined as an ejection fraction of lower than 40% in the presence of increased left ventricular dimensions")[132].

- Cardiac arrhythmia is due to a malfunction of the electrical impulses that coordinate the heartbeats. The heart will consequently beat too fast, too slow, or with an irregular rythm[9]. A heart normally beats 50 to 100 beats per minute[10]. The main form of arrhythmia is "atrial fibrillation" (AF), where rapid, unorganized" electrical signals cause the heart's two upper chambers (atria) to fibrillate". Unfortunately individuals who have AF may not feel symptoms and when this disease is unnoticed, it can increase the risk of

stroke[24]. In general, most sudden cardiac deaths (SCD) are caused by arrhythmias. Unlike heart attack, where a blockage of blood vessel stops the flow of blood to the ventricle, sudden cardiac death occurs "when the heart's electrical system" fails to function properly[12].

- Heart failure (or congestive heart failure) can occur when the heart does not efficiently pump the blood, due to a weakness of heart muscle or valvular problem. Contrary to heart attack, heart failure is a slow process. Approximately 50,000 Americans die annually of this condition[9].

- Valvular heart disease is related to the malfunction of the heart valves. The valves may narrow (stenosis) or not properly close all the way, leading to regurgitation, prolapse or close wrongly[9]. Valve disease may be asymptotic or have symptoms that worsen overtime. Monitoring LVEF can be crucial in managing this type of disease[134].

Unfortunately these forms of heart disease are common and can occur in children and adults of both sexes. Improving the overall prediction and early diagnosis of CVDs has become a public health priority. Achieving this goal would allow to reduce the burden of heart diseases in the upcoming years. There are many standard clinical tools and assessments such as Echo, MRI and Catheter tests that are available today in order to screen, prevent, and diagnose heart problems. These technologies allow the monitoring of the major heart health parameters.

1.2.4 Established Monitoring technologies

- Electrocardiogram (ECG or EKG)

This device is helpful in providing the graphic record of the electrical motion of the heart cycle. It allows the overall measurement of P, Q, R, S, T and U waves and related intervals. ECG also helps evaluate numerous heart parameters such as LVEF and CO. Abnormal ECG waves can often highlight problems linked to the electrical activities of the heart or show areas of damage. They can detect the following conditions:

- ☐ Abnormal heart rhythms (very fast, very slow or irregular).
- ☐ A heart attack or myocardial infarction that recently occurred or happened some time ago. ECG produces abnormal waves that show the damage of heart muscle.
- ☐ An enlarged heart that typically causes bigger impulses than normal [36.]

- Magnetic resonance imaging (MRI)

MRI is a non-invasive tool that employs powerful magnetic fields and radio waves to produce comprehensive images of the body parts. This technology is very helpful to evaluate the cardiovascular system. It can help assess the followings: "heart muscle damage after a heart attack, birth defects of the heart, heart tumors and growths", infections, inflammatory conditions, "weakening or problems with the heart muscle" as well as "symptoms of heart failure"[45, 46]. It can help evaluate LVEF and CO too.

- CT scan – or computed tomography scan:

This non-invasive device uses X-rays to produce images of the body. Unlike a conventional X-ray, it can provide amazing and very detailed pictures of the organs, by a movement of rotation around the body. The 64-slice scanner is better than a standard CT, because it can simultaneously and non-invasively produce an increased number of

detailed pictures[81]. CT angiography imaging emphasizes on the heart and its related arteries, helping to pinpoint “coronary artery disease”, or vessel obstruction problems. It also enables the measurement of the subject’s risk of heart attack[82]. CT has also the ability to estimate heart parameters such as LVEF. However, given its radiation issue, there has been resistance to use CT to measure LVEF[83]. Also, CT scans are very expensive and are typically billed at $500 to $1,500. They can involve unnecessary amounts of large radiations.

- Cardiac catheterization (or angiogram) and Ventriculography:

This invasive imaging procedure tests for heart disease by inserting “catheters" or long, thin tubes from the arms or legs through the arteries and heart. It can be helpful in highlighting almost all kinds of cardiovascular issues, such as valve or heart muscle problems or even congenital heart disease. The heart’s performance is assessed by the calculation of pressures as well as images of the ventricles in work[40]. A Ventriculography can be performed during catheterization to assess the LV function. The physician injects a dye into the subject’s heart that makes the inside of the heart show up on x-ray. The images are digitally recorded. A ventriculogram can show how efficiently the LV pumps blood (=LVEF). It can also reveal the size of the LV as well as how well blood flows through the heart valves[85].

1.3 Significance of the problem

The standard devices mentioned earlier are crucial for monitoring “cardio vascular health” but unfortunately they present numerous limitations and thus research remains ongoing for the perfect monitoring technique. Throughout this study, we

introduce IFs, a novel cardiovascular monitoring method that has the potential to circumvent the limitations of the established tools. If validated, the IFs technique would offer an effective, handy and inexpensive approach to heart health management and therefore have a significant impact on the field of cardiovascular monitoring. IFs could be used as an effective "biomarker" for CVDs, while addressing the limitations of the established tools. A description of the drawbacks of the conventional devices is provided in the next sections.

1.3.1 ECG limitations

A standard technique for the clinical measurement of LVEF, the 2D echocardiography presents many limitations. For example, it can lead to error if the imaging planes used for the measurement are inaccurate or wrong. Also, the accurate assessment of left ventricular performance by 2D echocardiographic tools often relies on geometric assumptions, which can make the calculations challenging or prone to errors. Indeed, when quantifying cardiac chamber volumes, mass or function, the operator relies on a few assumptions about the geometry of the chamber in order to use specific formulas for calculation of these parameters. As chambers become distorted in shape, the geometric assumptions about shape become less accurate as do the calculated values using these formulas. The 3D echocardiographic method decreases the limitations of 2D echocardiography and allows quantification of EF without geometric assumptions, however it is more expensive and thus less practical. Moreover, all echocardiographic methods require acoustic windows that allow adequate visualization of the blood and the endocardial border, to allow correct measurement and tracing. Usually, obese patients,

individuals with “chronic obstructive pulmonary disease” and patients with “limited space between the ribs” will obtain reduced image quality[73,74,75].

Furthermore, well trained technicians are needed to perform the procedure, otherwise misinterpretations can occur. Indeed, a study published in 2006 in the journal Circulation monitored five hospital Emergency Departments in California and Colorado over a two-year period to determine how often the treating Emergency physicians failed to identify “significant ECG changes” during a cardiac event. The conclusion was that 12% of the studied subjects “had a high-risk ECG abnormality”, which, failed to be detected by the Emergency Department provider[47]. The presence of providers that could interpret the results accurately and have the proper knowledge of manipulating the device is a must. When using ECG it is important to ensure that a good electrical conductivity between the body and electrodes is happening in order to produce correct waveforms with no noise pollution. Extracting the duration and amplitude of the wave itself can also be challenging because of the faint amplitude. Indeed, “ECG signal lies in frequency band of 1– 250 Hz, where flicker noise is dominant”, thus “common-mode interference from the main power line is likely to interfere with the diagnostic”[38]. ECG data may therefore not present the ideal method for cardiac health monitoring. It is an expensive test and a continuous cardiac monitoring process with ECG can be unviable. There is an urgent need to effectively address all these problems as they contribute to the increase of the cardiovascular death rate. Other types of tests (in addition to ECG) may sometimes become necessary to effectively monitor the cardiovascular health, such as cardiac catheterization.

1.3.2 Cardiac Catheterization limitations

The procedure of cardiac catheterization determines if there are blockages in the heart arteries (coronary arteries). To evaluate a heart valve, usually additional information is obtained through this method that is not available on other types of tests, including direct measurement of cardiac pressures. Regarding the evaluation of coronary arteries, a cardiac catheterization procedure would reveal "precisely" where the obstructions are. Cardiac Catheterization can thus provide a more comprehensive input compared to the standard non-invasive tests like ECG. Moreover, sometimes the cardiac catheterization can prove there is not a significant problem with the heart, even though non-invasive tests suggested there was an abnormality[48]. Although very helpful, the catheterization procedure has its own limitations: it is invasive, time consuming, risky and not practical (since it always requires a clinical setting involving numerous clinicians). Many clinical facilities include "Cath labs", which "include a table for the patient, x-ray tubes, and equipment to monitor the heartbeat and blood pressure. In addition to the physician performing the test, there is generally at least one technician or nurse who assists, and one who monitors various parameters who is outside the room"[49]. The actual process lasts approximately fifteen to thirty minutes, however the preparation and recovery phases could add several hours[49]. Furthermore, this procedure is very expensive as the "average cost of cardiac catheterization is between $1,500 and $4,000" [50]. Therefore this technique does not always represent a practical solution for monitoring the heart.

1.3.3 CT limitation

Computed Tomography Coronary Angiography can sometimes highlight conditions that do not really exist. Indeed, "when applied routinely in symptomatic patients at risk of coronary disease, in more than 50% of subjects", this tool "detected" coronary blockages that were actually absent! Stunningly, out of 98 patients in whom this device diagnosed "3-vessel coronary artery disease (CAD)", only 19 were having this condition, leading to a false-positive rate of 81%. Unfortunately, this "high false-positive rate" can have serious consequences and can lead to excessive and invasive tests that usually aggravate the medical costs[87]. A CT angiography fees are between $600 and $1,000[88].

1.3.4 MRI limitations

MRI is usually very reliable compare to similar devices. A comparative study showed that MRI efficiently highlighted all of the subjects' heart attacks, even the subjects with normal EKGs. MRI also revealed an increased number of subjects with unstable angina compared to the other standard procedures. In general of "the more than 5 million patients who visit emergency departments with chest pain each year, only about 40 percent can be immediately diagnosed with heart attack" using various standard tests[41.] Although MRI is an effective and painless method of detecting and diagnosing heart issues, unfortunately it is not practical because of its high cost. Indeed, MRIs charges are between $474 and $13,259, depending on the U.S State where they are administered. In addition to scan fees, the total bill for the MRI is usually higher as it

also includes the radiologist fees[42]. Moreover, this technology is time consuming and impractical, especially for the continuous monitoring process.

1.3.5 Why is there a need for a new cardiovascular monitoring method like IFs?

Numerous monitoring techniques are available today but most of them present several drawbacks. Moreover, these sophisticated tools require a clinical setting, which is not always available, nor affordable. There is an urgent need for a new monitoring method, such as IFs, that would address these limitations. This novel technique would offer a completely new insight into the field of cardiac performance evaluation. If validated, IFs would provide an inexpensive, handy and safe technique that could be used anytime and anywhere. IFs has therefore a potential to significantly impact the field of cardiovascular monitoring by rendering the health management process, stress free, practical, cost efficient and widespread.

1.4 Goals and Objectives

The purpose of this observational study is to find out if there is a significant and meaningful relationship between the new IFs method and the established cardiovascular monitoring techniques. The "IFs monitoring technique" includes a combination of explanatory variables consisting of the main indices that are mathematically extracted from the waveform, (BPM1, BPM2, Cratio and Envratio), as well as heart shape factors (NodeX, NodeY, Decoupling Factor, Duration) and a few physiological parameters. This "combination" of explanatory variables is used to provide measurements for LVEF, CO and PWV.

The objective of this research is to statistically compare the estimations of the dependent variables LVEF, CO and PWV, generated by the IFs technique to the values produced by the established devices such as Echocardiography, MRI and Tonometry. Any significant correlation is highlighted and assessed. The accuracy and precision of the IFs method is explored and the "clinical agreement" between IFs methodology and the standard techniques is ultimately examined. The goal of this study is thus to statistically validate the use of IFs methodology as a new, reliable, inexpensive and handy technique of cardiovascular monitoring, which could effectively address the drawbacks of the conventional methods mentioned earlier. The clinical data setting for this study is provided by Huntington Medical Research Institute (HMRI) and Framingham Heart Study (FHS), which is a long-term, ongoing cardiovascular study on adult subjects started in 1984.

1.5 Hypothesis and Research questions

The following is a list of research questions and related statistical hypothesis that are in alignment with the study's goals:

- Research questions 1

Is there a meaningful relationship between IFs technique and the established methods like MRI and Echo for the measurement of LVEF?

Or, more specifically:

- Is IFs_iPhone method significantly related to MRI?

- Is IFs_tonometry method significantly related to MRI or Echo?

- Null Hypothesis 1: there is not a statistically significant correlation between LVEF measurements obtained via MRI or Echo and LVEF values produced by IFs technique.
- Alternative Hypothesis 1: there is a statistically significant relationship between LVEF measurements obtained via MRI or Echo and LVEF values produced by IFs technique.

- Research question 2

Is there a meaningful relationship between IFs method and MRI for the measurement of CO?

- Null Hypothesis 2: there is not a statistically significant correlation between CO measurements obtained via MRI and CO values produced by IFs method.
- Alternative Hypothesis 2: there is a statistically significant relationship between CO measurements obtained via MRI and CO values produced by IFs method.

- Research question 3

Is there a meaningful relationship between IFs method and Tonometry technique for the measurement of PWV?

- Null Hypothesis 3: there is not a statistically significant correlation between PWV measurements obtained via Tonometry and PWV values produced by IFs method.
- Alternative Hypothesis 3: there is a statistically significant relationship between PWV measurements obtained via Tonometry and PWV values produced by IFs method.

CHAPTER II LITERATURE REVIEW

2.1 Introduction

With the rise of morbidity, disability and cost related to CVDs, a new reliable, functional and low priced monitoring device is urgently needed. Many studies have been published in reference to heart performance monitoring methods. They are mainly investigating a better technology that could safely and reliably measure hemodynamic parameters.

This review presents a brief description of the cardiovascular monitoring technologies that measure various hemodynamic indices. It also offers an overview of the studies in which, researchers have statistically evaluated a number of old and new monitoring devices. The last section of this review includes a study related to the newly introduced IFs, in which a group of scientists from Caltech have demonstrated that IFs indices could be used as an effective biomarker for cardiovascular diseases.

2.2 Monitoring Methods for Pulse Rate

Monitoring heart rate is important as it represents a risk factor for heart disease. Indeed, it has been demonstrated "that an increase in heart rate by 10 beats per minute was associated with an increase in the risk of cardiac death by at least 20%"[110]. Arterial pulse was explored in China approximately 2,000 years ago. The ancient Chinese would simply assess the pulse beats (by using both wrists) to diagnose a disease[107]. Then

Santorio Santori with the use of Pulsilogium, a form of pendulum based on the work by Galileo Galilei tried to perform a more accurate measurement of HR[108]. Nowadays, doctors use 4 main methods: touch or palpation, ear or auscultation, monitor or ECG recorder[109]. Recently though, a group of scientists from MIT created an algorithm in a related software that can measure a subject's pulse, including a baby's heart rate, by simply pointing a camera at their face, rendering the overall pulse rate monitoring much easier. They originally developed this method to evaluate the vital signs of babies that are just born, without touching them. It is performed by "amplifying the subtle changes in motion" and color in "a video". Indeed, through the examination of a video, the algorithm analyses "the elements of the video that change over time, and then dramatically amplifies those motions". For example, as the ventricle ejects blood into the body, the individual's face and skin becomes slightly redder, which is difficult to see. A tool used by the software "Eulerian Video Magnification (EVM)", can measure the color variation to accurately estimate the subject's heart rate. The "MIT computer scientist Fredo Durand predicts that his algorithm will be used primarily for remote medical diagnostics"[57,58,59]. This novel technology offers a new and practical approach for monitoring pulse-wave.

2.3 Monitoring methods for Ejection Fraction

The Ejection fraction is often measured with traditional imaging technologies such as Echocardiogram, Cardiac Catheterization, MRI and CT.

2.3.1 Echocardiogram

This non-invasive technology is based on sound waves. The tool produces pictures of the ventricles and the related arterial dynamics during the pumping mechanism.

2.3.2 Cardiac Catheterization

This invasive tool involves the insertion of a thin catheter into the blood vessels from the arm/leg in the direction of the heart. Then, through the assessment of pictures taken during catheterization, the physician evaluates the ventricle's pumping activity.

2.3.3 MRI

During a cardiovascular MRI, magnetic field and radio waves are generated, producing cross-sectional pictures of the heart. This non-invasive tool enables the clinician to evaluate the pumping mechanism of the ventricle (especially the left ventricle).

2.3.4 CT

During a cardiac CT scan, EF is evaluated through X-ray method, which, creates "cross-sectional images" of the heart[111].

As mentioned previously, all these technologies are expensive and time consuming and thus, monitoring ejection fraction can become difficult, impractical and risky, exposing the subject to unnecessary radiation. Therefore, new non-invasive math-based techniques are emerging to allow a better monitoring. These new approaches rely on the analysis of blood pressure waveforms and aim to estimate cardio vascular indices.

2.3.5 Estimating EF from a model-based analysis of pressure wave (Windkessel).

A recent analysis published by Mukkamala et al. demonstrated the feasibility of estimating EF from a model-based analysis targeting pressure wave. They "measured aortic pressure waveforms, reference EF and EDV" through traditional echocardiography from 6 dogs and compared them with calculated EF and EDV, which, were obtained via a non-invasive method relying on pressure wave. The pressure waveform was symbolized by a "lumped parameter circulatory" model based on Windkessel model, which, was introduced in the late 1800's by the German physiologist Otto Frank. He described the cardiovascular system as a closed hydraulic circuit, which contains a "water pump connected to a chamber, filled with water except for a pocket of air". When it is pumped, "the water compresses the air, which in turn pushes the water out of the chamber". Windkessel models are often used to explain the role assumed by the heart throughout the cardiac beat. It explains the hemodynamics of the arterial system in terms of P, aortic pressure, R, peripheral resistance of the arterial tree to ventricular ejection of the blood, C, arterial compliance, the elasticity and extensibility of the major artery during the cardiac cycle and Elv, time varying ventricular elastance function [25,97]. The following diagrams feature the model.

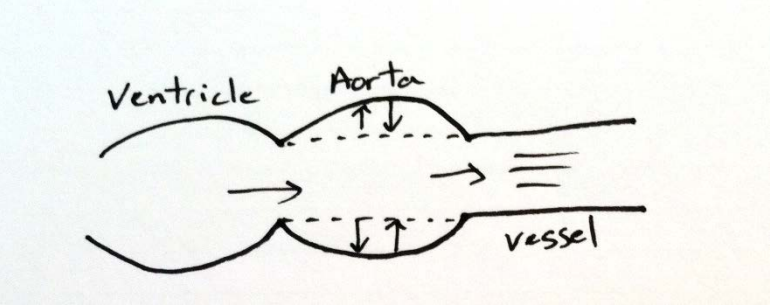

Figure 4: Representation of ventricular ejection of blood and arterial circulation

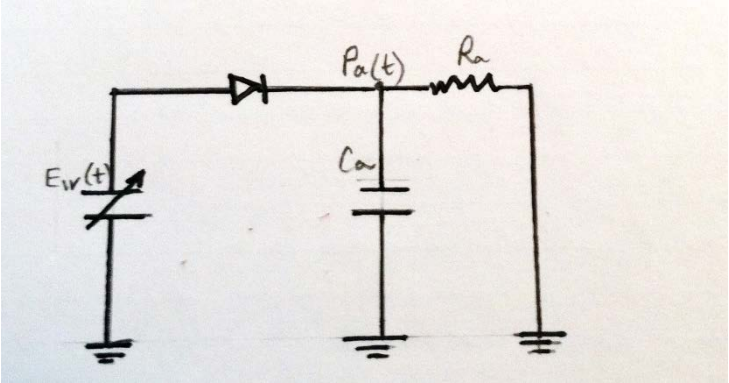

Figure 5:
Lumped parameter model of the LV and arterial tree
(Adopted from "Continuous LVEF monitoring by central aortic pressure waveform analysis")[25]

As per Mukkamala et al., EF was computed as follow for each heart beat[25]:

$$EF = \frac{\frac{SV}{C_a}}{\frac{EDV}{C_a}} = \frac{\frac{P_a(n_{bs}T)}{C_a E_{lv}(n_{bs}T)} - \frac{P_a(n_{es}T)}{C_a E_{lv}(n_{es}T)}}{\frac{P_a(n_{bs}T)}{C_a E_{lv}(n_{bs}T)} + \frac{V_{lv}^0}{C_a}}$$

C_a: arterial compliance
E_{lv}: time varying ventricular elastance function
EDV: LV end diastolic volume
n_{bs}: index corresponding to the start of the systolic ejection phase
n_{es}: index corresponding to completion of the systolic ejection phase
SV: left ventricular stroke volume
T: sampling period
V^0_{lv}: left ventricular unstressed volume[25]

The advantage of this method is that this algorithm can be embedded into a software and EF can be automatically measured in outpatient medical settings or even at home through commercial noninvasive transducers such as Portapres. Researchers

showed that the data produced by their mathematical model was as good as the data obtained through echocardiography. The average RMSE for EF was 5.6% .

This method can provide a continuous and practical hemodynamic monitoring. However, there are a number of assumptions. For example as we mentioned above, the analysis is based on a lumped parameter symbolization of the arterial pressure waveform. Unfortunately arteries are more than a simple lumped system. Indeed, the arterial tree is composed of bifurcations and ramifications which, have to be considered in the formula in order to produce reliable results. Also, another assumption is that we have a constant arterial compliance over a monitoring period. Studies have shown that "Ca tends to decrease with increasing arterial pressure"[25].

2.4 Monitoring left ventricular cardiac indices: CT, CVG and Echo monitoring methods compared to MRI technique

A study led by Greupner et al. in 2012, compared the performance of CT, CVG and Echocardiography with MRI (which was used as the reference method) in estimating left ventricular cardiac indices[86]. The study group consisted of 36 patients with suspected or known coronary disease. They all underwent all 5 diagnostic tests, which were performed within an individual period of 24h. The left ventricular cardiac indices such as EF, End diastolic volume, End systolic volume and Stroke volumes were measured via 64-row CT, CVG, 2D Echo and 3D Echo. These values were compared to MRI's values using Pearson's correlation (r) and limits of agreement (LA) which were equal to +/- 1.96 x SD of the differences, as defined by Bland- Altman. The study highlighted the following results:

- CT:

It did not overestimate or underestimate EF, EDV, ESV in comparison with MRI. However, it significantly overestimated SV. The limits of agreement of CT versus MRI was +/- 14.2 % for LVEF, which was the lowest compare to the other tests. Also it showed an excellent correlation with MRI for EF (r=0.89), as well as a good correlation for SV (r=0.55).

- CVG:

It significantly overestimated EF. SV, EDV, ESV. The limits of agreement of CVG versus MRI is +/- 20.2 % for EF. It "showed significantly larger limits of agreement than CT for EF and SV, whereas for EDV and ESV there was no significant difference". The correlation with MRI regarding EF was good (r=0.77), but moderate in case of SV.

- 2D Echo:

It displayed no significant overestimation or underestimation for EF. However, it underestimated EDV, ESV, SV. The LA were also wider for SV. The correlation with MRI regarding EF was good (r=0.79), but was low for SV (r=0.31)

- 3D Echo:

It showed no significant overestimation or underestimation for EF. It displayed a significant underestimation for EDV, ESV. The LA were larger than for CT in case of LVEF (+/- 21.2%); the LA were also larger than for CT in case of SV. The correlation with MRI regarding EF was good (r=0.79), but very weak in case of SV (r=0.27).

As a conclusion, researchers demonstrated that 64-row CT seemed to be more reliable and superior to CVG, 2D Echo and 3D Echo when MRI was used as the tool reference for the evaluation of global LV function[86].

2.5 Techniques for the measurement of blood pressure

Estimating blood pressure (BP) is very important as it contains underlying and pertinent information about the subject's cardiovascular health. Producing reliable measurements for blood pressure is crucial in order to make adequate medical diagnosis. The non-invasive measurements are mainly performed by 3 different technique[96]:

- The Auscultatory method (*mercury*-sphygmomanometer)
- The Oscillometric method (Omron)
- The Penaz/Wesseling method (Portapres and Finapres)

For years, the mercury sphygmomanometers have been the "gold standard" tools for blood pressure estimations but they are being substituted in hospitals due to environmental matters. For example they have been banned in Veterans Administration Hospitals[93]. Tools such as the automated Oscillometric blood pressure device or "Finapres" and "Portapres" are being adopted instead, in which the systolic and diastolic BP are mathematically estimated via the form of Oscillometric amplitudes and heart rate.

2.5.1 Omran's measurements

In a study led by Ostchega and published in 2012, researchers compared Omron's measurements with the golden standard, sphygmomanometer[89]. The number of observations used for systolic BP was 6,461 (individuals>=8 years old) and for diastolic

BP it was 6338. The subjects had 3 mercury and Omron systolic readings as well as 3 diastolic readings. The conclusion of the study was the following: there was a statistically significant high correlation between the two devices regarding Systolic blood pressure (r=0.92) and a good relationship for diastolic blood pressure (r=0.79)[89]. These graphs also show that the regression line was under the line of equality for Systolic blood pressure, implying that Omran understimated the mean of systolic blood pressure compared to mercury. Regarding the diastolic blood pressure, omran overestimated the mean measurements for lower BP values and underestimated it for high diastolic values.[89]

The main disadvantage of oscillometric method is that sometimes curves are hard to read correctly. Ocillometry is easily affeted by the movements related to the bandwidths of signals, thus the clinician should ensure that the arm is immobile otherwise this method can be prone to errors when there is excessive patient arm movement[90].

2.5.2 Wesseling technique

This method is based on the volume-clamp method of Penaz which relies on the principal of dynamic unloading of the arteries in the finger. The "finger arterial pressure" is estimated by "a finger cuff and an inflatable bladder" combined with "an infrared plethysmograph" that "consists of an infrared light source and detector". Then, "the infrared light is absorbed by the blood, and the pulsation of arterial diameter" during a heartbeat produces a "pulsation in the light detector signal"[94]. The following figure illustrates this technique:

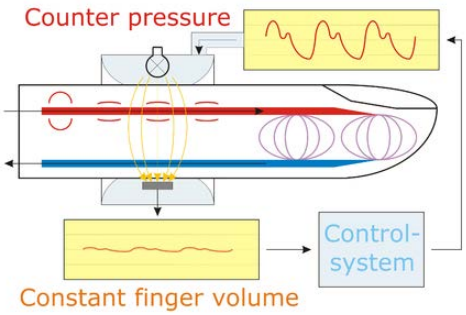

Figure 6: Principle of the Vascular Unloading Technique [98]

The Finapres's Portapres device uses this technique to determine both BP and CO noninvasively. In a study within an emergency department of a hospital, which was published in 2013, Does et al. tried to find out if the medical staff can use this device as a triage aid to "recognize patients in early phases of shock"[95]. To reach this goal, they verified if the methods of Finapres Portapres and automatic Sphygmomanometry for measuring BP produce close results. They computed the correlation coefficient r as well as the mean bias and limits of agreement (through Bland-Altman analysis). A total of 97 patients from the emergency department were included in the study. The related r results were moderate: "0.50 for SBP, 0.53 for DBP and 0.54 for MAP". The study generated a "Bland Altman bias of 11.3 (upper limit 65.3, lower limit -42.8) and 7.7 (39.2, -23.7) for SBP and DBP respectively".

The conclusion of this study was that Finapres Portapres was not interchangeable with automated Sphygmomanometry.

2.6 Cardiac Output measurement

Many invasive and noninvasive algorithms exist today for the measurement of CO, each with its own advantages and drawbacks. However, no standard or reference

measurement against which "all" of these methods can be compared exists. Many researchers try to validate a new CO device by comparing it to thermodilution method, however the "precision (i.e., 95 % confidence intervals) of thermodilution measurements is quoted as ± 20 % and recent data suggests these limits could be even wider"[105]. Moreover, the use of this method is quite risky.

In this section we describe various methods in use today, including bolus thermodilution.

2.6.1 Fick's method

As per Geerts et al., this old technique based on the Fick's mathematic formula can produce "cardiac output (CO) indirectly from whole body oxygen consumption (VO_2) and the mixed venous (CvO_2) and arterial oxygen concentrations (CaO_2)"[92]:

$$CO = VO_2/(CaO_2\text{-}CvO_2)$$

Skilled researchers consider this method very reliable and claim that it should be used as a reference method to which other techniques should be contrasted. However, it can become truly laborious and many variables need to be calculated, which can lead to errors. Furthermore, the circulation needs to be stable when the data is acquired. Moreover, this method involves a pulmonary artery catheter (PAC) that involves risks for the patient and is also expensive[92].

Besides the Fick method, there are other techniques are being used too, which are based on "indicator dilution".

2.6.2 Indicator Dilution method

Four types of "indicator dilution" method exist, such as the "pulmonary artery catheter (PAC) thermodilution with bolus injection of cold fluid, the PAC continuous thermodilution, the transpulmonary bolus thermodilution and the transpulmonary lithium bolus dilution method". They follow the same principle despite the indicator used (dye, temperature) and "have in common that the computation of cardiac output is based on a mass balance"[92]:

$$mi = \int q(t) \times c(t) dt$$

In this previous formula, "mi is the amount of indicator injected, q(t) is instantaneous blood flow and c(t) is concentration as function of time. Thus with these methods CO is based on the following well-known Stewart Hamilton equation"[92]:

$$CO = \frac{mi}{\int c(t) dt}$$

"where $\int c(t)dt$ is the area under the indicator dilution curve (c(t) is concentration as function of time)". To apply this formula, "complete mixing of blood and indicator, with no loss of indicator between place of injection and place of detection" are assumed. Also, "we further assume blood flow to be constant"[92,99].

In general, most errors related to indicator dilution methods are due to violation of the assumptions cited earlier, the wrong use of the technique and the "anatomic abnormalities"[92,99]. Moreover, indicator dilution methods are invasive because of the use of PAC and thus they involve related risks such as "arrhythmias, valvular lesions, infection, pulmonary emboli, pulmonary infarction, and pulmonary artery rupture"[100].

Even though the thermodilution technique is considered the "golden standard" for clinical method of estimating CO by many scientists, it is not continuous and involves a PAC for the duration of CO monitoring and also requires a well-trained technician to operate the device adequately in order to avoid inaccurate measurements. Researchers are therefore looking for minimally invasive tools that could generate reliable measurements of CO while being non-invasive and easy to use.

2.6.3 Esophageal Doppler method

The Esophageal Doppler (ED) monitor is a non-invasive technique that measures the speed of blood flow in the aorta via an ultrasound probe. It also can be used to provide values for the stroke volume or CO. However, this tool requires a clinical staff that knows how to correctly place the probe in order to ensure a reliable reading of CO. This device's use presents also another limitation: its use assumes "that the division of the blood flow from the descending aorta is constant with even distribution to the brachiocephalic and coronary arteries, which is not always true in very ill patients"[102].

2.6.4. Pulse contour analysis

According to Porhomayon et al the arterial pressure waveform is targeted in this technique. For example, "CO is computed from the area under the curve of the systolic portion of the arterial pressure waveform divided by the aortic impedance multiplied by the heart rate". Currently, various CO devices are marketed based on Pulse Contour Analysis (PCA) technique. One of the recent tools is Picco.

2.6.5 Picco

This minimally invasive technique "uses the pulse contour method based on the Wesseling algorithm for the calculation of CO"[102]. It "requires a thermistor-tipped central venous catheter and an arterial line usually introduced via the femoral, axillary, or brachial artery. After central venous injection of the cold indicator, the thermistor" located "in the tip of the arterial catheter measures the downstream temperature changes". The Stroke Volume or CO is consequently computed by the study of the thermodilution plot, "using a modified Stewart-Hamilton algorithm"[102]. Pulse contour analysis continuously measures stroke volume and arterial pressure, the following figure was adopted from "Applications of minimally invasive cardiac output monitors"[102] and shows how Stroke volume is computed:

Figure 7: PiCCO system[102]**:**

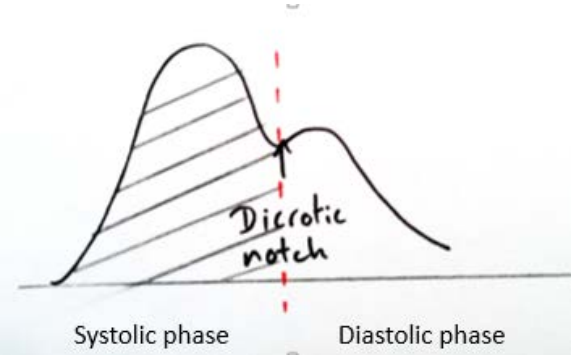

Stroke volume = (Shaded area corresponding to the systolic period + aortic compliance) × shape of pressure curve[102].

PICCO remains relatively invasive (carrying risks such as bleeding, deep venous thrombosis) and requires well trained technicians[101]. Thus researchers continued their quest for a less invasive tool such as VolumeView.

2.6.6 VolumeView

A new and less invasive pulse wave analysis method called VolumeView has been recently developed to monitor CO in a continuous way. According to the inventors, the related algorithm is based on an improved version of Wesseling technique. It "consists of a "thermistor -tipped femoral arterial catheter (the VolumeView™ catheter) and the EV1000™ monitoring" platform which aim "to continuously assess CO based on the femoral arterial pressure curve signal". Through an observational study, including 72 ill patients, Bendjelid and his team compared" the performance of the VolumeView method and of the PICCO pulse contour method" with reference trans-pulmonary thermodilution (TPTD) CO measurements. They used regression and Bland Altman analysis and obtained the following results. The bias for CO (VolumeView) was -0.07 l/min and LA were +/-2, with a percentage error (PE) of 29%. The bias and limits of agreement for CO (PICCO) was 0.03 l/min +/- 2.48, with a PE of 37%. The Pearson correlation values for both these methods were 0.83 and 0.76 respectively. The conclusion of their paper was that the performance of VolumeView CO technique is as reliable as PICCO when targeting critically ill subjects. Furthermore, the precision was better with VolumeView CO[129].

2.6.7 Modelflow

Modelflow (from Finapres) is a noninvasive technique based on Windkessel method and arterial pulse wave analysis. A group of scientists studied whether Modelflow could be validated for the evaluation of CO. They compared non-invasive Modelflow results with an indicator dilution: thermodilution cardiac output (TDCO)

measurements (obtained during right-sided heart catheterization) in 28 healthy elderly subjects, aged 70 +/-4 years (mean+/-S.D.). Modelflow calculated CO from arterial pressure wave acquired non-invasively from Finapres Windkessel method.

The two methods were statistically compared. Thermodilution was 6.4+/-1.1 L/min (mean+/-S.D.) and Finapres's MFCO was 4.7+/-1.3 L/min with P<0.001. The correlation between the two measurements was not significant (r=0.28, P=0.13). Mean difference (bias) was -1.7 L/min (S.E.M. 0.27 L/min) and the LA were -4.6 to +1.1 L/min. Therefore, non-invasive Finapres values showed no significant correlation with invasively determined TDCO values in the normal range. Although easy to use and safe, the Finapres Modelflow method showed that it is not reliable for assessment of cardiac output[91]. More research need to be done to validate this method.

2.6.8 Nexfin

Nexfin Co-trek relies on "finger arterial pressure pulse contour analysis" method to continuously assess blood pressure as well as estimate the cardiac output. . Nexfin is totally noninvasive and easy to use. The measurement of finger arterial pressure is performed via "an inflatable cuff around the middle phalange of the finger. The pulsating finger artery is clamped to a constant volume by applying a varying counter pressure equal to the arterial pressure using a built-in photoelectric plethysmograph and an automatic algorithm" (Physiocal). Then, "the resulting finger arterial pressure waveform is reconstructed into a brachial artery pressure waveform" by a generalized mathematical expression. CO is obtained "by a pulse contour method" (CO-TREK) "using the

measured systolic pressure time integral and the cardiac afterload determined from the Windkessel model"[101,112].

There are many studies trying to validate the use of Nexfin. For example, scientists have recently done an observational analysis in 45 mixed surgical/medical and burns critically ill patients in order to compare Nexfin to Thermodilution invasive technique. They found moderately good results with TDCO (R^2 0.68) and CCO (R^2 0.71) with p values < 0.001 for both. Mean NexCO was 6.1 ± 2.3 which is comparable to mean TDCO,6.6 ± 2.2. They also applied Bland-Altman analysis for exploring the agreement between NexCO and TDCO and obtained a mean bias of 0.4 and LA of +/- 2.32 L/minute leading to a Percentage error of 36.1%. The results regarding the comparison between NexCO and CCO led to a bias of 0.2 and LA of +/- 2.3 L/min with a Percentage error 37% [101]. Even though the overall results seemed to be good, the calculated percentage errors (PE) were too high to meet the criteria for general "interchangeability" as suggested by Critchley et al.[103]. In general, "the main statistical method used to validate CO monitors is comparison with single bolus thermodilution by Bland–Altman and calculating the percentage error, a parameter calculated from the limits of agreement of the analysis over the mean CO"[105]. Thus, PE=[(1.96 * *SD of the differences)/ Mean CO of the targeted standard technique]. As mentioned previously, thermodilution measurement has a precision of "+/-20 %". Thus, "to equal or better this by the new method, it is widely agreed that the percentage error should be less than 30 %"[105]. In this study, CO obtained by Nexfin showed an adequate relationship with CO (TDCO) and CO

(CCO) obtained by PiCCO, but the PE was too high to allow an absolute interchangeability[101].

Another study performed by Broch et al. [106] led to the conclusion that Nexfin is a consistent method of estimating CO values "during and after cardiac surgery". They showed that when comparing Nexfin to thermodilution (invasive pulmonary procedure), the bias was -0.1 and the LA = +/- 0.55 L/min "before cardiopulmonary bypass", with a PE of 23% and -0.1 (unbiased LA=+/-0.7 L/min with a PE of 26% "after the bypass". The results for the correlations were R^2=0.72 and R^2=0.76 respectively for before and after the bypass with $p< 0.001$[106].

Although these analysis showed a good relationship between Nexfin and the established methods, studies are still ongoing to validate the use of Nexfin. Indeed, three other recent studies "performed after a fluid challenge in cardiac surgical or critically ill patients showed a weak correlation between changes in CO between both devices", Nexfin and the pulmonary artery catheter, as well as PE above 50%[104]. As per Fisher et Al., we really need additional studies to evaluate Nexfin[104].

2.6.9 Link between CO and Body Surface Area

In order to validate a new method of evaluating CO, it may be important to consider body surface area (BSA) of the subject. Indeed, according to a study lead by Jegier et al.[131], CO (as well as SV) are linked to the "size" of the individual. The association is approximately the same for height, weight, and surface area. Indeed, the study showed the following correlation results[131]:

CO and BSA: r=0.85

CO and Weight: r= 0.86

CO and Height: r= 0.84

In a report written by Williams and sponsored by the department of energy in 1994, different methods of CO evaluation are explored[137]. Some scientists use Cardiac Index instead of Cardiac output since the formula for CI includes BSA: CI =CO/BSA. However, a number of investigators have suggested that a multiple regression of CO on several variables such as height, weight, or age would be more adequate than using BSA as the standard for comparison. In the same report, Williams includes suggested reference values for CO and CI, according to age.

The report also pointed out that over the entire age range, the correlation in each sex category between CO and anyone of the variables, weight, height, or BSA was greater than 0.6. The correlation between CO and BSA was roughly the same as that for either of the other variables including (weight)[137].

In the above sections, we noticed that many techniques have been created for the estimation of cardiac output, but they all have limitations and the new non-invasive methods such as Nexfin need further validation. The 'holy grail' for the evaluation of cardiac output would be a technique that is reliable, safe, handy and inexpensive and which, does not require a well-trained technician. To this date scientists are still looking for the ideal method[92]. According to Critchley, we are presently missing a reliable

"method of measuring CO in the clinical setting against which we can evaluate our new and emerging CO technology"[105].

2.7 PWV measurement

Arterial stiffness is a crucial biomarker for cardiovascular disease. This parameter is assessed by pulse wave velocity (PWV). Traditional techniques such as Doppler Ultrasonography, Magnetic Resonance Imaging (MRI) and Pulse Waveform Analysis are used to measure PWV but they are all expensive, complex and need to be performed within a medical setting with well-trained operators.

New devices are therefore emerging, which claim to be a better and more practical tool in monitoring PWV.

2.7.1 PulseTrace, Complior, PulsePen methods compared to tonometer technique

A review study lead by Salvi et al in 2008 compared PWV measurements via 2-tonometers (reference method) of 50 subjects between the ages of 20 and 84 years, with the values obtained through three devices: Complior, PulsePen and PulseTrace[126].

With Complior, the general procedure for estimating PWV is summarized below: Pulse wave Velocity is computed as the Distance between the two waveforms locations divided by Time delay between the feet of the two waveforms. The technician places one probe at carotid location and a second probe at the femoral location. The sensor captures the signal and a proprietary algorithm is consequently generated to calculate PWV.

With PulsePen, "PWV is calculated as the distance (L) between the two recording sites divided by the pulse transit time, obtained by the time delay between the

electrocardiogram and the carotid pulse (Ta) subtracted from the time delay between electrocardiogram and the femoral pulse (Tb)"[126].

With PulseTrace, the Stiffness Index is estimated by exploring the "photoplethysmo-graphic" signals obtained on the fingertip. SI is computed as follows: SI = Height/Time delay (between the waveform's "first systolic peak and early diastolic peak").

The measurements of these devices were compared to the ones generated by the reference method, which consisted of simultaneously acquiring waveforms through 2 tonometers. The results of the study were the followings:

PulsePen versus 2-tonometers: r=0.99

Complior versus 2-tonometers r=0.83

PulseTrace versus 2-tonometers r=0.55

The Bland–Altman analysis showed, "mean differences of values ±2s.d. versus the reference method of _0.15±0.62 m/s, 2.09±2.68 m/s and _1.12±4.92 m/s, for PulsePen, Complior and Pulse-Trace, respectively")[126].

In conclusion of their study, Salvi et al., affirmed that PulsePen and Complior were more reliable than PulseTrace in measuring PWV values. However, both PulsePen and Complior are "based on the delay between carotid and femoral pressure pulses in estimating PWV", which is similar to the reference method. On the contrary PulseTrace device, uses a totally different method and this fact may explain the low correlation with the reference method. According to Salvi et al, it is mandatory to establish reference values for each monitoring tool and it is crucial to homogenize the algorithms used for

these different devices to be able to compare them and also to obtain similar PWV values. In particular, many other new devices, such as Vicorder or Colins system are emerging today in order to measure PWV and the values of PWV obtained with these devices may considerably vary from one device to the other depending on the technique, the type of probes and algorithms used to define PWV. Salvi et al. argued that it is mandatory to evaluate and compare different devices to standardize PWV values, and to at least define reference values[126].

2.7.2 Link between PWV, Age and BP

In a study published by European heart journal in 2010, scientists tried to define reference values for carotid femoral PWV[130]. They collected data from 16 867 individuals from thirteen various centers across 8 European countries, in which PWV and other important indices were measured. Before performing the "data pooling, PWV values were converted to a common standard using established conversion" formula and individuals were categorized by both age decade and blood pressure. They demonstrated that PWV increases with "age and BP category" and thus created related PWV reference measurements linked to both of these variables [130].

2.8 Intrinsic frequencies, a new approach to heart health evaluation

Intrinsic frequencies (IF) are two recently discovered indices, two dominant frequencies or signals that are mathematically extracted from the arterial pressure waveform: ω_1 and ω_2, or BPM1 and BPM2. Their measurements could possibly carry important information regarding the health of the cardio vascular system. These indices

could be used as effective biomarkers in order to predict heart disease or monitor the overall cardiovascular performance. Pahlevan et al. demonstrated the following trend: if the wave ω1 and ω2 "graphed as a function of HR, the two curves" will "always intersect at the optimum HR value". This suggests that the total frequency variation, TFV ($\Delta\omega=\omega1-\omega2$) is close to "zero at young ages", when the cardiovascular system is functioning near "the optimum state" and that this variation "increases with age" or heart diseases. They showed that at an increased level of "aortic rigidity, the optimum HR shifts to the right"[29].

Therefore studying ω_1, ω_2 and TFV can be crucial as they can be used as predictive values of cardiac health. Through the study of waveforms, Pahlevan et al. performed blind test examples to predict the health status of a subject without consulting a physician. For example by applying STFR method to the waveform of a subject, which had a HR of 79.4, they calculated the intrinsic values: ω_1 =73.2, ω_2 = 52.3 and $\Delta\omega=\omega1-\omega2$=20.9. The following observations were subsequently made about this subject: ω_1 is less than HR indicating LV dysfunction (thus severe abnormality), ω_2 is low indicating mild arterial rigidity which is consistent with 35-45 year old male or 55-65 year old female and delta w was low indicating good heart aorta coupling. In fact, the subject was a 66 year old female without any history of hypertension and she had a normal EF however presented with atypical chest pain with indeterminate cause. Another example of this method's application on a subject with an HR of 97.5 led to the calculated ω_1=121.4, ω_2 =44 and $\Delta\omega=\omega1-\omega2$=77.4. The following observations were subsequently made: ω_1 was high pointing out to LV dysfunction, ω_2 was very low indicating severe arterial rigidity (which is consistent with 60+ year old male) and delta w was very high

highlighting a severe arterial rigidity and heart diseases). In reality the patient was a 65 year old male with severe coronary disease. He had a poor LV function with a very low EF(25%).

Pahlevan et al. consequently created a table, which displays possible diagnoses associated with the subject IF values. This method can be implemented with a programmable logic device. Indeed, the intrinsic algorithm can be directly embodied in a software module executed by a processor. The system can thus acquire and calculate intrinsic frequency values and subsequently provide prediction(s) related to the cardiac health status of the individual[28,29,30].

Further studies based on IFs are still needed that could produce a database and propose correlations between the IF values and various cardio vascular diseases. The clinical data used in Pahlevan et al. study was gathered from previously published work or from retrospective databases and the number of pressure waveforms attained was limited. Moreover IFs can estimate the values of major cardiac health parameters, including LVEF, PWV and CO, however no studies were done yet to validate this claim and therefore additional research needs to be performed.

2.9 Research gap

The publications that we reviewed earlier have shown that research is still ongoing for a reliable, handy, cost-effective and safe cardiovascular monitoring technology. CVDs have reached epidemic proportions and thus, improved methods are urgently needed. The purpose of this study is to analyze, test and validate a new noninvasive method of estimating cardiovascular performance parameters (such as

LVEF, CO and PWV). This technique offers a new vision to cardiovascular health management since it is easy to use and therefore, it can render the monitoring of hemodynamic parameters widespread. Indeed, it exclusively relies on the shape of the pressure pulse-wave and not its magnitude, thus IFs values and a combination of heart shape factors can easily be extracted via an algorithm that can be embedded in small, handy and lightweight technologies, such as an iPhone. This new IFs technique is therefore very safe and inexpensive. If validated, it could possibly circumvent the limitations of the standard assessment devices described earlier and therefore offer a simple, non-invasive and practical way of monitoring cardiovascular health. Ultimately, it can help eliminate the burden of CVDs and save lives. The next sections provide statistical details on the database used for this study as well as different analytical methods.

CHAPTER III METHODS

3.1 Research Overview

Heart disease is the main cause of death in this country. Many devices and techniques are currently in use to manage cardiovascular health, however they present numerous limitations. To address the drawbacks of the current technologies, this study statistically evaluates a new method based on IFs methodology. This novel method has the potential of rendering the overall process of cardiovascular monitoring easy, safe and cost efficient.

Throughout this study, we statistically analyze the relationships between the estimates of LVEF, CO and PWV produced by IFs method and the values of these parameters generated by the established devices. The goal of this observational study is to find out if the new IFs technique generates reliable measurements. This chapter presents an overview of the methodology used to address the above objective, including the study design, sampling and data analysis methods.

3.2 Research Design

This study is divided into 3 main sections. Each part targets the heart parameter that we aim to estimate via IFs technique. Thus, the first part emphasizes on LVEF, the second part on CO and the last part on PWV. Each of these heart parameters constitutes the "dependent" variable. A "Multivariable regression" method is applied to various

observational databases in order to investigate the correlation between the dependent and independent variables. The "independent" variables include IFs indices as well as a number of heart shape factors. IFs indices are preliminary extracted from the carotid pulse (waveform), which is captured via various devices:

- Tonometry: this device captures the pulse over carotid arteries using a modified stethoscope.
- iPhone camera: the algorithm related to the extraction of Intrinsic frequency values is loaded onto a smartphone. The phone captures a waveform by simply placing it lightly over the subject's neck where the carotid pulse can be felt
- Cardius: it consists of a newly patented small device connected to a monitor that captures the waveform from the subject's neck.

An algorithm (based on the modified sparse time frequency) is applied on the captured carotid waveforms (figure 8) to "simultaneously" extract IFs indices consisting of BPM1, BPM2, Cratio and Envratio. A number of heart shape factors are simultaneously computed too:

NodeX = Coupling period

NodeY = Decoupling period

Duration = Time corresponding to 1 heart cycle.

Decoupling Factor (DF) = the point where heart and aorta decouple.

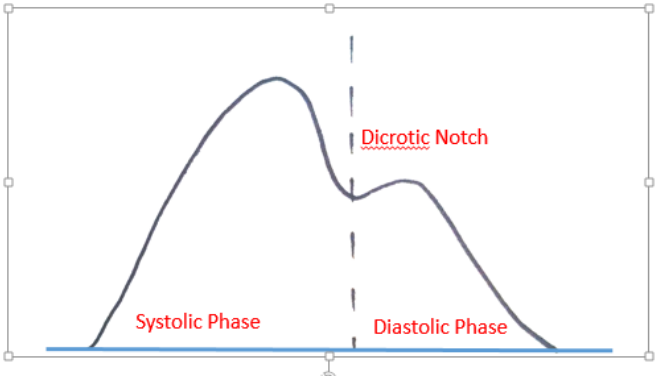

Figure 8: IFs explanatory variables, simultaneously generated from the shape of a simple arterial waveform.

The above eight variables constitute IFs "core independent variables". A few physiological variables such as, Age or Weight are occasionally considered as independent variables. Combinations of these variables are used to estimate the values of the dependent variables, LVEF, CO and PWV. These calculated measurements are then compared to the measurements produced by the established techniques. Any correlation is thoroughly investigated. To evaluate the "clinical agreement" between the IFs methodology and the established monitoring techniques, Bland Altman analysis is applied.

3.3 Research Questions and associated Hypothesis

Throughout this study, the following research questions and related statistical hypotheses are addressed:

- Is there a meaningful relationship between IFs method and established methods like MRI or Echo for the measurement of LVEF?

- Null Hypothesis 1. There is not a statistically significant correlation between LVEF measurements obtained via MRI or Echo and LVEF values produced by IFs method.
- Alternative Hypothesis 1. There is a statistically significant relationship between LVEF measurements obtained via MRI or Echo and LVEF values produced by IFs method, thus at least one of the independent variables (BPM1, BPM2, NodeX, NodeY, Cratio, Envratio, Duration…) is useful in explaining or predicting LVEF.

- Is there a meaningful relationship between IFs method and MRI for the measurement of CO?

- Null Hypothesis 2. There is not a statistically significant correlation between CO measurements obtained via MRI and CO values produced by IFs method.
- Alternative Hypothesis 2. There is a statistically significant relationship between CO measurements obtained via MRI and CO values produced by IFs method, thus at least one of the independent variables (BPM1, BPM2, NodeX, NodeY, Cratio, Envratio, Duration…) is useful in explaining or predicting CO.

- Is there a meaningful relationship between IFs method and Tonometry technique for the measurement of PWV?

- Null Hypothesis 3. There is not a statistically significant correlation between PWV measurements obtained via Tonometry and PWV values produced by IFs method.
- Alternative Hypothesis 3. There is a statistically significant relationship between PWV measurements obtained via Tonometry and PWV values produced by IFs method, thus at least one of the independent variables (BPM1, BPM2, NodeX, NodeY, Cratio, Envratio, Duration…) is useful in explaining or predicting LVEF

3.4 Population and Sample Data

This observational study determines the followings:

- How intrinsic frequency LVEF measures compare to MRI or Echocardiogram values.

- How CO measures compare to MRI values

- How PWV estimations compare to Tonometry values.

A number of training and testing datasets is used to accomplish the above objectives. This study was approved by Caltech IRB committee.

3.4.1 Datasets for LVEF, CO and PWV analysis:

3.4.1.1 HMRI

We use Huntington Medical Research Institute (HMRI) as our setting to evaluate IFs method for LVEF and CO estimations. The database inclusion and exclusion criteria are:

- Inclusion criteria: adults (both male and female) between the ages 18 and 90 years with normal and abnormal cardiac function.
- Exclusion Criteria:

- Inability to lie flat for 30 minutes with periodic breath holding
- Metal implants or other standard contraindications to MRI
- Acute cardiac decompensation (active chest pain, shortness of breath)
- Hypotension (SBP<90 mm Hg)
- Claustrophobia
- Patient too large to fit in closed MRI

The arterial waveforms or cycles (beat per minute) are captured from each subject via Tonometry, iPhone or Cardius devices. For every single cycle, few recordings are obtained per subject and thus, IFs core independent variables are extracted. They are filtered by Dr. Pahlevan, who is conducting this study at HMRI. There is a need for filtering since a number of these values are defective, usually due to the quality of the signal itself (which is sensitive to noise), or because of other causes. The filtering process takes place as follows: for each subject, a number of waveforms is obtained, from

which IFs core indices are extracted and plotted. These indices are filtered and kept within the following interval: +/- 15. Then, the average of these filtered indices is computed and considered. The remaining indices are excluded from the database. Therefore only recordings of high quality are kept. After the filtering process, the followings sets

- HMRI_Tonometry database

We use this database to train our data for both EF and CO estimations. It includes 124 useable random observations (multiple recordings per subject) with actual EF and CO values from MRI.

- HMRI_ iPhone databases

It includes two sets of databases that we use to train and test our data for our iPhone study.

- Dataset 1 or the training set: it includes 82 random observations, with the actual EF values from MRI. The IF and shape factor values are from waveforms captured via the following devices: Tonometry, iPhone and Cardius.
- Dataset 2 or the testing set consists of 64 random observations, with actual EF values from MRI; and IF and shape factor values from waveforms solely captured via iPhone.

3.4.1.2 Framingham:

The data collected as part of the Framingham longitudinal epidemiological cohort study, is used as our testing set for LVEF and CO measurements. It is then used as both our training and testing sets for PWV estimates. "The Framingham Heart Study is a long term ongoing cardiovascular study on residents of the town of Framingham in Massachusetts, which began in 1948 with adult subjects from Framingham, and is now on its third generation of participants"[113]. It includes 6,500 observations targeting both male and female adults between the ages of 19-99. This database includes actual LVEF and CO values from echocardiogram, as well as tonometry derived cycles (waveforms) from which, IFs core variables are extracted. It also includes actual PWV measures. For every single cycle (which consists of one recording per subject), the IFs values and a number of heart shape factors are obtained and then filtered the same method as described earlier.

3.4.1.2.1 Database for LVEF testing:

Initially a small subset of this database with 400 unfiltered observations was available. We call this database FHS-400. After filtering, 170 useable observations were available for the initial testing (out of 400). Then, a larger database (FHS_6500) with a total of 3,556 useable observations became available. It also included FHS_400. This larger database, was subsequently used to perform further testing on the trained models. A major issue with Framingham dataset was the fact that it had a very limited number of low LVEF values.

3.4.1.2.2 Database for PWV training and testing:

- **FHS Training Database:**

For training our data in reference to PWV estimations, we use FHS_400 (a subset of FHS_6500). It includes the actual PWV values from tonometry as well as tonometry derived waveforms (cycles) from which IFs and shape factors are extracted. After filtering our waveforms, the training database consists of 279 useable observations.

- **FHS Testing Database:**

For testing our PWV results, we use FHS_6500 database. After filtering and removing the observations with missing values, we have 5,684 useable observations to test our training data. This database includes our training set of FH_400.

Notes: The sample sizes used in the study are selected based on the need to have sufficient statistical power in order to prevent type 2 error and also to avoid problems regarding overfitting the data. In general, we ensure to have a minimum of 10 to 15 data-points per predictor.

A p-value<0.0001 is considered, which reduces the probability of committing type 1 error.

3.5 Data analysis

The main objective of this study is to explore relationships between measures generated via IFs technique and results produced by gold standard devices such as MRI, Echo and Tonometry. The methods used in this paper include supervised machine

learning with regression analysis and Bland Altman evaluation. In order to perform our data analysis, we used the following statistical packages: SAS, JMP and Matlab.

3.5.1 Supervised Machine learning for Modeling

Machine learning consists of the "creation and evaluation of algorithms that facilitate pattern recognition and prediction, based on models derived from existing data"[115]. The objective of "supervised machine learning" is to construct a model that makes predictions through an algorithm, which uses a training dataset. Through the use of the training dataset, the supervised learning algorithm aims to "learn" and "train" a model that generates reasonable estimations for the response values to a new database. Then a "test" database is applied to assess the model and evaluate its prediction error. Often, using larger training datasets produces" models with higher predictive power that can generalize well for new datasets"[114]. In this study we use "Multiple regression" to generate a "learned" or "trained" algorithm and then we use "Bland Altman" to re-evaluate the selected model. The general workflow is presented below:

Figure 9 - Data Analysis: general workflow

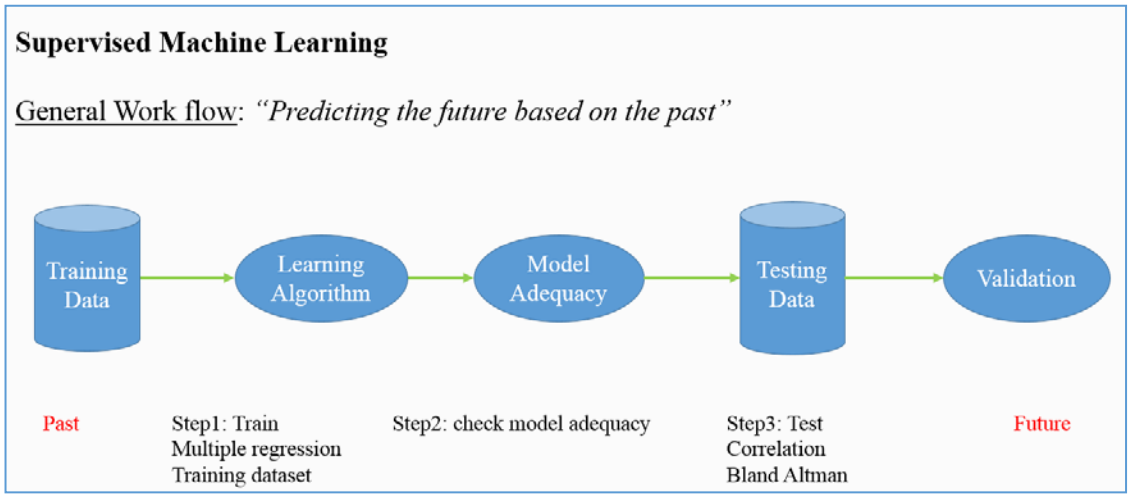

3.5.2 Multivariable Regression Analysis

3.5.2.1. General Equation

Regression analysis is a technique that helps model the relationship between variables. A multiple linear regression equation is applied to our study:

$\hat{y} = \beta_0 + \beta_1 x_1 + \beta_2 x_2 + ... + \beta_k x_{k+} \varepsilon$

- $\hat{y}$ is the predicted value for the response variable. In our study $\hat{y}$ respectively consists of estimated values for LVEF,CO and PWV.
- β_0 represents the intercept.
- K consists of the number of predictors in the model
- β_1 to β_k represent the regression coefficients for the independent variables within the model.
- x_1 to x_k consist of the values for the k regressor variables. In our study they include the "core variables": BPM1, BPM2, NodeX, NodeY, Decoupling Factor, Duration, Cratio and Envratio. They also occasionally include physiological variables deemed necessary, such as Age or Weight.
- ε=random error

The following regression assumptions are required:

- On the regression: the relationship between the response and explanatory variable(s) is linear or approximately linear.
- On the errors: the error term ε has zero mean and constant variance. The errors are uncorrelated (independent) and normally distributed[116].

Using the regression formula, our main hypotheses are:

- H_0: there is no relationship between the response variable and our predictors, thus $\beta 1 = \beta 2 = ... = \beta p\text{-}1 = 0$.
- H_1 Alternative Hypothesis: there is a relationship, thus at least one of the independent variables is useful in explaining or predicting Y', therefore at least one $\beta i \neq 0$

After we fit a linear model using multiple regression analysis, we determine how well the model fits the data. The overall significance of the model is tested using the ANOVA approach (F test). The threshold for statistical significance is $p < 0.0001$. The statistical significance of each predictor's coefficients is tested via t-test. This test shows if a predictor contributes significantly to the equation. We check the value of R^2, which is equal to Explained variation / Total variation (or Sum of Squares of Regression/Sum of Squares Total).

$$R^2 = \frac{SSR}{SST} = \frac{\sum (\hat{y}_i - \bar{y})^2}{\sum (y_i - \bar{y})^2}$$

This value is between 0 and 1 and "the more closely the points in the scatter diagram are dispersed around the regression line, the higher the proportion of variation will be explained by the regression line, thus the greater R^2 value"[123]. R^2 value is important, but can sometimes be misleading and may not show the real relationship between the response and explanatory variables. Indeed, the more variables are added into a regression, the higher the R^2 value, even if there is absolutely no relationship between the additional variables and the target variable. Indeed the likely improvement in fit would

happen because each new predictor would randomly account for some of the variation in the response variable. Thus R^2 alone does not work alone as a means of deciding the number or type of variables to include. One remedy to this problem is to use the Adjusted R^2 (Adjrq) which, reduces the value of R^2 each time a predictor is added to a model. This adjustment attempts to compensate for purely random fit improvements. This is useful to prevent fitting pure random noise or overfitting the data[135]. Our statistical analysis is therefore based on maximizing the value of Adjrq.

The formula for Adjrq is:

$$\bar{R}^2 = 1 - (1 - R^2)\frac{n-1}{n-k-1}$$

With n being the sample size and k being the number of predictors.

After finalizing a regression algorithm, the related model is checked for adequacy We review the validity of regression assumptions. To perform this task, we check the diagnostic fits, the residuals plots and outliers and ensure that multicollinearity is minimized:

3.5.2.2 Checking the residuals

The residuals from a regression model can be written as "ei= yi- ŷi where yi is an actual observation and ŷi is the corresponding fitted value from the regression model"[121]. The study of residuals helps the process of "checking the assumption that the errors are approximately normally distributed with constant variance"[121]. Standardized residuals plot can be checked too. They are residuals divided by the SD of the residuals. They can create a guideline for what is a large residual. If they are larger than 1.96, then they are

the extreme 5% of values. If the model is inadequate, changes are made and the parameters are estimated again. The normality assumption is also be checked by analyzing the QQ plot. If the assumption is satisfied, the residual points on a QQ plot are approximately falling along the diagonal $y=x$ line.

3.5.2.3 Influence of Outliers

We can check for anomalous values in the data by looking at the plot of outliers and leverage. According to Montgomery et al., data points for which Cook's D value is greater than 1 could be influential and of concern since the related outlier can drag the regression line toward itself[116]. It is also useful to check "Studentized" residual greater than 3 in order to pinpoint an outlier. In this study we evaluate all the related plots.

3.5.2.4 Multicollinearity

Multicollinearity occurs, when a few predictors in a multiple regression model are strongly correlated. According to Montgomery et Al., "the diagnosis treatment of multicollinearity is an important aspect of regression modeling" as multicollinearity can make

the coefficients of the predictors very unstable[116]. For example a particular regression coefficient should be positive while the actual estimate of the parameter is negative. In order to minimize multicollinearity and have the least amount of variability, variance inflation factor (VIF) is checked for each predictor and a VIF threshold of 10 is targeted in our modeling selection. VIFs larger than 10 indicate serious problems with multicollinearity[116].

3.5.2.5 Transformations

To further ensure that all assumptions are valid or to increase the strength of the relationship, we either apply a transformation on our response variable or a polynomial transformation on our predictors. We also add additional predictors when required.

- Transformation on the Response variable:

Box-Cox procedure can help find an adequate transformation. The statisticians George Box and David Cox created a method to find an adequate exponent (lambda) to apply on the data in order to turn it into a "normal shape." and address heteroscedasticity. This method does not "guarantee" normality but verifies for "the smallest standard deviation"[136]. "The assumption is that among all transformations with Lambda values between -5 and +5, transformed data has the highest likelihood – but not a guarantee – to be normally distributed when standard deviation is the smallest"[136]. The Lambda pinpoints to the power to which all data should be raised, meaning the "best" power transformation for the response. Thus, the transformation is y to the power of lambda. To apply this method, the SAS Box-Cox automated procedure is used. It explores values from Lambda -5 to Lamba +5 until the most adequate value is found[136].

$$Y' = Y^{\lambda} \qquad \text{When } \lambda \neq 0$$

$\lambda = 2$	$Y' = Y^{2'}$
$\lambda = 0.5$	$Y' = \sqrt{Y}$
$\lambda = 0$	$Y' = Log_e Y$
$\lambda = -0.5$	$Y' = \frac{1}{\sqrt{Y}}$
$\lambda = -1$	$Y' = \frac{1}{Y}$

- Transformation on predictors:

We transform our predictors using Parseal

Wilson and Matlab software. Parseal Wilson is a proprietary algorithm recently created

by Dr. Tavallali, of Caltech. This algorithm transforms the predictors based on the following criteria: VIF and Adjrq. In order to obtain regression models that would best fit the data, the algorithm involves:

1) A polynomial transformation on the predictors. We have the liberty of setting the degree (power) of this transformation.
2) An interaction among the predictors. In general, "an interaction occurs when an independent variable has a different effect on the outcome depending on the values of another independent variable"[122]. For example, an Interaction occurs between adding sugar to tea and stirring the tea. Neither of the two distinct variables has much effect on sweetness but a combination of the two does. An additional level of regression analysis is thus employed here by allowing the exploration of the synergistic effects of combined variables. We can set the interaction level (or Mix) to a specific level of interest.

The overall goal of our regression model(s) is to determine the values of the beta parameters that minimize the sum of the squared residual values (difference between predicted and observed values) for the set of observation. Therefore the learned algorithm (or model) should offer the best prediction possible of our dependent variable, minimizing the amount of errors. After performing all the required transformations and checking the model adequacy, we run a Bland Altman analysis to reckon the magnitude of *agreement* between the methods. The purpose of this analysis is to ensure that the selected models generates reasonable and acceptable results. The selected models are thus further evaluated for their accuracy and precision.

3.5.3 Bland Altman method to evaluate degree of agreement

We need to evaluate the degree of agreement between the results obtained with our new method and the measurements generated by the established technologies to find out if they agree enough for the new to be exchanged with the old. According to Bland and Altman, the correlation coefficient is not sufficient and "a high correlation does not mean that the two methods agree: *r* measures the strength of a relation between two variables, not the agreement between them". They maintain that the "perfect agreement" is reached only if the data points lie along the line of equality, whereas a perfect correlation can be reached if the points lie along any straight line[117, 119]. Also, the "correlation coefficient can be close to 1 even when there is considerable bias between the two methods". For instance, "if one method gives measurements that are always 10 units higher than the other method, the correlation will be 1 exactly, but the measurements will always be 10 units apart"[119].

Thus Bland Altman introduced a plot that would assess the agreement between the measurements of two different devices[60]. The "method calculates the mean difference between two methods of measurement (the bias), and 95% limits of agreement (LA), as the mean difference +/- 1.96 standard deviation of the differences"[61]. This method depends on the following assumptions:

- Bias and SD of differences are constant
- SD of differences are generated from a roughly Normal distribution.

We can use graphs to check these above assumptions: a scatterplot of the mean of the two methods against the differences as well as a histogram plot of the differences.

This method also offers an important parameter, called percentage error (PE) which can be used to assess the error between the two methods: *PE= [LA/Mean of the reference method (or Mean of the response]*. According to various publications, the PE number for CO estimations should be less than 30%[118]. Since the established thermodilution method "has a precision of +/-20%, to equal of better this by the new method, it is widely agreed that the PE should not be over 30%". However there has been debate about this benchmark by various literature since "many validation studies have provided PE way above 30%"[118]. Regarding LVEF and PWV, it is also useful to compute the PE value, however there is no defined benchmark for these parameters.

Therefore, throughout this study, we compare the limits of agreement of IFs method to established monitoring techniques of LVEF, CO and PWV. A general example of a Bland Altman plot is featured below:

Figure 10: Example of a Bland Altman plot

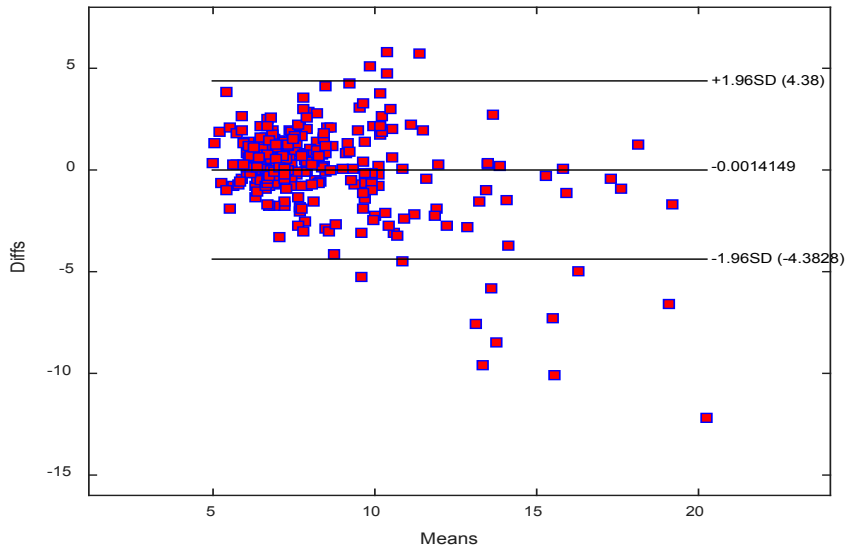

CHAPTER IV RESULTS AND DISCUSSION

4.1 Results

In order to estimate LVEF, CO and PWV values, we first extract IFs indices from the shape of the waveform. Thus, we capture the subject's carotid pressure waveform via any of these distinct non-invasive devices: Tonometer, iPhone and Cardius. Then, we mathematically (simultaneously) extract BPM1,BPM2, Cratio, Envratio and a number of heart shape factors such as NodeX, NodeY, Decoupling Factor and Duration. These "IFs explanatory variables" are subsequently used to estimate the values of LVEF, CO and PWV. We compare these values to the actual measurements generated by various reference methods currently in use, in order to investigate any existing relationship(s). We explore the correlation and agreement between the IFs and the standard methods of cardiovascular evaluation. The units of measurement are the followings throughout the study: LVEF (%), CO (L/min) and PWV (m/s). We perform this analysis through three main sections:

- In the first section we emphasize on LVEF:

  - IFs estimations (computed from tonometry waveforms) are compared to MRI and Cardiac Echo measurements.

  - IFs estimations (computed from iPhone waveforms) are compared to MRI measurements.

- In the second section we target CO:

IFs values (computed from tonometry waveforms) are compared to MRI measurements.

- In the third section we focus on PWV:

IFs values (from tonometry waveforms) are compared to 2-tonometers measurements.

4.1.1 Data analysis: estimating LVEF with IFs methodology

4.1.1.1 Estimations (IFs_Tonometry) compared to values from established devices

IFs methodology views the carotid pressure waveform as a combination of BPM1, BPM2, Cratio and Envratio indices, as well as a number of heart shape factors: NodeX, NodeY, Decoupling Factor and Duration. All these variables constitute IFs core independent variables. We are looking for a model that would possibly include the best combination of predictors in order to estimate LVEF.

4.1.1.1.1 Training process – Modeling the relationship between IFs and MRI:

Before exploring various models, we neglect heart shape factors and focus on the main IFs frequencies, which are BPM1 and BPM2. We use our tonometry database that includes 124 useable observations (HMRI database) and apply a linear regression analysis with the following formula: Estimated LVEF= $\beta_0 + \beta_1$ BPM1 + β_2 BPM2. We obtain table 1 and figure 11:

Model 1: PredictedLVEF = f(BPM1 BPM2)

Table 1: LVEF - Model 1

Results of Analysis of Variance - Obs=124

Source	DF	Sum of Squares	Mean Square	F Value	Pr > F
Model	2	8400.16553	4200.08276	53.63	<.0001
Error	121	9475.34439	78.30863		
Corrected Total	123	17876			

Root MSE	8.84922	**R-Square**	0.4699
Dependent Mean	57.45081	**Adj R-Sq**	0.4612
Coeff Var	15.40312		

Parameter Estimates

Variable	Label	DF	Parameter Estimate	Standard Error	t Value	Pr > |t|	Variance Inflation
Intercept	Intercept	**1**	123.95443	6.60240	18.77	<.0001	0
BPM1	BPM1	**1**	-0.80627	0.07832	-10.29	<.0001	1.34905
BPM2	BPM2	**1**	0.18229	0.04279	4.26	<.0001	1.34905

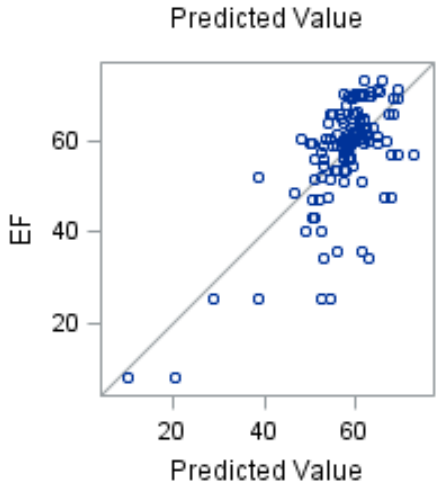

Figure 11: LVEF-Model1

This preliminary analysis shows that both BPM1 and BPM2 are significantly related to our response variable, the multiple correlation coefficient R is 0.69 and Rsquare is 0.47 ($p<0.0001$). The value for the Adjrq (0.46) is moderately high, which

indicates that a good percentage of the variation (out of the total variation) is explained by our regression line. However, we can perhaps improve this relationship by including Cratio and Envratio as well as a combination of heart shape factors obtained from the carotid waveform: NodeX, NodeY, Decoupling Factor and Duration. In order to target the best combination of predictors, we begin exploring the scatterplot matrix of variables:

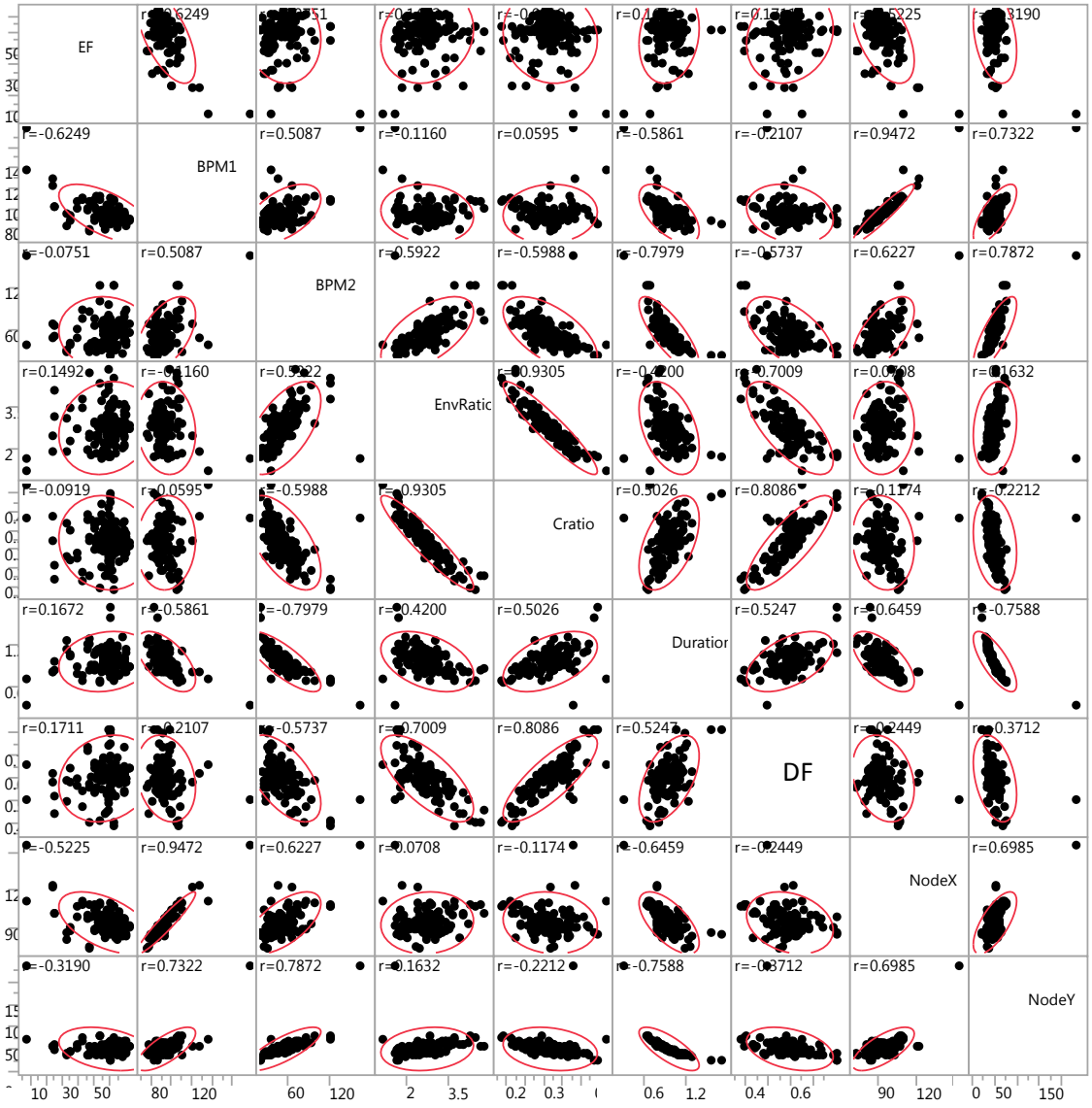

Figure 12: LVEF – Scatterplot Matrix of variables

We observe that most of these variables could to some extent contribute to our regression model. We also notice that BPM1 and NodeX are greatly correlated to each other (figure 12). Furthermore, they are both highly related to our response variable ($p<0.0001$). This information suggests that we may encounter multicollinearity in our analysis, and thus we need to establish a system in order to manage this issue. We consequently perform a linear regression analysis with a full set of explanatory variables and explore the "VIF" value of each variable within the overall relationship. Using our training database with 124 observations, we attain the following results.

Model 2 : Predicted LVEF = f(Core variables)

Table 2: LVEF-Model2

Analysis of Variance - Observations = 124					
Source	**DF**	**Sum of Squares**	**Mean Square**	**F Value**	**Pr > F**
Model	8	10186	1273.29707	19.04	<.0001
Error	115	7689.13334	66.86203		
Corrected Total	123	17876			

Root MSE	8.17692	**R-Square**	0.5699
Dependent Mean	57.45081	**Adj R-Sq**	0.5399
Coeff Var	14.23291		

Parameter Estimates							
Variable	**Label**	**DF**	**Parameter Estimate**	**Standard Error**	**t Value**	**Pr > |t|**	**Variance Inflation**
Intercept	Intercept	**1**	128.01920	24.09900	5.31	<.0001	0
BPM1	BPM1	**1**	-1.81814	0.45142	-4.03	0.0001	52.49259

Parameter Estimates							
Variable	**Label**	**DF**	**Parameter Estimate**	**Standard Error**	**t Value**	**Pr > |t|**	**Variance Inflation**
BPM2	BPM2	**1**	0.25234	0.10441	2.42	0.0172	9.40523
NodeX	NodeX	**1**	0.90260	0.46130	1.96	0.0528	40.53810
NodeY	NodeY	**1**	-0.01669	0.10486	-0.16	0.8738	7.93391
DF	DF	**1**	-11.93369	26.31503	-0.45	0.6510	7.99957
Duration	Duration	**1**	-19.87948	8.29258	-2.40	0.0181	3.92302
Cratio	Cratio	**1**	111.78374	65.20695	1.71	0.0892	20.91980
EnvRatio	EnvRatio	**1**	-1.89247	3.41757	-0.55	0.5808	9.88237

According to the above results (table 2) and as guessed earlier, both BPM1 and NodeX display an excessive VIF value, suggesting a high multicollinearity. As mentioned before, this issue can complicate or prevent the identification of an optimal set of explanatory variables for a statistical model. In order to address this problem, one approach is to eliminate the predictor with the highest VIF, and recalculate all VIF values with the new set of variables. In this case, the highest VIF belongs to BPM1, however, we choose to keep BPM1 since it shows a significant relationship with our response variable. Instead of eliminating BPM1, we proceed to exclude NodeX, the next variable with the highest VIF. This variable is not significantly related to LVEF within the above analysis (contrary to BPM1).

We recalculate therefore the VIF values with our new set of variables. We notice that Cratio continues displaying a high VIF, thus we decide to eliminate it. Now with our new reduced-size model, VIF values are all below the benchmark of 10 (table 3):

Model 3 : Predicted LVEF = f(BPM1 BPM2 NodeY Decoupling Factor Duration Envratio)

Table 3: LVEF-Model 3

Analysis of Variance – Obs=124					
Source	**DF**	**Sum of Squares**	**Mean Square**	**F Value**	**Pr > F**
Model	6	9897.54203	1649.59034	24.19	<.0001
Error	117	7977.96789	68.18776		
Corrected Total	123	17876			

Root MSE	8.25759	**R-Square**	0.5537
Dependent Mean	57.45081	**Adj R-Sq**	0.5308
Coeff Var	14.37332		

Parameter Estimates							
Variable	**Label**	**DF**	**Parameter Estimate**	**Standard Error**	**t Value**	**Pr > |t|**	**Variance Inflation**
Intercept	Intercept	**1**	142.04527	21.36987	6.65	<.0001	0
BPM1	BPM1	**1**	-0.93952	0.10572	-8.89	<.0001	2.82300
BPM2	BPM2	**1**	0.35553	0.09075	3.92	0.0002	6.96768
NodeY	NodeY	**1**	-0.12642	0.08778	-1.44	0.1525	5.45133
DF	DF	**1**	32.80510	14.71430	2.23	0.0277	2.45251
Duration	Duration	**1**	-16.44184	7.84684	-2.10	0.0383	3.44433
EnvRatio	EnvRatio	**1**	-4.47610	2.33394	-1.92	0.0576	4.51941

These results reveal that after performing a selection based on VIF, the standard error estimates of the coefficients becomes smaller, thus adding stability to our regression

equation and model. For example the standard error estimate for BPM1's coefficient dropped from 0.45 to 0.1. This equation has a better chance to hold when applied to a new dataset. Moreover, this dimension reduction makes our model simpler with an Adjrq (0.53) that remains moderately high. The overall regression equation is significantly related to the response variable ($p<0.0001$). The multiple correlation coefficient R is equal to 0.74, which seems to be a good fit for our data, but we need to run the fit diagnostics and residuals by regressors for EF in order to check the adequacy of the model. The following figure features the related plots.

Figure 13: Graph combination related to LVEF-Model 3

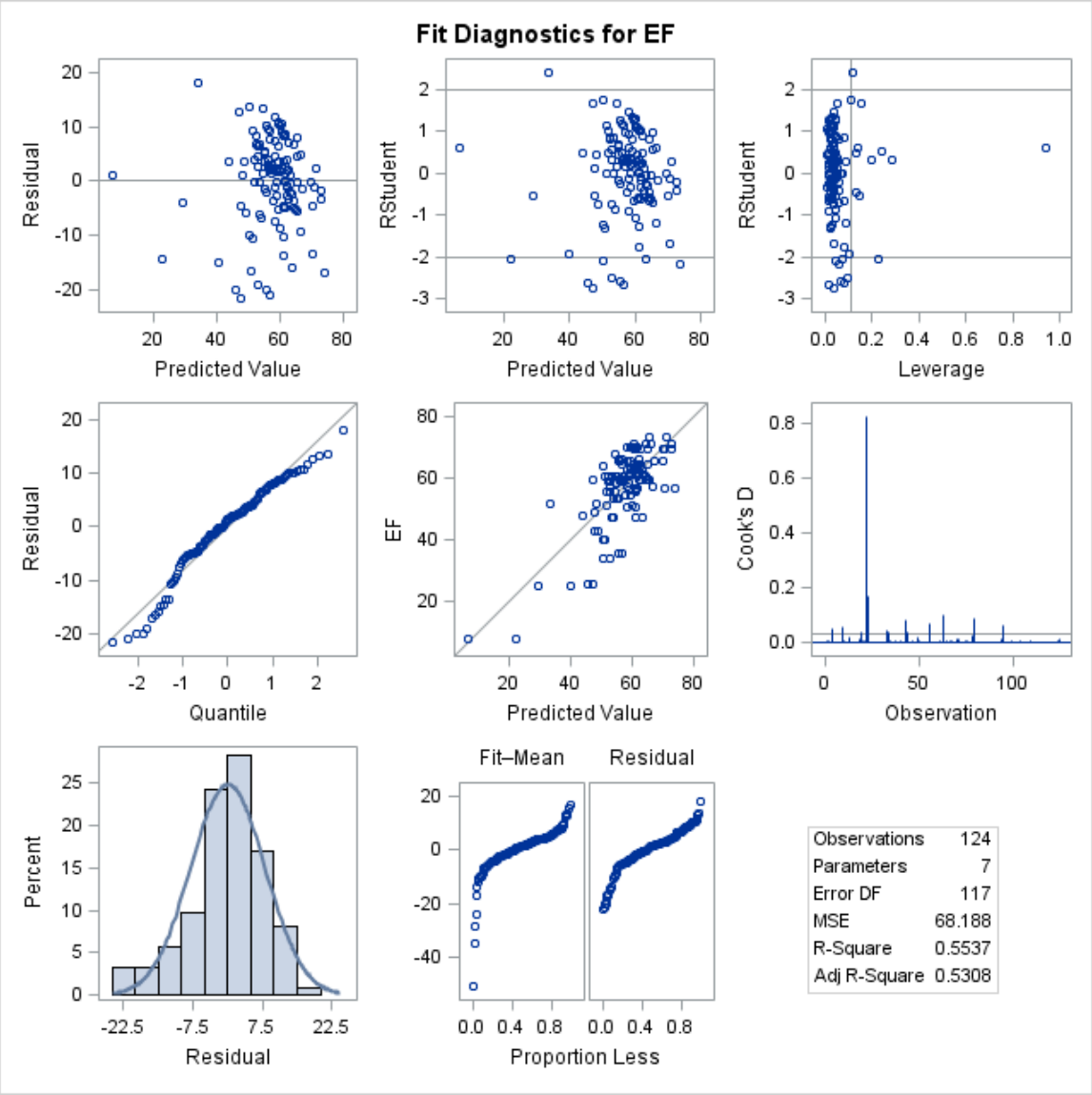

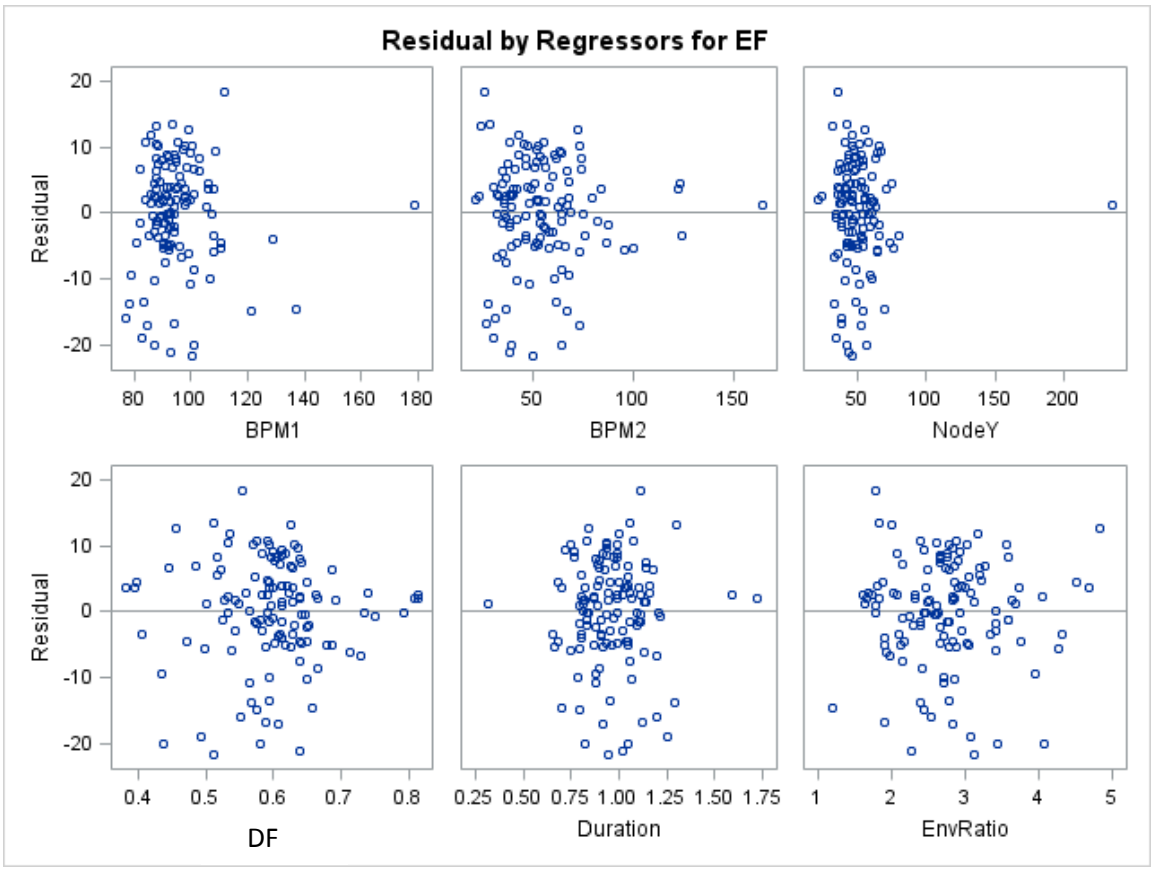

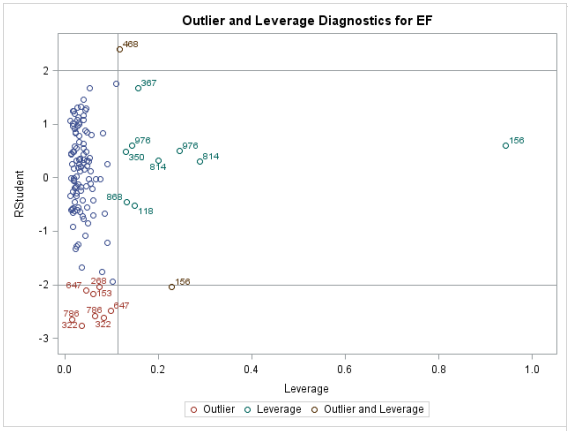

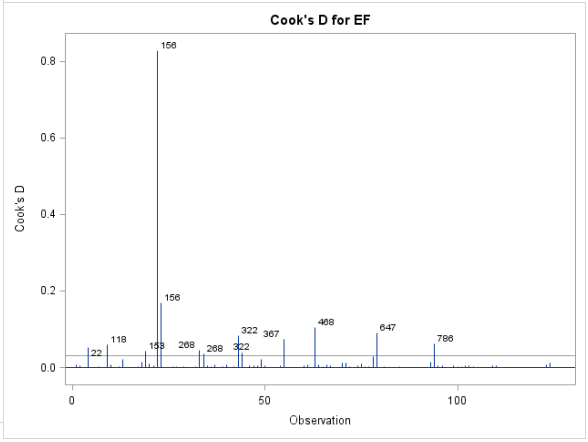

According to the above graph combination, the points on the quantile (or QQ) plot fall approximately on a straight line. The plots of the residuals display a random pattern and do not show any violation of the regression assumptions. We notice an outlier though, on the outlier and leverage plot, which can be influential, dragging the regression

line toward itself. We need to review this data-point and check its validity. It corresponds to SUBID 156 which displays an actual LVEF value of 7.8. This data-point is related to IFs signals that are derived from tonometry (right side). The actual LVEF value related to this point is very low, and the removal of this data-point drops Rsquare of the calculated EF from 0.55 to 0.48 (with RMSE=8.28) making this data-point to some extent influential, but since it is a legitimate point and is not arising from errors, we decide to keep it. Moreover, the related Cook's D value is below the threshold of 1. Further evaluation of this model shows that only one explanatory variable (among all 6), is significantly contributing to the relationship. Moreover, the plot featuring predicted EF values versus MRI measures, reveals a degree of non-linearity. Thus, we may obtain a better fit of the data and improve the plots and strength of the relationship if we apply a transformation on the variables. We first try a Boxcox transformation on our response variable. The best lambda is 2.25, suggesting that squaring our response variable may improve the QQ plot. However, after applying this power transformation, we notice that Adjrq drops from 0.53 to 0.45 and the related plots show no significant improvement (Figure 14):

Figure 14: Graphs combination related to Boxcox transformation on LVEF-model 3

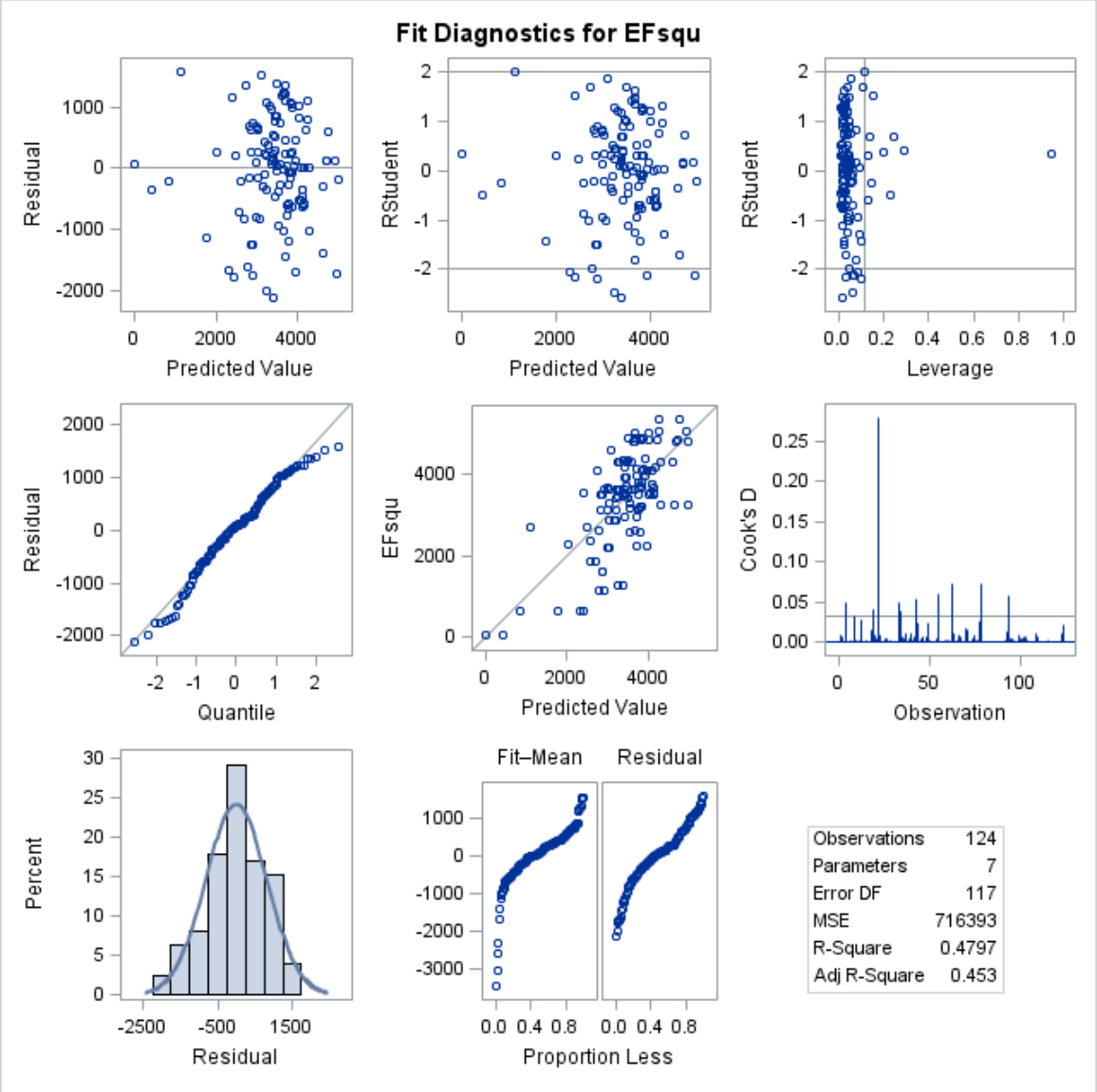

In order to address the non-linearity issue of our data, we decide therefore to apply a polynomial transformation on our "predictors" instead of the response variable. To reach this goal we use Parseal Wilson, which automatically selects the best subset of explanatory variables based on the following criteria: VIF and Adjrq. Parseal Wilson can

apply a “power” transformation on the predictors while adding interaction terms. The presence of a significant interaction (or mix) can indicate that the effect of one predictor variable on the response variable is different at various values of the other predictor variable, which can improve the overall result of our regression analysis. We also decide to add a new variable to the existing set of predictors: “square root of Duration”, as it was recently found by Dr. Pahlevan, that this variable can have some physiological impact on LVEF. Thus, using Parseal Wilson, we set the “mix” feature to 3 (meaning that a new predictor can be built from the interaction of up to 3 variables) and we also set the polynomial power to 2. We generate the following regression formula:

Model 4:

Predicted EF = f(Var1 Var2 Var3 Var4)

Predicted_EF = 196.04722 - (0.00922 * ((BPM1^2) * (SqrtDuration))) - (0.01578 * ((BPM1^2) / (BPM2* Cratio^2))) + (0.02982 * ((BPM1^2) / (BPM2* DF^2))) - (8358.33754 * ((Duration * NodeY) / (NodeX^2))) ;

We obtain therefore 4 explanatory variables in this new model with an intercept of 196.05:

Var1 = ((BPM1.^2) .* (sqrtDuration))

Var2= ((BPM1.^2) ./ (BPM2.* Cratio.^2))

Var3= ((BPM1.^2) ./ (BPM2.* DF.^2))

Var4= ((Duration .* NodeY) ./ (NodeX.^2))

The subsequent results (table 4 and figure 15) show that our regression model is significant (Rsquare=0.62, $p<0.0001$, R(multiple correlation coefficient)=0.79) and its

prediction strength has greatly improved: Adjrq (0.61) has increased and RMSE (7.51) has remained low. Also, according to the below table, almost all predictors show a significant relationship with the response variable. The outlier corresponds to SUBID 156, which has been previously resolved. There is also another outlier, which relates to SUBID 468 (waveform from tonometry carotid_rightside). This outlier adds only 2.55 percent to Rsquare (which is equal to 0.65 without this datapoint) and therefore this datapoint is not very influential. Moreover it displays a Cooks'D value of 0.5989, which is below the threshold of 1 and therefore negligible. We conclude that this datapoint is legitimate and must stay in our database. Table 4 and figure 15 provide more details:

Table 4: LVEF-Model 4

Analysis of Variance – Observations = 124					
Source	**DF**	**Sum of Squares**	**Mean Square**	**F Value**	**Pr > F**
Model	4	11163	2790.72116	49.47	<.0001
Error	119	6712.62529	56.40862		
Corrected Total	123	17876			

Root MSE	7.51057	**R-Square**	0.6245
Dependent Mean	57.45081	**Adj R-Sq**	0.6119
Coeff Var	13.07304		

Parameter Estimates							
Variable	**Label**	**DF**	**Parameter Estimate**	**Standard Error**	**t Value**	**Pr > |t|**	**Variance Inflation**
Intercept	Intercept	**1**	196.04722	17.38359	11.28	<.0001	0
Var1	Var1	**1**	-0.00922	0.00109	-8.45	<.0001	7.25070

Parameter Estimates							
Variable	**Label**	**DF**	**Parameter Estimate**	**Standard Error**	**t Value**	**Pr > |t|**	**Variance Inflation**
Var2	Var2	**1**	-0.01578	0.00268	-5.89	<.0001	3.58954
Var3	Var3	**1**	0.02982	0.00847	3.52	0.0006	5.72223
Var4	Var4	**1**	-8358.33754	1582.36767	-5.28	<.0001	5.23540

Figure 15: Graphs combination related to LVEF-Model 4

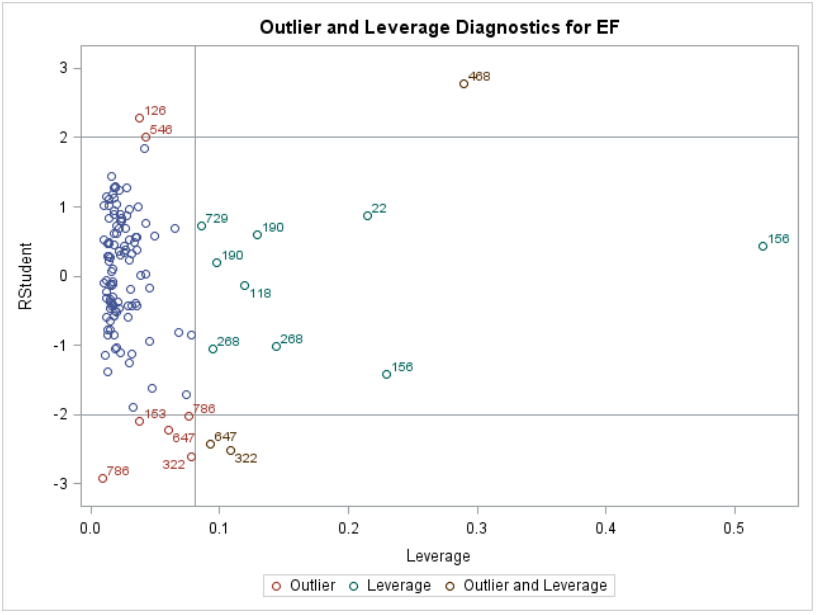

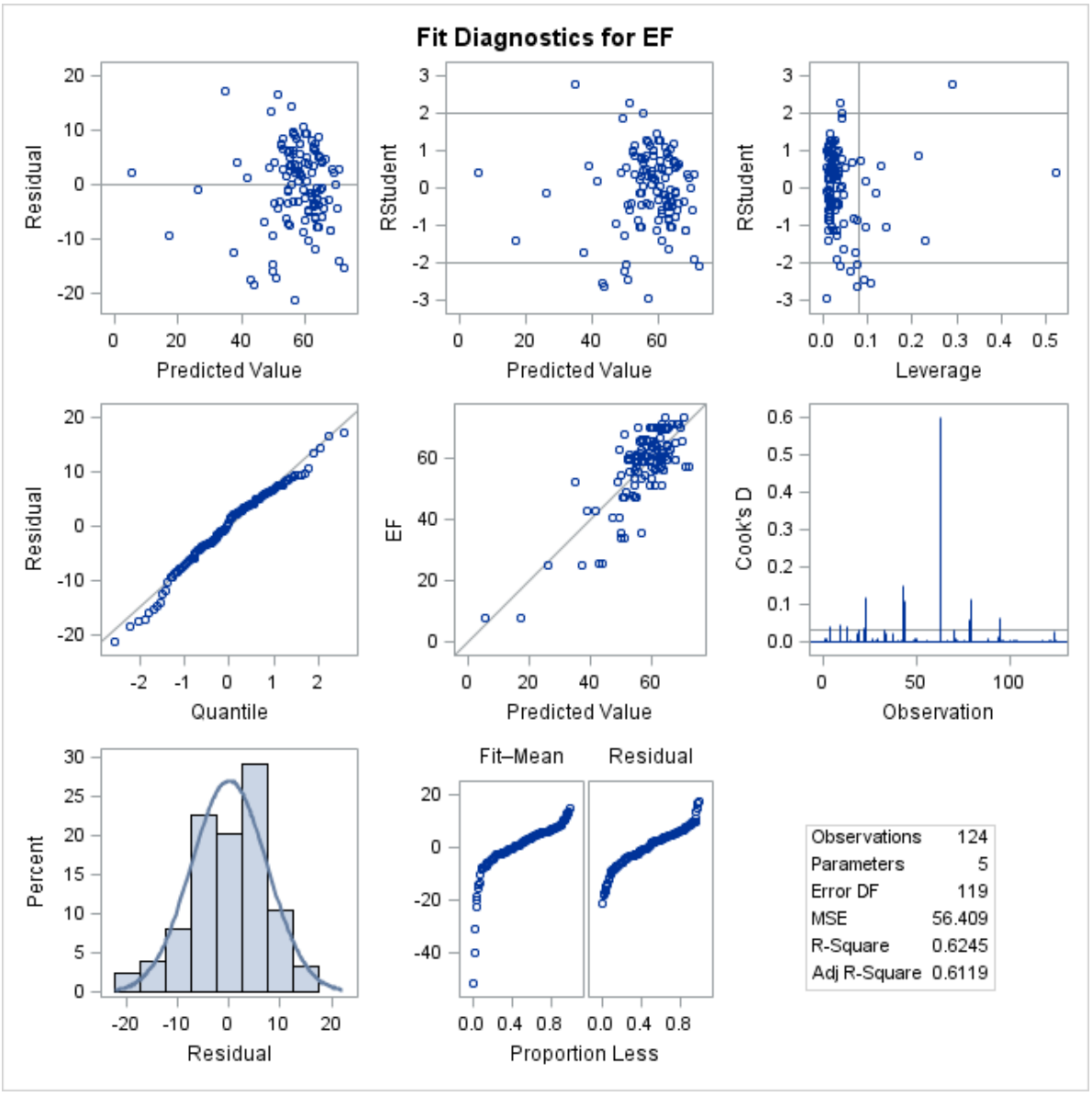
Fit Diagnostics for EF
Residual
Predicted Value
RStudent
Predicted Value
RStudent
Leverage
Residual
Quantile
EF
Predicted Value
Cook's D
Observation
Percent
Residual
Fit–Mean
Residual
Proportion Less
Observations 124
Parameters 5
Error DF 119
MSE 56.409
R-Square 0.6245
Adj R-Square 0.6119

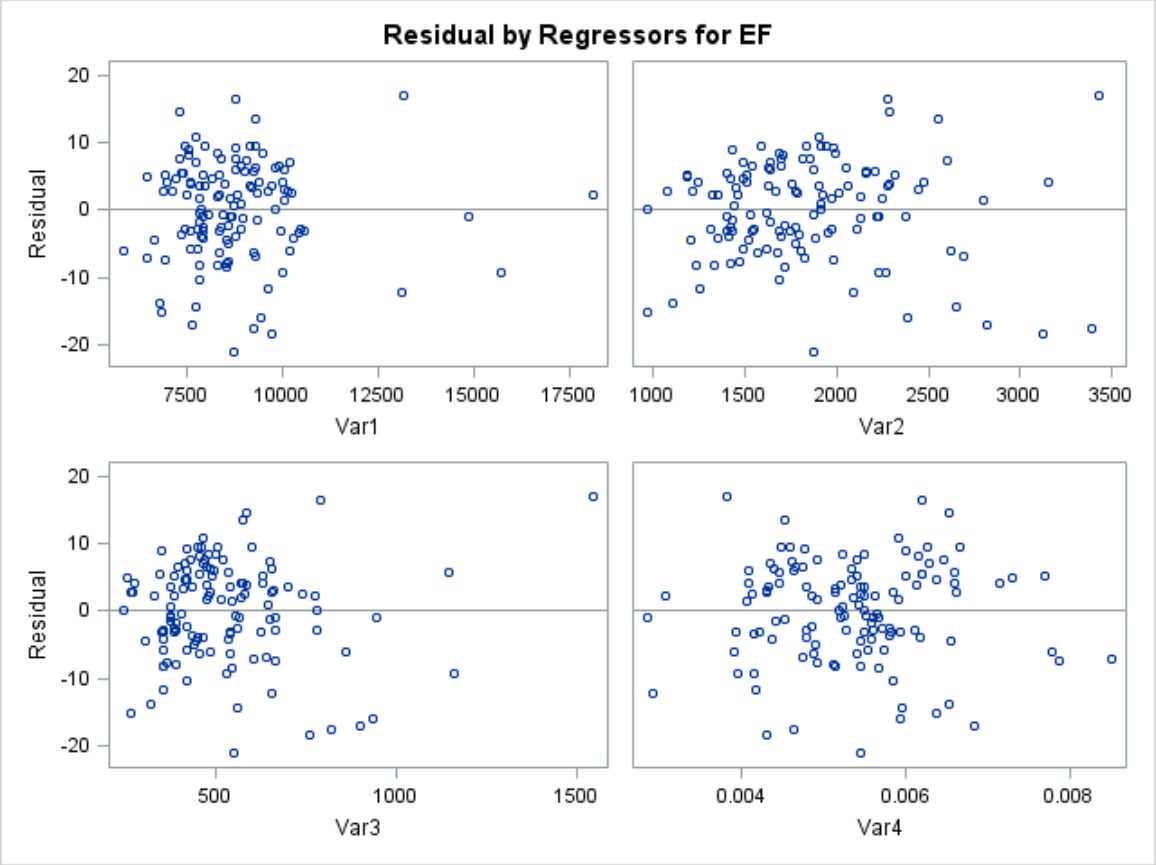

This model presents an overall good fit for our training data. The plotted residuals on figure 15, appear to behave randomly and the QQ plot reveals points that are close to the line, showing no major deviation from the assumption of residuals' normal distribution. Our two methods of measurement are therefore closely related. However, do they "agree"? We use Bland Altman analysis to further evaluate Model 4 and study the agreement between the two techniques.

According to Bland and Altman, a high correlation value does not always guarantee that the two methods are in agreement. The coefficient (r) "reflects the noises and direction" of regression relationship. We can achieve a complete and absolute correlation if all the observations lie along any straight line. For example, we can still have r=1 when we compare two devices even though one device consistently overestimates the other device by a factor of 2. In this situation, we have a perfect correlation but no agreement between the two methods of measurement. The correlation coefficient obtained can thus be improper as it only measures the "degree" of a linear relationship between variables. The coefficient of determination R^2 and Adjusted R^2, being linked to the correlation coefficient are based on a similar concept and are therefore not adequate for evaluating agreements[123].

To investigate if these two methods agree, we review the plot of identity, a simple scatterplot of the two methods along with the line of equality (at 45 degrees to the axes). If the measurements (Y and X) are in basic agreement then the datapoints in the scatterplot would line up close to the line $y = x$

Figure 16: Plot of identity for Model4

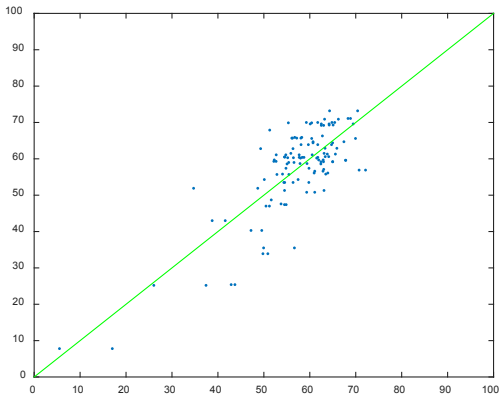

According to the previous graph (figure 16), which displays predicted LVEF versus actual values, the observations lie close to the line of identity, however the plot reveals that a few low LVEF values are not predicted reasonably. Indeed, it seems that there is a wider gap between predicted and actual values concerning low LVEF measures. To assess how far apart all points are, we need to compute the limits of agreement. The 95% LA can be calculated as follow: (mean of diffs) ± 2 * (S.D of diffs). The following graph is obtained using Matlab software:

Figure17: Bland Altman plot for Model 4 – HMRI training set

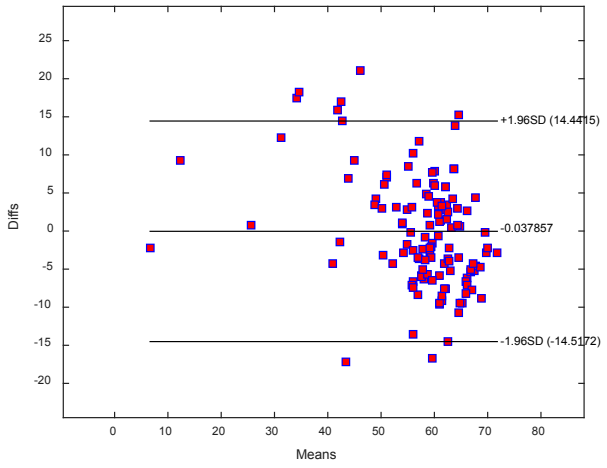

According to the Bland Altman graph, we observe that the bias is very low (-0.04%), meaning that the accuracy of the estimated measurements is adequate. As mentioned earlier, the accuracy shows how close the estimated measurements are to the referenced values. The unbiased limits of agreement are approximately (+/-14.48%), reflecting a narrow range and thus a reasonably good precision. The Percentage Error (PE) is computed as follow:

PE = (1.96*SD Bias/Mean of Standard Method) * 100 = (14.47/57.45081) * 100= 25%.

After performing both regression and Bland Altman analysis on our training database, we can state that these two methods reveal a close relationship and are in good agreement. However, in order to further validate this statement, we test the trained regression equation (Model 4) on two additional databases: FHS_400 and FHS_6500. We specifically need to investigate if our model can predict low LVEF values reasonably and if it produces a low percentage error (PE).

4.1.1.1.2 Testing process:

- FHS_400 (LVEF_IFs versus LVEF_Echo):

Our testing dataset consists of a study panel in which the actual LVEF values are generated via echocardiogram (instead of MRI). This database originally included 400 observations (FHS_400), however many of the actual LVEF values were missing and also a number of waveforms were problematic and had to be filtered before generating IFs values. We obtained 170 "useable" observations. We use this database to test and validate the "trained" regression algorithm obtained with Model 4. We explore the agreement between Model 4 estimates and cardiac Echo measures (our reference method of LVEF evaluation). Bland Altman analysis generates the following results:

Figure 18: Bland Altman and identity plots for Model 4 – FHS_400 testing set

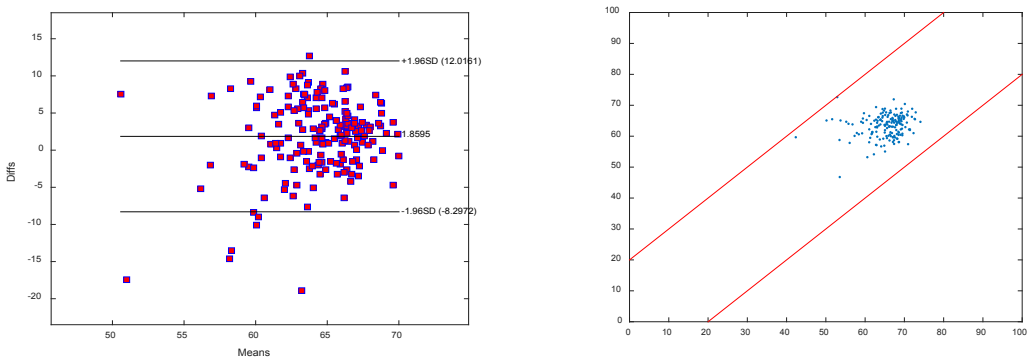

According to Bland Altman plot, after applying the algorithm of Model 4 on the testing dataset, the mean bias (or the average of the differences between the two methods) slightly increases, but remains low. The unbiased limits of agreement are narrow and acceptable, but r drops:

Mean Bias = 1.8595% LA = +/- 10.17 % r=0.19

PE = (1.96SD of Differences/Mean of the reference Method) * 100 = 10.17/63.39 = 16.04%.

- FHS_6500 (LVEF_IFs versus LVEF_Echo)

We test the regression equation of Model 4 on this larger database too. It contains 3,556 useable observations (out of 6500). We obtain the following results:

Bias=1.62% LA = +/- 10.71% r=0.2

PE = 10.71/63.73 = 16.8%

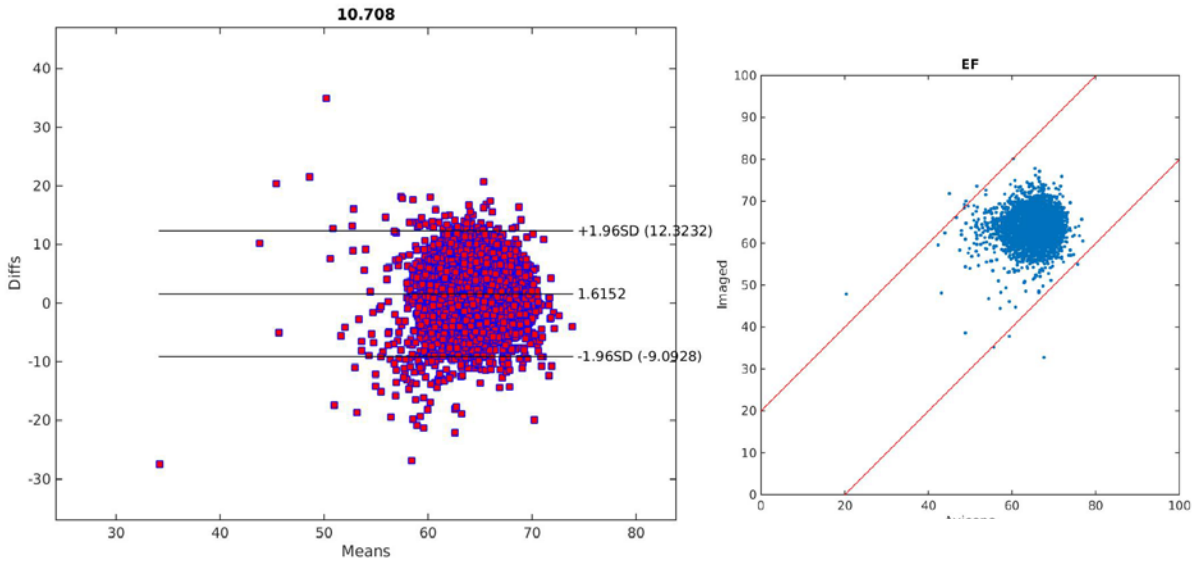

Figure 19: Bland Altman and Identity line for Model 4 – FHS_6500-testing set

These results show that the agreement between the two methods is good, with narrow bands for precision and a low percentage error. However, the correlation coefficient drops. Also, from the line of identity plot, we can observe that some of the low LVEF values are still estimated unreasonably. These results are thus not conclusive.

4.1.1.2 Estimations (from IFs_iPhone) compared to actual values

In the above section, we estimated LVEF from IFs method based on "pressure wave signals obtained from Tonometry". In this section, we perform a similar analysis but with different datasets. Our training set is based on HMRI database and IFs core values are derived from: Tonometry, iPhone and Cardius. Our testing set is also based on HMRI database, but IFs values are derived from wave signals exclusively captured from "iPhone" device.

4.1.1.2.1 Training process – Modeling the relation between EF_iPhone and EF_MRI

This training set consists of 82 observations from HMRI database which, includes IFs and heart shape factors simultaneously extracted from pressure waves via Tonometry, iPhone and Cardius devices. We use this set of data to train the best fit model based on VIF and Adjrq criteria. The actual LVEF values are generated via MRI. We obtain the following results:

Model 1: LVEF = f(BPM1 BPM2 Duration Envratio DF)

Table 5: LVEF-iPhone-Model 1

Analysis of Variance – Obs =82					
Source	**DF**	**Sum of Squares**	**Mean Square**	**F Value**	**Pr > F**

Analysis of Variance – Obs =82					
Source	**DF**	**Sum of Squares**	**Mean Square**	**F Value**	**Pr > F**
Model	5	5158.53706	1031.70741	11.88	<.0001
Error	76	6598.28014	86.81948		
Corrected Total	81	11757			

Root MSE	9.31770	**R-Square**	0.4388
Dependent Mean	57.84024	**Adj R-Sq**	0.4018
Coeff Var	16.10937		

Parameter Estimates							
Variable	**Label**	**DF**	**Parameter Estimate**	**Standard Error**	**t Value**	**Pr > |t|**	**Variance Inflation**
Intercept	Intercept	**1**	149.52612	27.94455	5.35	<.0001	0
DF	DF	**1**	8.96062	14.93199	0.60	0.5502	3.19206
Duration	Duration	**1**	-15.90961	9.72912	-1.64	0.1061	2.90363
BPM1	BPM1	**1**	-0.76450	0.12093	-6.32	<.0001	1.74974
BPM2	BPM2	**1**	0.09251	0.08354	1.11	0.2716	2.67880
EnvRatio	EnvRatio	**1**	-4.96299	2.87286	-1.73	0.0881	3.35461

Figure 20: Graphs Combination related to LVEF iPhone– Model 1

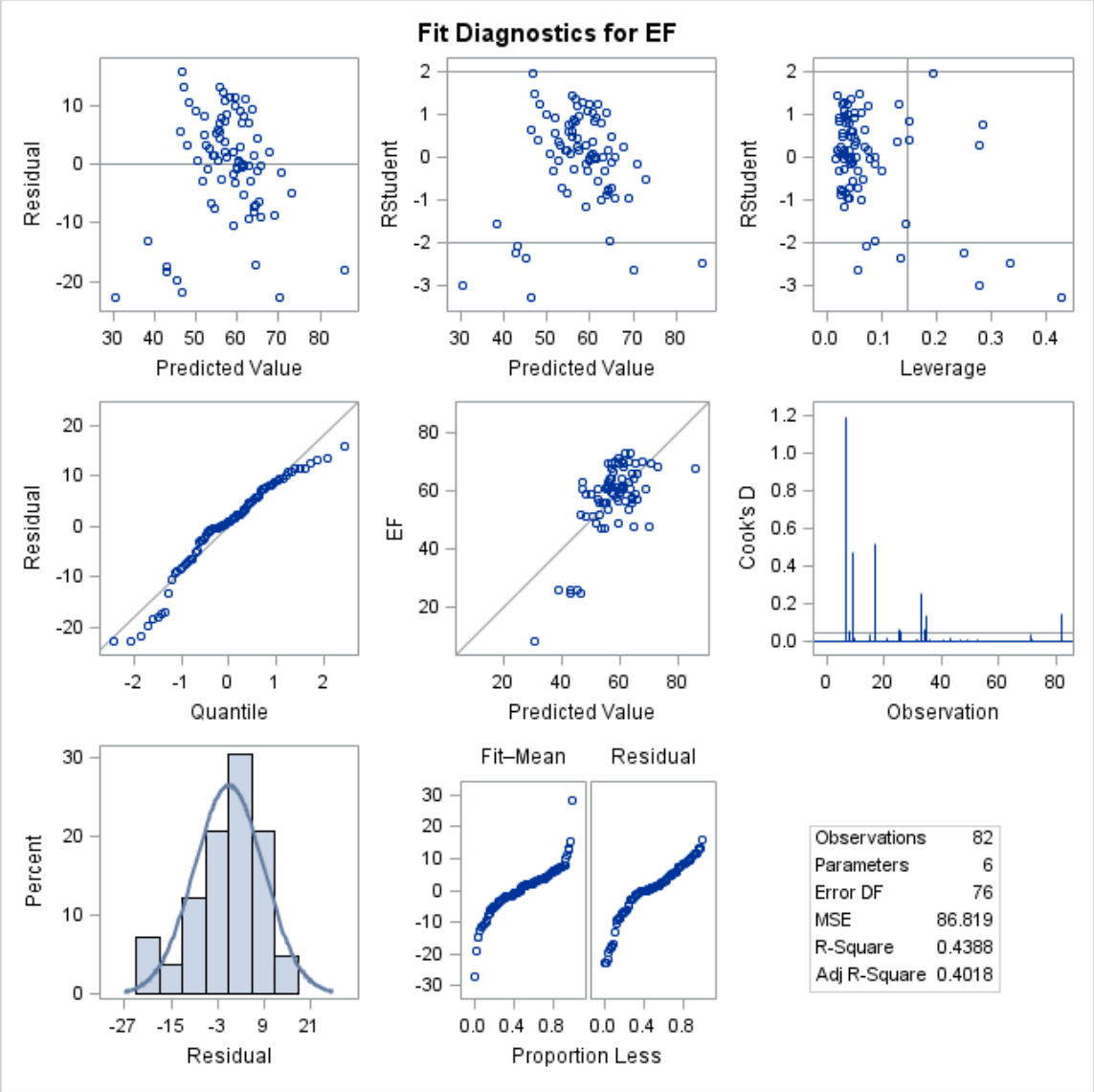

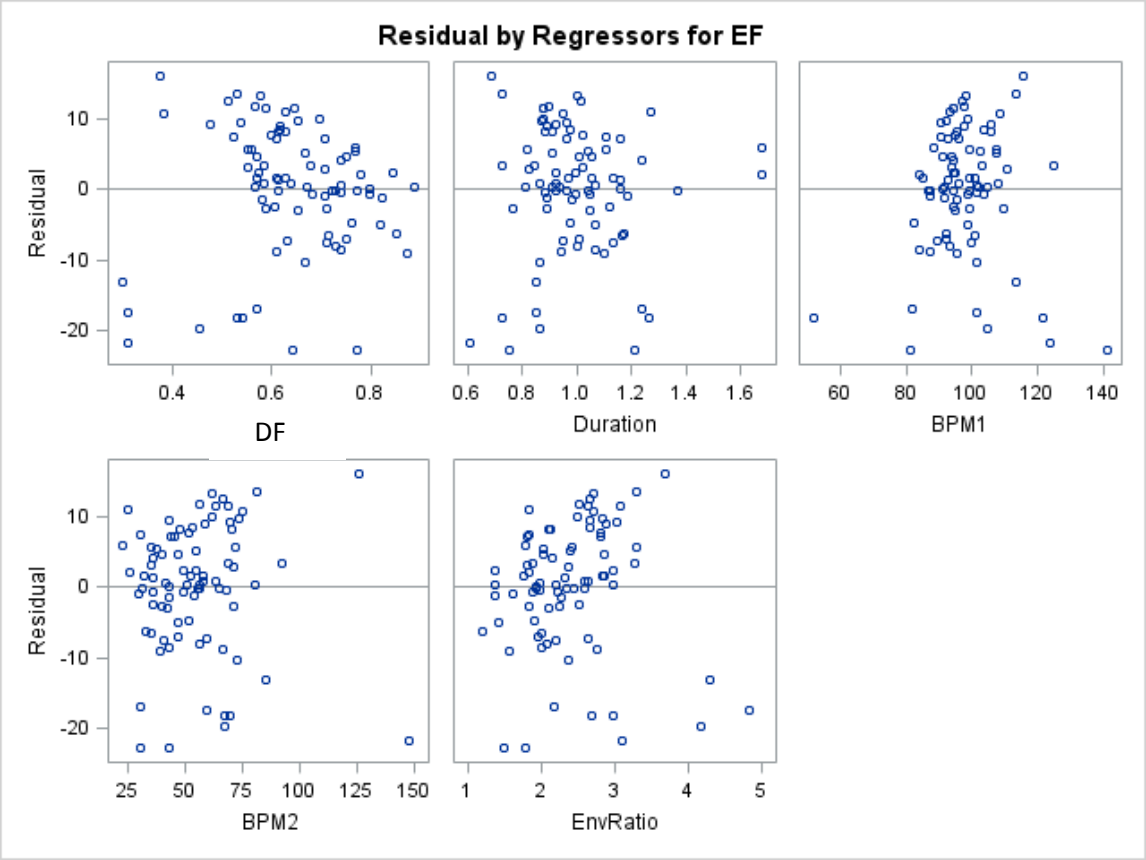

According to the above results, the overall relationship is moderately high and significant (R=0.66, Rsquare=0.44, p<0.0001) with an Adjrq of 0.4. The plots of residuals (elements of variation unexplained by the fitted model) show a relatively random pattern. However, this model needs to be improved because the related QQ plot reveals a small deviation from the assumption of normal distribution of residuals. Indeed, there is some departure from the diagonal line. There is also an outlier which needs to be further investigated. It corresponds to SUBID 95. Thus, in order to obtain an overall better model, we use Parseal Wilson with a selection based on VIF and Adjrq. We also include two additional explanatory variables, called Omega1Bar and Omega2Bar, which are variations of BPM1 and BPM2. Indeed Omega1Bar= BPM1 *

Dicrotic Notch and Omega2Bar = BPM2 * (Duration – Dicrotic Notch). With additional research, we noticed that the use of these two variables could enhance the regression model. Parseal Wilson produced a few models, among which the regression model 2 (Mix 1, Power1) generated the best results (table 6, figure 21).

Model 2 equation:

Predicted LVEF = 326.55832 - 0.74613 BPM1 - 3.76920 Omega1Bar + 0.13117 Omega2Bar -10.63547 EnvRatio - 35.01137 Duration - 19.76155 DF - 0.31504 NodeY;

Model2:

LVEF = f(BPM1 Omega1Bar Omega2Bar NodeY DF Duration Envratio)

Table 6: LVEF-iPhone-Model 2

Analysis of Variance – Obs = 82					
Source	**DF**	**Sum of Squares**	**Mean Square**	**F Value**	**Pr > F**
Model	7	5911.48853	844.49836	10.69	<.0001
Error	74	5845.32867	78.99093		
Corrected Total	81	11757			

Root MSE	8.88768	**R-Square**	0.5028
Dependent Mean	57.84024	**Adj R-Sq**	0.4558
Coeff Var	15.36592		

Parameter Estimates							
Variable	**Label**	**DF**	**Parameter Estimate**	**Standard Error**	**t Value**	**Pr > |t|**	**Variance Inflation**
Intercept	Intercept	**1**	326.55832	74.45140	4.39	<.0001	0
NodeY	NodeY	**1**	-0.31504	0.29197	-1.08	0.2841	8.33766

Parameter Estimates							
Variable	**Label**	**DF**	**Parameter Estimate**	**Standard Error**	**t Value**	**Pr > |t|**	**Variance Inflation**
DF	DF	**1**	-19.76155	17.89146	-1.10	0.2729	5.03694
Duration	Duration	**1**	-35.01137	16.26785	-2.15	0.0346	8.92268
BPM1	BPM1	**1**	-0.74613	0.11845	-6.30	<.0001	1.84485
EnvRatio	EnvRatio	**1**	-10.63547	3.41104	-3.12	0.0026	5.19790
Omega1Bar	Omega1Bar	**1**	-3.76920	1.84223	-2.05	0.0443	2.88594
Omega2Bar	Omega2Bar	**1**	0.13117	0.22762	0.58	0.5662	2.60447

Figure 21: Graphs Combination related to LVEF-iPhone-Model 2

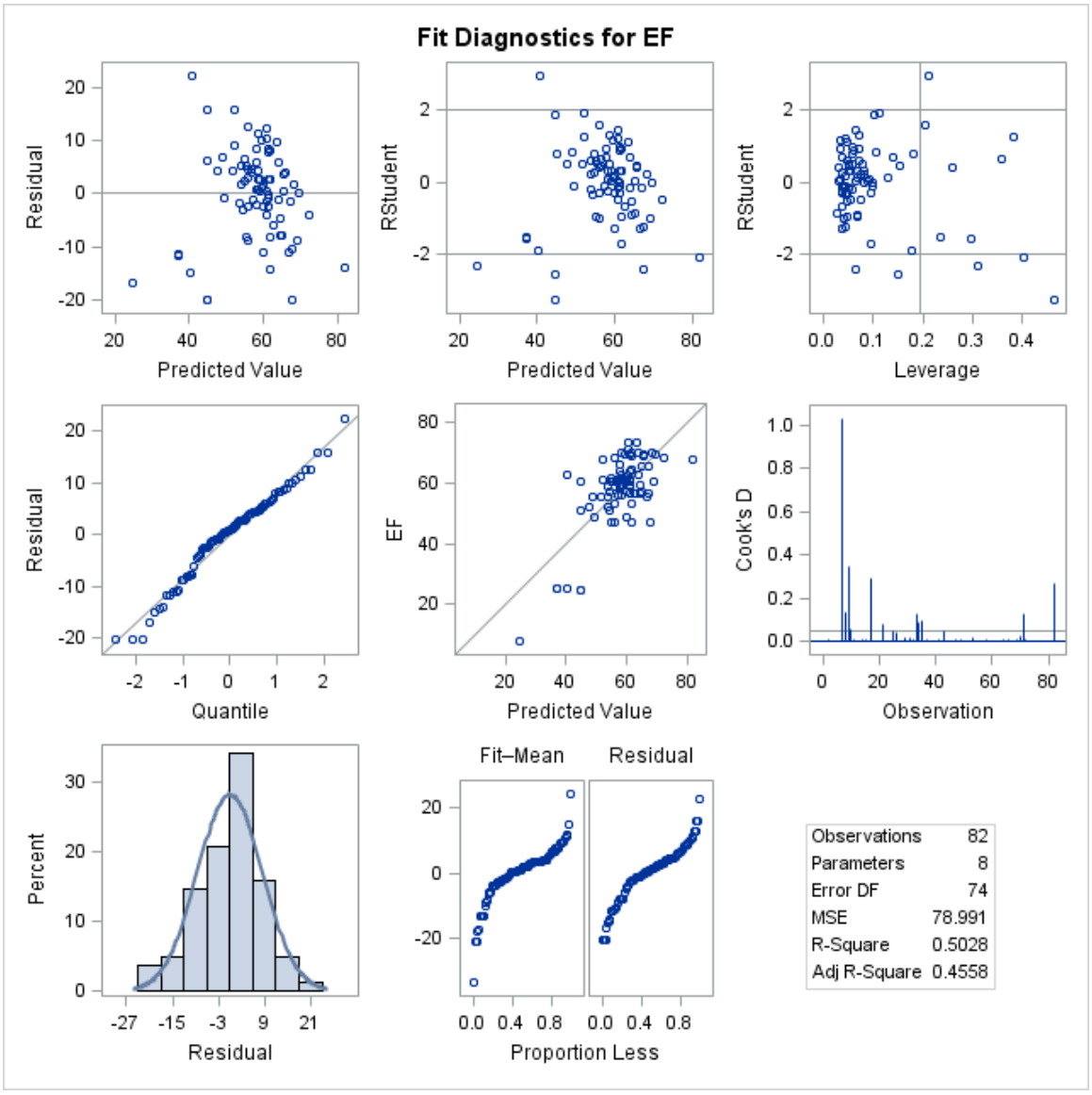

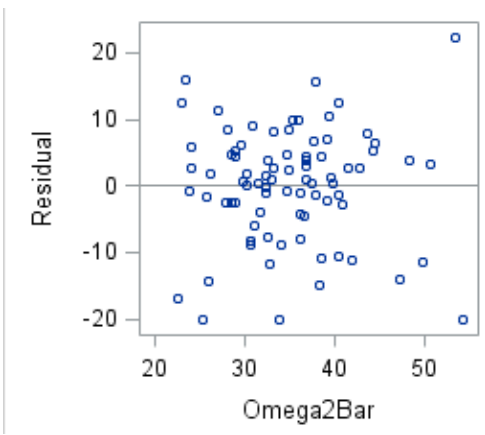

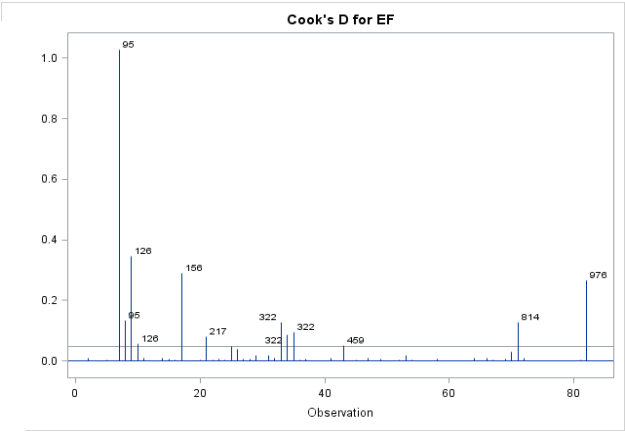

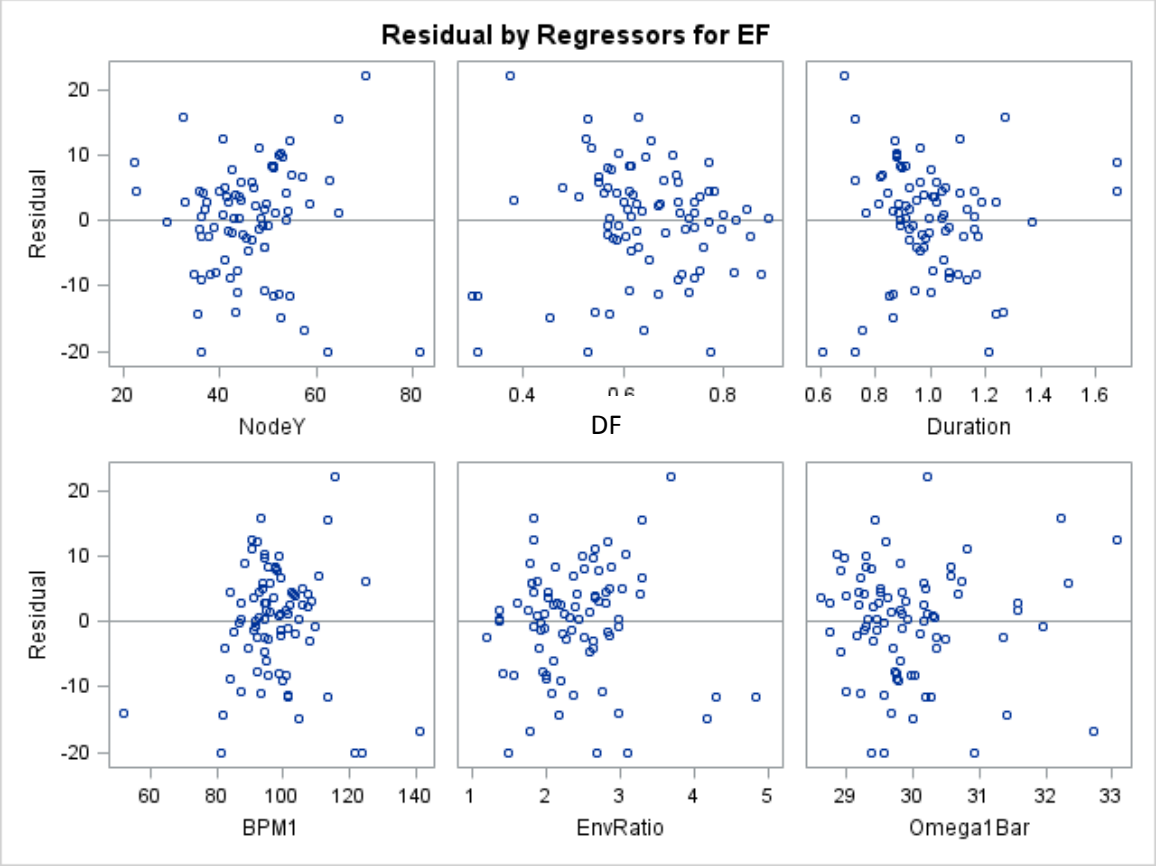

This model seems to be a better fit for our iPhone data. Indeed, according to table 6 and figure 21, Adjrq value increases from 0.4 to 0.46 and RMSE drops to 8.89. QQ-plot improves too, showing data points that are marked closer to the diagonal line. We still need to check the outlier, which corresponds to SUBID 95. This data point is related to the waveforms obtained from Cardius device (right carotid). The removal of this outlier does not have a large impact on Rsquare value. Indeed, it slightly increases its value from 0.5 to 0.5215 and RMSE (8.35) remains approximately the same. Further analysis of this observation reveals that it corresponds to a high Omega2Bar value,

however it is not a defective point. Since the related Cooks'D value is almost equal to 1, we decide to keep this point in our analysis. This model seems overall reasonable, however many variables are not significantly related to our response variable. Perhaps a few of these predictors can be removed without impacting the overall regression results. We proceed to a variable dimension reduction. Since the residual plots corresponding to NodeY and Duration show a slight funnel distribution and the VIF values for both NodeY and Duration are close to the threshold number, we decide to exclude NodeY and Duration. We thus obtain a reduced version of Model 2, which generates the following results:

Model 3: LVEF = f(BPM1 Omega1Bar DF Envratio)

Table 7: LVEF-iPhone-Model 3

Analysis of Variance Obs = 82					
Source	**DF**	**Sum of Squares**	**Mean Square**	**F Value**	**Pr > F**
Model	4	5275.35704	1318.83926	15.67	<.0001
Error	77	6481.46015	84.17481		
Corrected Total	81	11757			

Root MSE	9.17468	**R-Square**	0.4487
Dependent Mean	57.84024	**Adj R-Sq**	0.4201
Coeff Var	15.86211		

Parameter Estimates							
Variable	**Label**	**DF**	**Parameter Estimate**	**Standard Error**	**t Value**	**Pr > |t|**	**Variance Inflation**

Parameter Estimates							
Variable	**Label**	**DF**	**Parameter Estimate**	**Standard Error**	**t Value**	**Pr > |t|**	**Variance Inflation**
Intercept	Intercept	**1**	291.90163	58.10555	5.02	<.0001	0
BPM1	BPM1	**1**	-0.53779	0.09525	-5.65	<.0001	1.11943
Omega1Bar	Omega1Bar	**1**	-4.85132	1.46927	-3.30	0.0015	1.72264
DF	DF	**1**	-21.34073	17.44237	-1.22	0.2249	4.49243
EnvRatio	EnvRatio	**1**	-9.40723	3.46082	-2.72	0.0081	5.02120

Figure 22: Graphs Combination related to LVEF-iPhone-Model 3

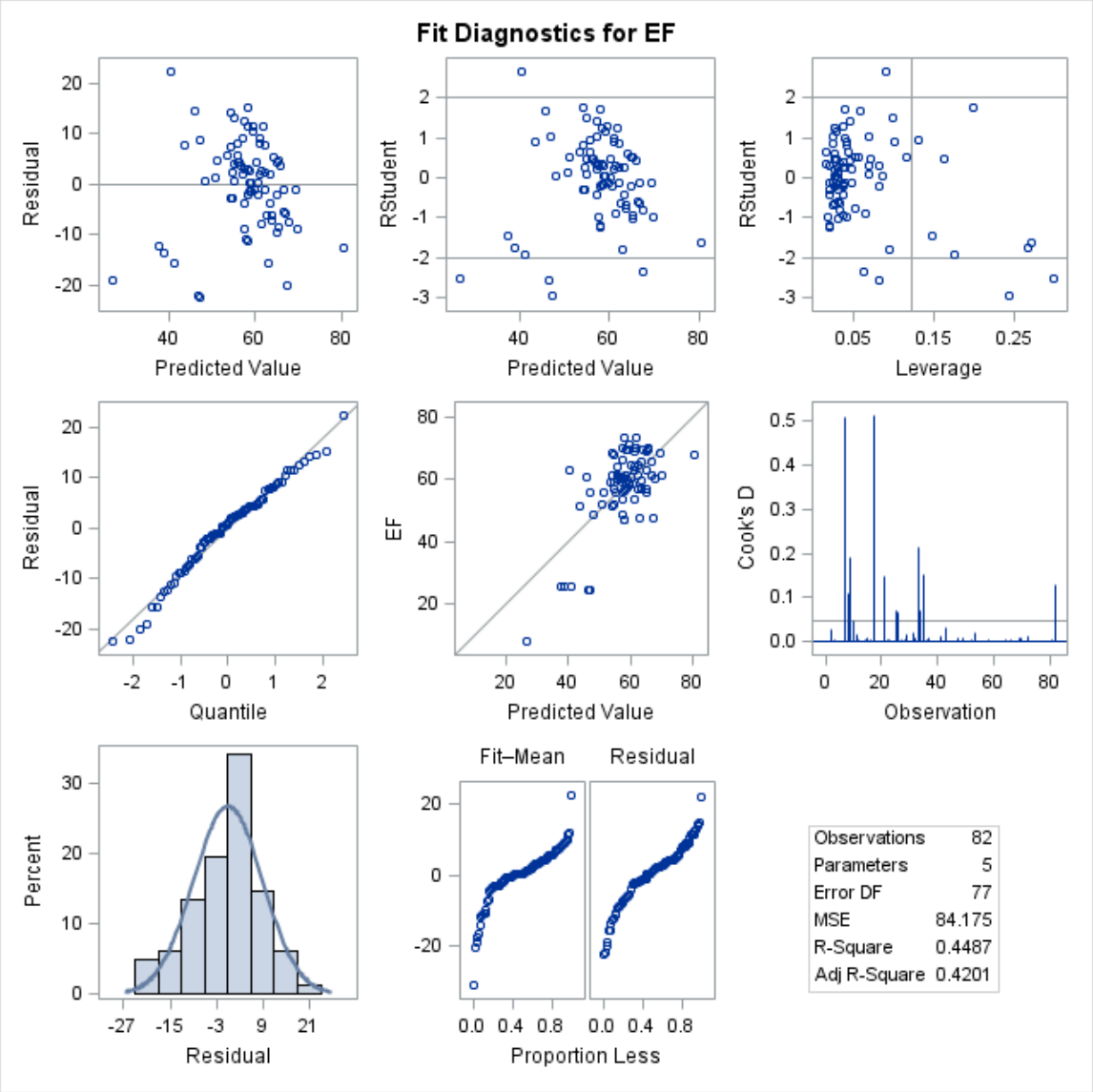

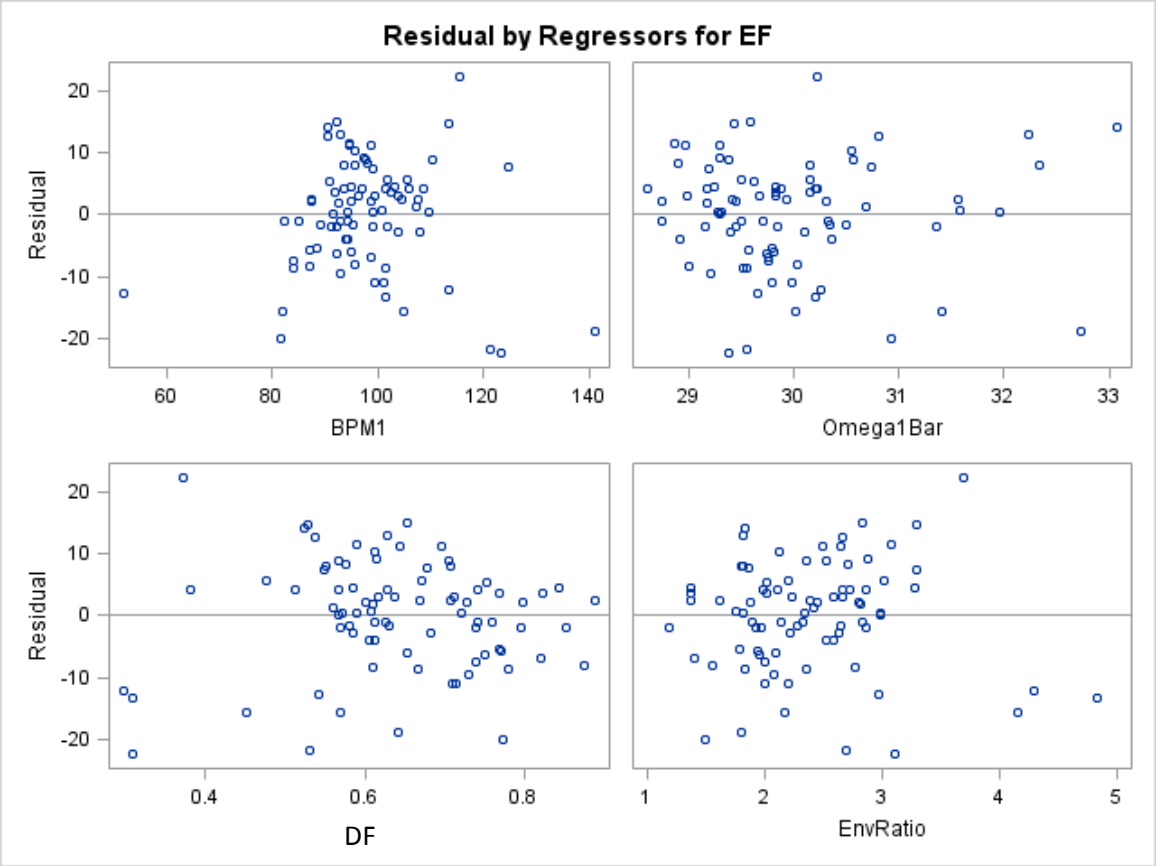

We notice that this reduced version slighly drops Adjrq from 0.46 to 0.42. However, it is a simplified model and shows improved values for standard errors of most coefficients (table 7). Residual plots show random distributions and all VIF values are much smaller. There are no major influential outliers and QQ-plot is fairly adequate (figure 22).

Aside from this model, we decide to review Model 2 and eliminate the variables generating low P-values. We obtain the below results:

Model 4: LVEF = f(BPM1 Omega1Bar Envratio Duration)

Table 8: LVEF-iPhone-Model 4

Analysis of Variance - Obs =82					
Source	**DF**	**Sum of Squares**	**Mean Square**	**F Value**	**Pr > F**
Model	4	5693.53882	1423.38470	18.08	<.0001
Error	77	6063.27838	78.74388		
Corrected Total	81	11757			

Root MSE	8.87377	**R-Square**	0.4843
Dependent Mean	57.84024	**Adj R-Sq**	0.4575
Coeff Var	15.34187		

Parameter Estimates							
Variable	**Label**	**DF**	**Parameter Estimate**	**Standard Error**	**t Value**	**Pr > |t|**	**Variance Inflation**
Intercept	Intercept	**1**	267.63997	38.24557	7.00	<.0001	0
BPM1	BPM1	**1**	-0.70049	0.11464	-6.11	<.0001	1.73368
EnvRatio	EnvRatio	**1**	-7.16875	1.74327	-4.11	<.0001	1.36189
Omega1Bar	Omega1Bar	**1**	-3.48653	1.20066	-2.90	0.0048	1.22969
Duration	Duration	**1**	-19.81013	7.53566	-2.63	0.0103	1.92061

Figure 23: Graphs Combination related to LVEF-iPhone-Model 4

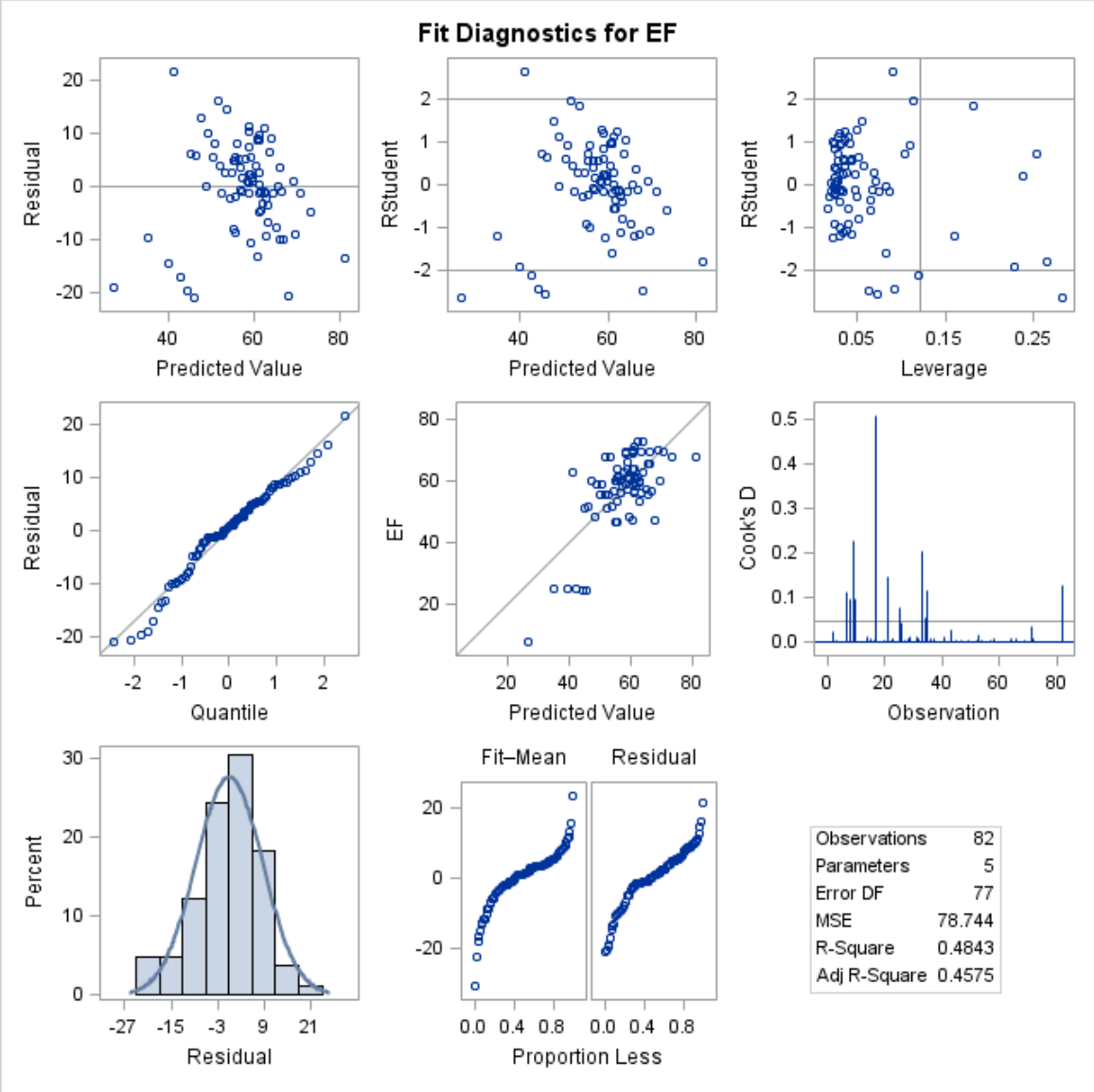

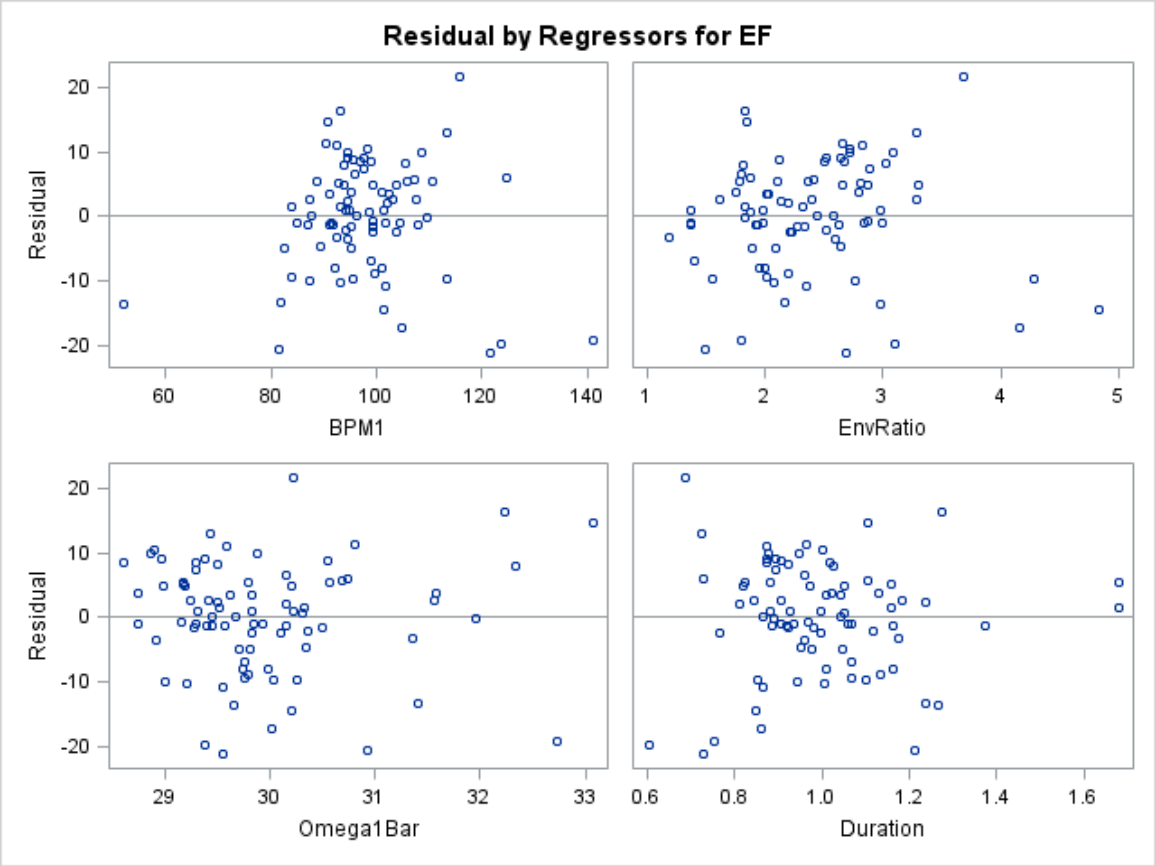

As per the above table and results, we can notice that in this simplified model, Adjrq increases again to 0.46. This value is approximately equal to the one generated for Model 2 (table 6), however fewer predictors are involved, leading to a simpler model. We observe that EnvRatio becomes significantly related to the response variable (table 8). All residual plots are adequate (figure 23).

In conclusion, the trained Models 2, 3 and 4, they all display a moderately strong relationship between the response variable and the predictors, but they need to be tested

on a new database. Indeed, we need to find out if these results hold in real world and if our models can predict LVEF values with low percentage error.

4.1.1.2.2 Testing process:

The HMRI testing database includes 64 observations generated from pressure waveforms captured via iPhone device only. It also has actual LVEF values from MRI. We run a Bland Altman analysis to test our three trained models and explore which equation produces a better agreement:

Testing Model 2

According to the below graph, the mean bias or the average of the differences between the two methods is relatively low and the unbiased limits of agreement are narrow:

Mean bias = 1.763% LA = +/- 17.44% r=0.79 p<0.0001

PE = (17.44/55.83) * 100 =31.2%

IFs results seem thus fairly good. The narrow range for the limits of agreement reveals the moderately high precision of IFs measures. However, we observe that there are a few low LVEF observations that are not estimated reasonably (figure 24 and 25)

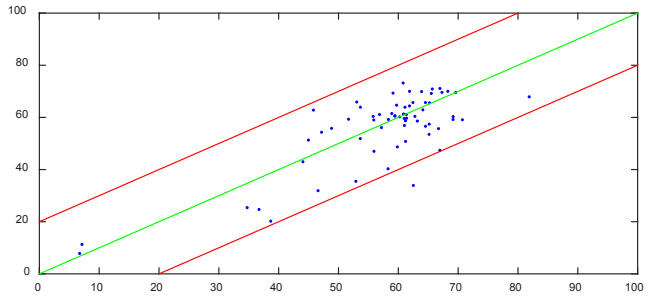

Figure 24: Identity line for LVEF-iPhone-Model 2 –HMRI test set

Figure 25: Bland Altman for LVEF-iPhone- Model 2 –HMRI test set

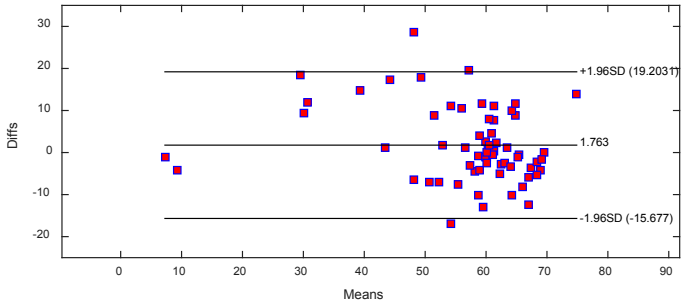

Testing Model 3:

This model involves 4 predictors only. We notice that the mean bias has improved, showing a better accuracy (figure 26). The precision of the measurements has slightly degraded. The unbiased limits of agreement have increased from 17.44 to 18.53, revealing a modest change from the previous model:

Mean bias = 1.1378% L.A=+/- 18.53 %

PE = (18.53/55.83) * 100 =33.2% r=0.76 p<0.0001

Figure 26: Bland Altman and Identity line for LVEF-iPhone- Model 3 –HMRI test set

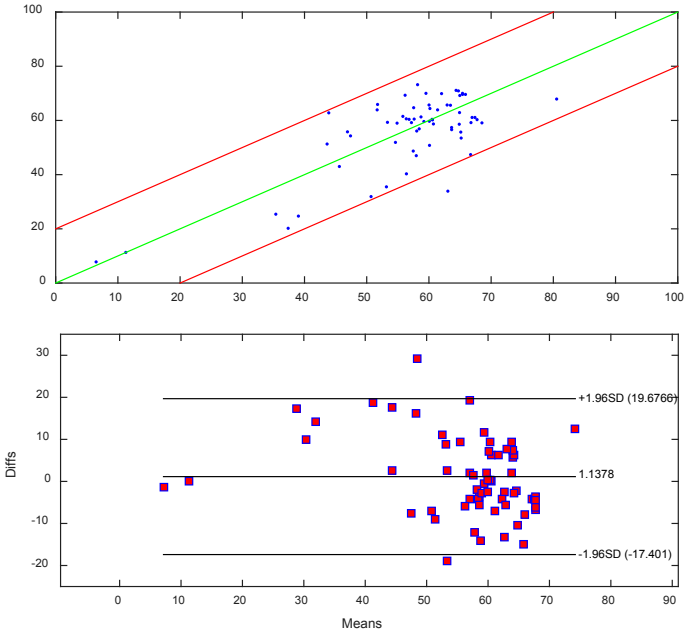

Testing Model 4:

This reduced model includes 4 predictors too. The Bland Altman analysis produces the following results:

Mean Bias= 2.19% L.A = +/- 18.2% PE = 18.2/55.83=32.59% r=0.76

p<0.0001

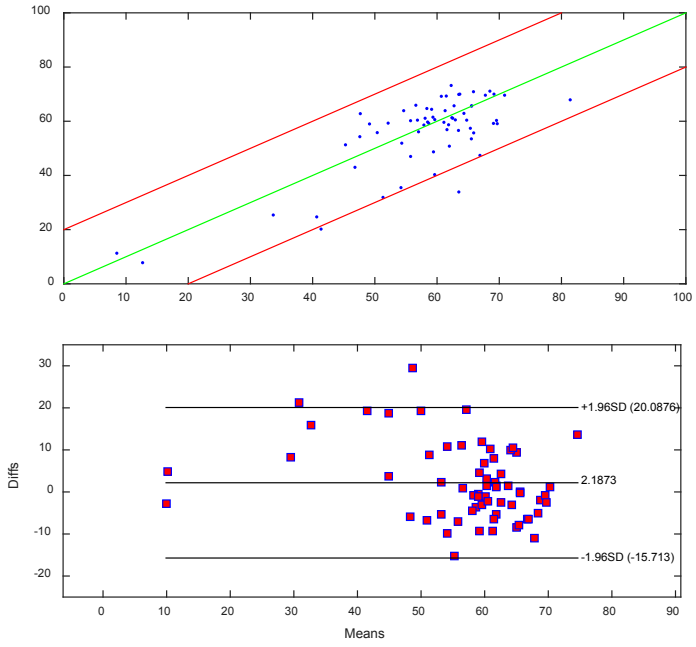

Figure 27: Bland Altman and Identity line for LVEF-iPhone-Model 4 –HMRI Test set

4.1.2 Data analysis: Estimating CO with IFs methodology

With IFs methodology, we can also produce estimates of CO. We use the same HMRI training database that we used for LVEF, which has 124 observations and IFs derived from tonometry waveforms. The actual values of CO are generated from MRI. We first run a scatterplot matrix to have an overall picture of the existing relationships between all variables. The following graph features the related results:

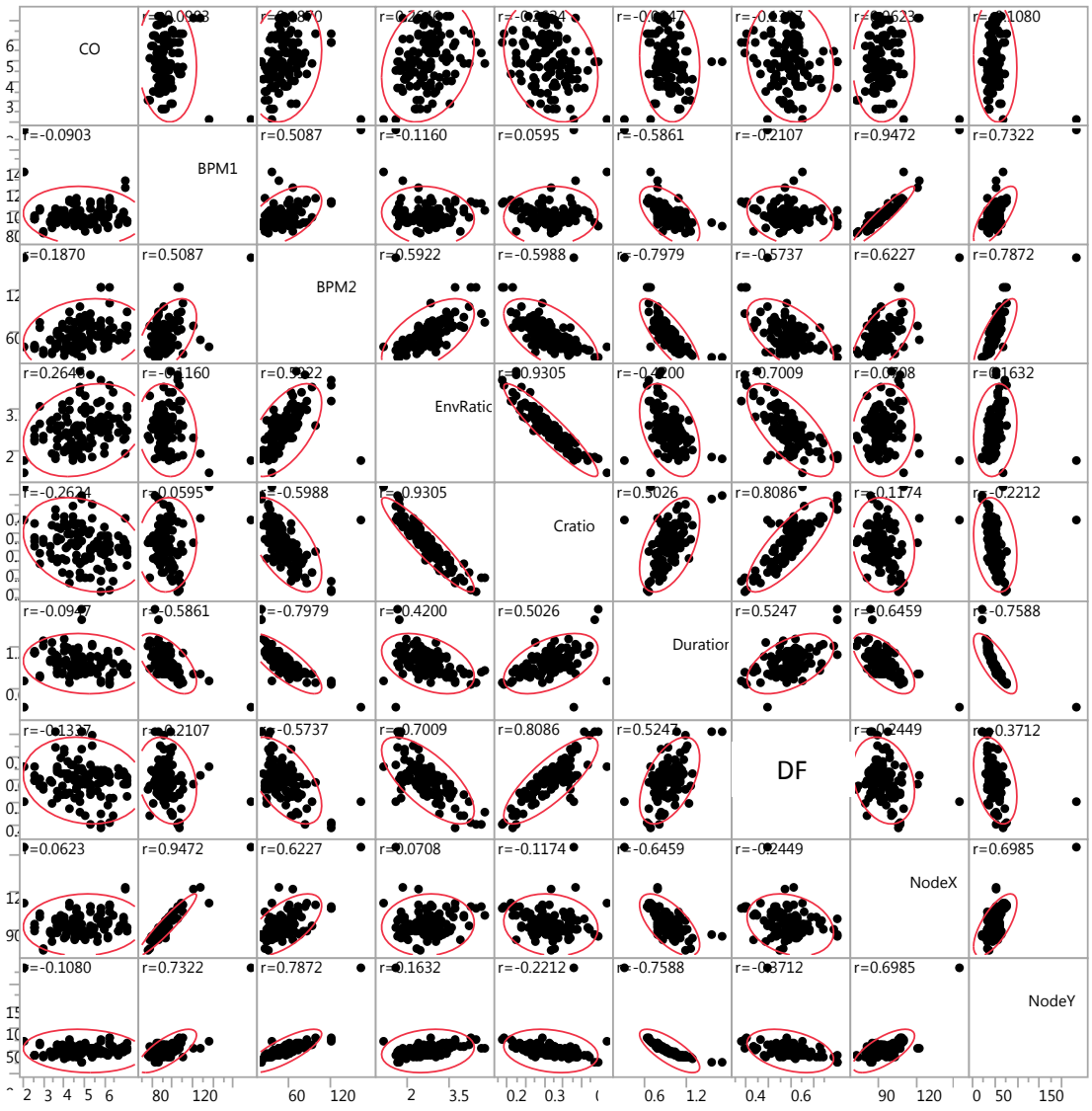

Figure 28: Scatterplot Matrix for CO

According to the above matrix, most of the variables can contribute to some degree to regression equation that we are investigating. We can notice again that BPM1 and NodeX are closely related (figure 28). Thus, in order to avoid multicollinearity, we decide to perform a multiple regression analysis based on VIF criterion. We also choose

our model based on Adjrq to minimize noise. We generate the following preliminary results:

Model 1: CO=f(BPM1 BPM2 NodeY DF Duration EnvRatio)

Table 9: CO-Model 1

Analysis of Variance Obs = 124					
Source	**DF**	**Sum of Squares**	**Mean Square**	**F Value**	**Pr > F**
Model	6	39.78044	6.63007	5.41	<.0001
Error	117	143.28325	1.22464		
Corrected Total	123	183.06369			

Root MSE	1.10664	**R-Square**	0.2173
Dependent Mean	4.98761	**Adj R-Sq**	0.1772
Coeff Var	22.18769		

Parameter Estimates							
Variable	**Label**	**DF**	**Parameter Estimate**	**Standard Error**	**t Value**	**Pr > |t|**	**Variance Inflation**
Intercept	Intercept	**1**	6.30545	2.86387	2.20	0.0296	0
BPM1	BPM1	**1**	0.00221	0.01417	0.16	0.8764	2.82300
BPM2	BPM2	**1**	0.04574	0.01216	3.76	0.0003	6.96768
NodeY	NodeY	**1**	-0.05131	0.01176	-4.36	<.0001	5.45133
DF	DF	**1**	0.01690	1.97193	0.01	0.9932	2.45251
Duration	Duration	**1**	-0.83420	1.05159	-0.79	0.4292	3.44433
EnvRatio	EnvRatio	**1**	-0.22957	0.31278	-0.73	0.4644	4.51941

Figure 29: Graphs Combination related **to** CO-Model 1

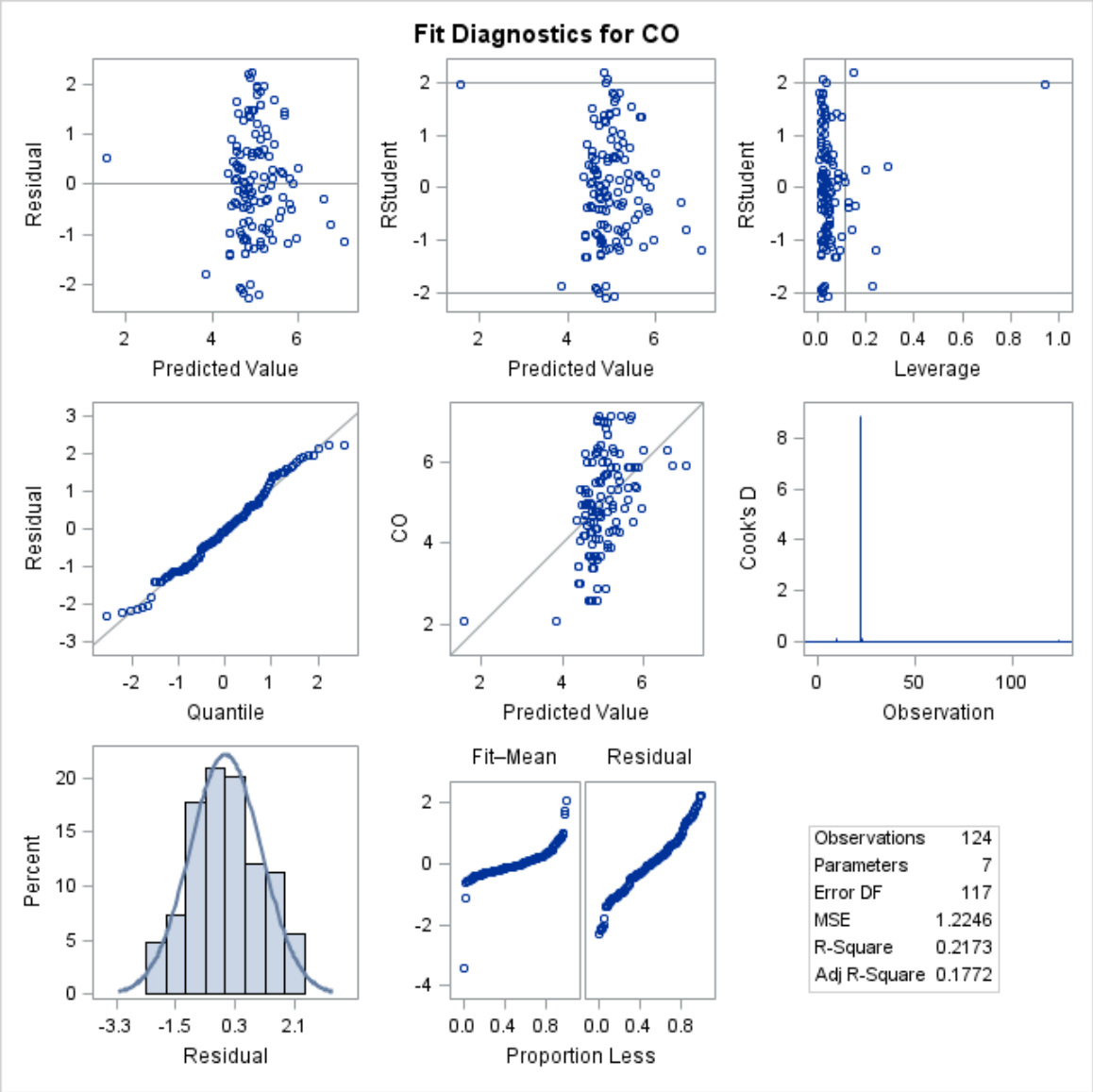

These preliminary results indicate that the model needs improvement. The Cooks D plot reveals an important influential point with a value over 8. With further investigation we find that this data-point corresponds to SUBID 156, which has a very low LVEF value. Since this model generates a very small Rsquare, in order to enhance the correlation among the response and explanatory variables, we decide to add new

predictors such as Omega1Bar and Omega2Bar, which as we mentioned previously are variations of BPM1 and BPM2. We run a pairwise analysis between these two predictors and CO to evaluate their correlation (table 10):

Table 10: correlation between Omega1Bar, Omega2Bar and CO

Pearson r	CO	Omega1Bar	Omega2Bar
CO	1.0000	-0.4288	0.4617
Omega1Bar	-0.4288	1.0000	-0.6835
Omega2Bar	0.4617	-0.6835	1.0000

Both Omega1Bar and Omega2Bar show a moderate correlation with CO, thus we re-perform a regression analysis including these two variables and obtain the following results (table 11):

Model 2 CO = f(Omega1Bar Omega2Bar NodeX DF Duration EnvRatio)

Table 11: CO_Model2

Analysis of Variance – Obs=124					
Source	**DF**	**Sum of Squares**	**Mean Square**	**F Value**	**Pr > F**
Model	6	49.76762	8.29460	7.28	<.0001
Error	117	133.29606	1.13928		
Corrected Total	123	183.06369			

Root MSE	1.06737	**R-Square**	0.2719
Dependent Mean	4.98761	**Adj R-Sq**	0.2345
Coeff Var	21.40046		

Parameter Estimates							
Variable	**Label**	**DF**	**Parameter Estimate**	**Standard Error**	**t Value**	**Pr > |t|**	**Variance Inflation**

Parameter Estimates							
Variable	**Label**	**DF**	**Parameter Estimate**	**Standard Error**	**t Value**	**Pr > |t|**	**Variance Inflation**
Intercept	Intercept	**1**	20.19265	6.72911	3.00	0.0033	0
NodeX	NodeX	**1**	-0.00239	0.01363	-0.18	0.8610	2.07693
Omega1Bar	Omega1Bar	**1**	-0.42272	0.15434	-2.74	0.0071	3.24793
Omega2Bar	Omega2Bar	**1**	0.07660	0.02758	2.78	0.0064	3.22594
DF	DF	**1**	-3.93479	2.28149	-1.72	0.0872	3.52893
Duration	Duration	**1**	-0.20832	0.85630	-0.24	0.8082	2.45496
EnvRatio	EnvRatio	**1**	-0.76549	0.33218	-2.30	0.0230	5.47929

Figure 30: Graphs Combination related to CO_Model 2

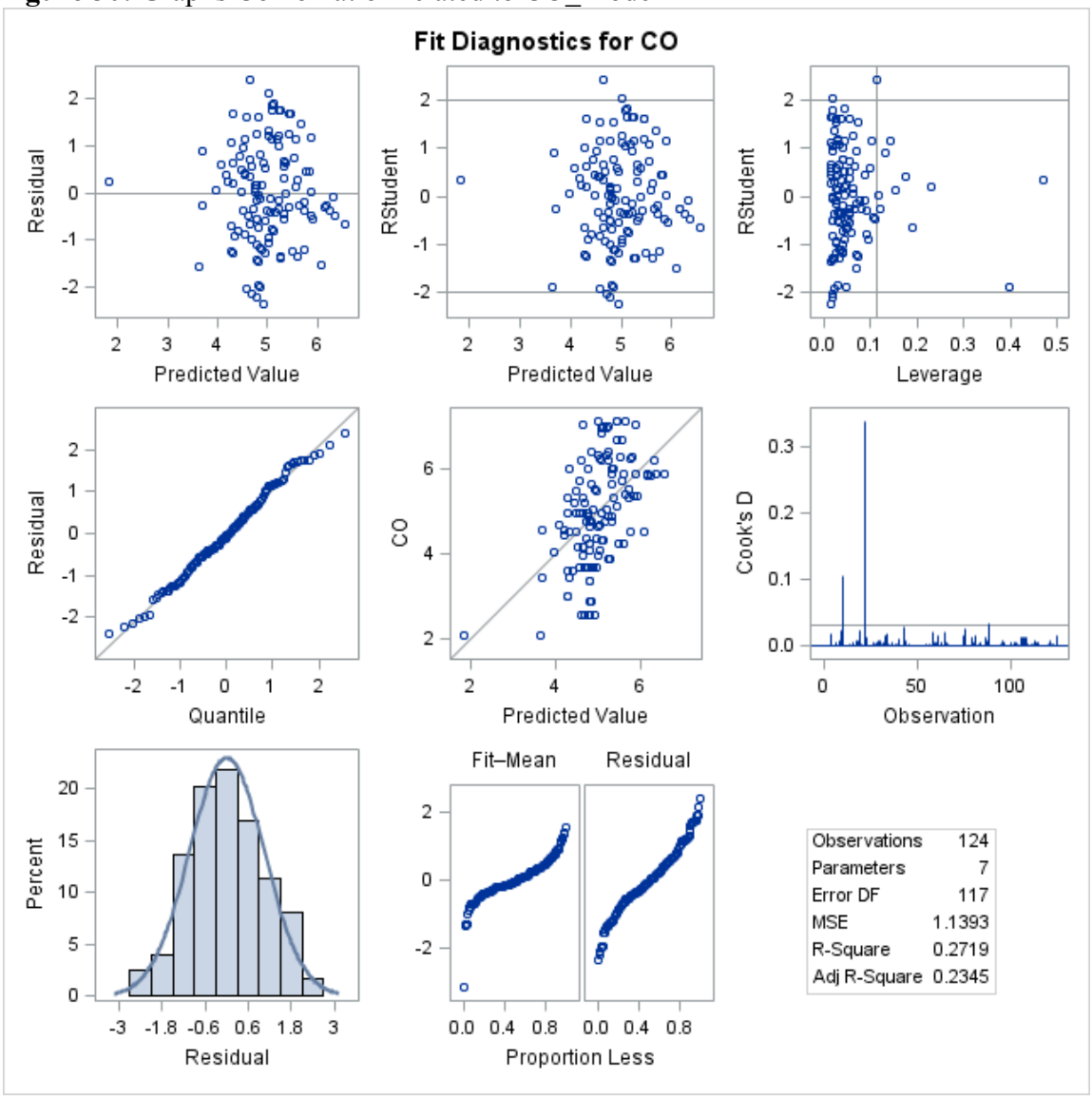

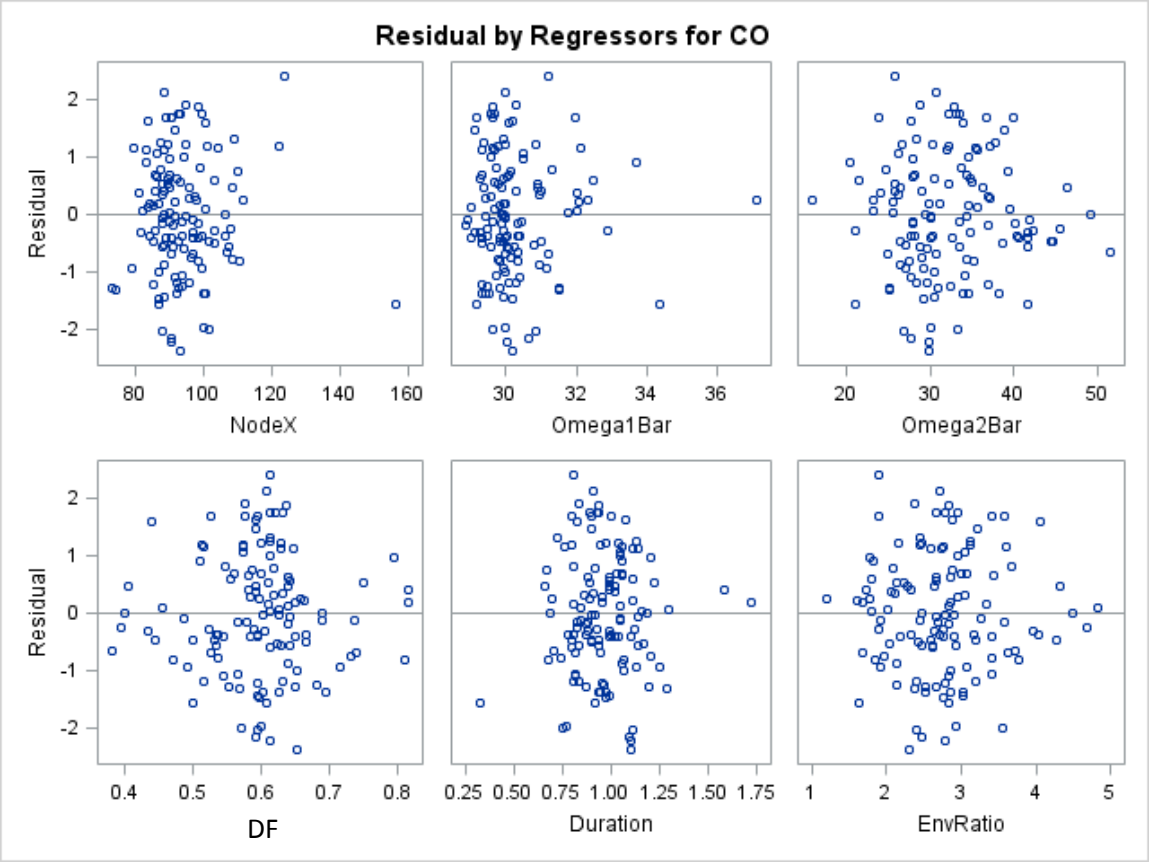

According to the above results, Adjrq increases from 0.18 to 0.23 and there is no longer an influential outlier in our new model. The residual plots show a random distribution. This model shows a weak multiple correlation coefficient (r=0.52) between CO and IFs. We use Parseal Wilson (mix2, power2) with Omega1Bar Omega2Bar NodeX Nodey DF Duration Cratio and Envratio to explore transformations on the predictors, and thus possibly improve our results, but the related Rsquare value increases to 0.29 only. The related Bland Altman results would need improvement too as they show a slightly wide limits of agreement, with a high PE, compared to the benchmark of 30% for CO (below figure):

Bias = 0 LA = +/- 2.04 L/min

PE = (1.96 * SD of Bias/Mean CO of reference method) * 100 = (2.04/4.988) * 100 = 41%

Figure 31: Bland Altman analysis of CO-Model 2

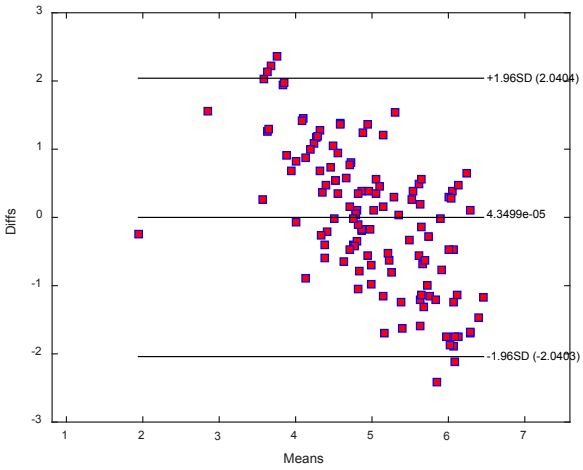

A better model is therefore needed to improve the agreement between these two techniques. We start investigating the effect of physiological predictors such as Age or Weight. When we add Age to the above Model, Rsquare increases slightly and reaches 0.35 (Adjrq=0.3), however when we add Weight, Rsquare jumps to 0.47. This variable can according to White et al. be related to CO values in small mammals[127]; and we can observe this claim in our current study. Thus, we decide to include Weight in our analysis to improve both our correlation and agreement results. First, we perform a regression targeting only CO and weight to evaluate the strength of the simple relationship (figure 32). Then we produce a multivariable regression equation using a combination of predictors including Weight.

Model 3: CO=f(Weight)

Figure 32: Correlation between CO and Weight

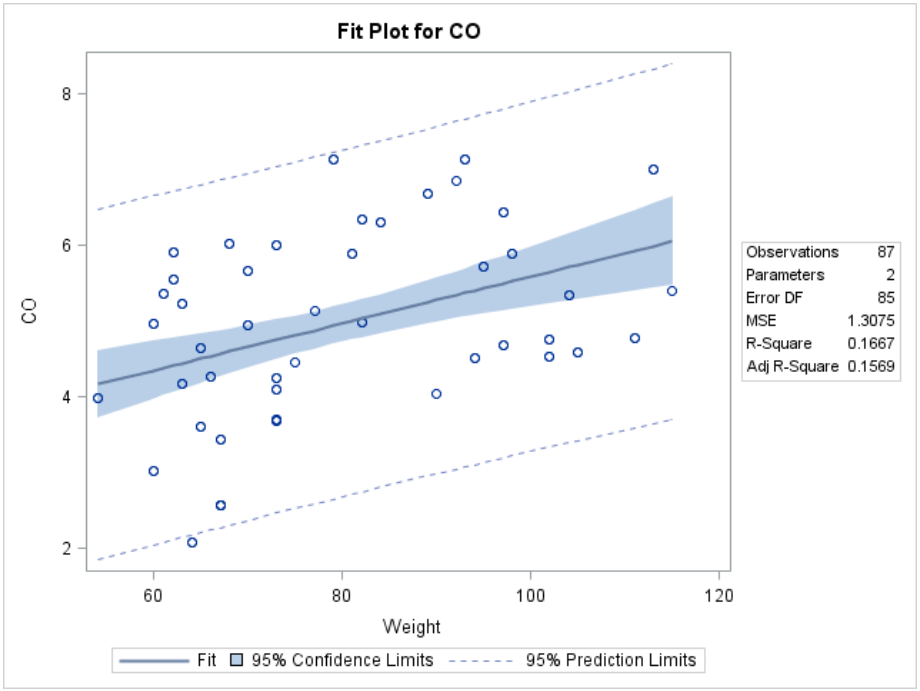

We obtain a weak to moderate correlation (r=0.41) between CO and Weight. Now we include IFs and heart shape factors to find out if this correlation can be improved. We generate the following results:

Model 4 : CO = f(Omega1Bar Omega2Bar NodeX Duration DF Envratio Weight)

Table 12: CO_Model 4

Number of Observations Read	124
Number of Observations Used	87

Number of Observations with Missing Values	37

Analysis of Variance – Obs=87					
Source	**DF**	**Sum of Squares**	**Mean Square**	**F Value**	**Pr > F**
Model	7	62.07928	8.86847	9.83	<.0001
Error	79	71.28565	0.90235		
Corrected Total	86	133.36493			

Root MSE	0.94992	**R-Square**	0.4655
Dependent Mean	4.94801	**Adj R-Sq**	0.4181
Coeff Var	19.19803		

Parameter Estimates							
Variable	**Label**	**DF**	**Parameter Estimate**	**Standard Error**	**t Value**	**Pr > |t|**	**Variance Inflation**
Intercept	Intercept	**1**	10.03292	7.14074	1.41	0.1639	0
NodeX	NodeX	**1**	-0.01658	0.01439	-1.15	0.2528	2.18513
Omega1Bar	Omega1Bar	**1**	-0.21839	0.15962	-1.37	0.1751	3.91465
Omega2Bar	Omega2Bar	**1**	0.06616	0.02838	2.33	0.0223	3.39292
DF	DF	**1**	0.79390	2.57542	0.31	0.7587	4.42141
Duration	Duration	**1**	-1.49559	0.84861	-1.76	0.0819	2.46984
EnvRatio	EnvRatio	**1**	-0.06509	0.40311	-0.16	0.8721	7.21843
Weight	Weight	**1**	0.02736	0.00647	4.23	<.0001	1.07755

Figure 33: Graphs Combination related to CO_Model 4

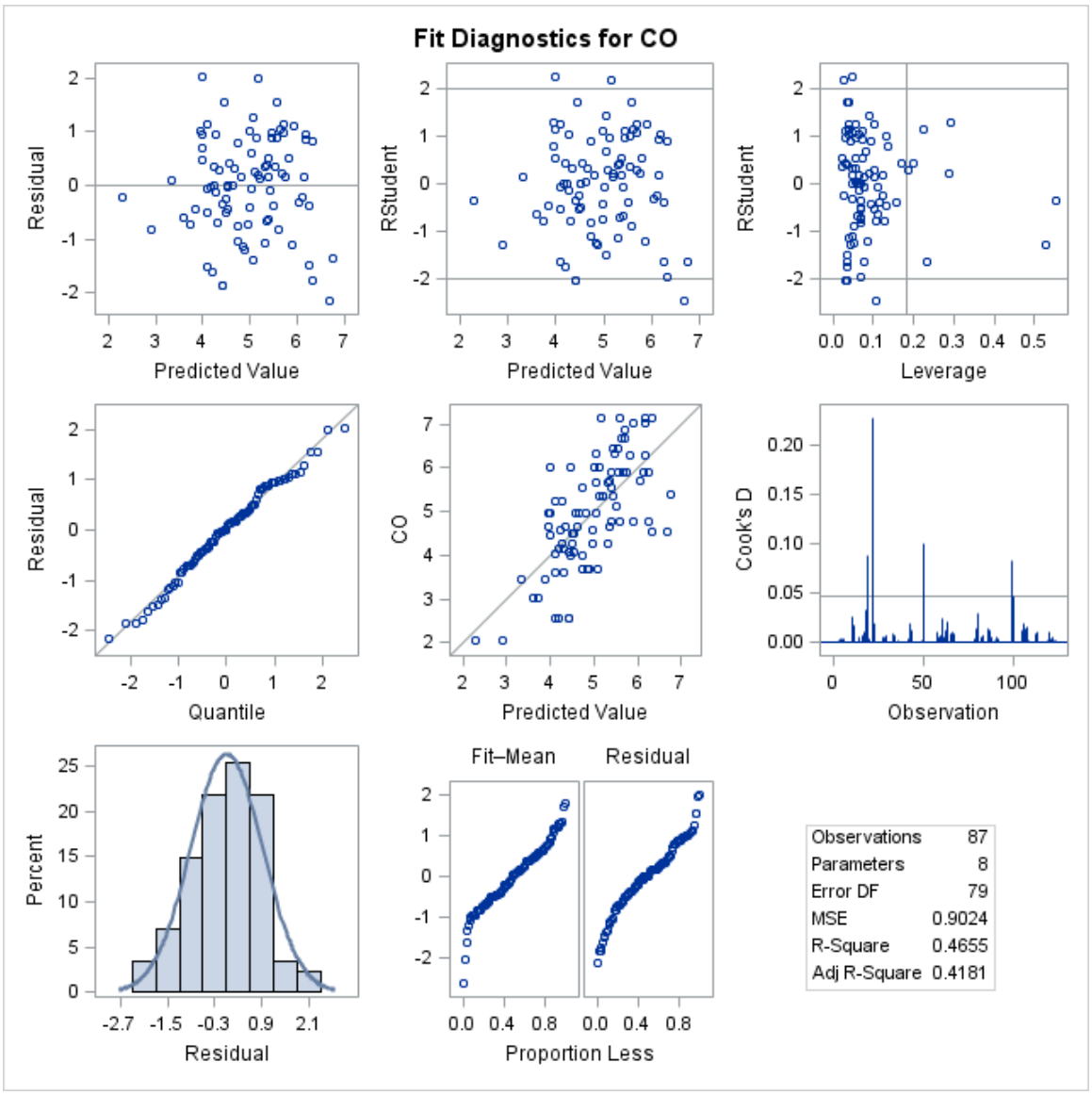

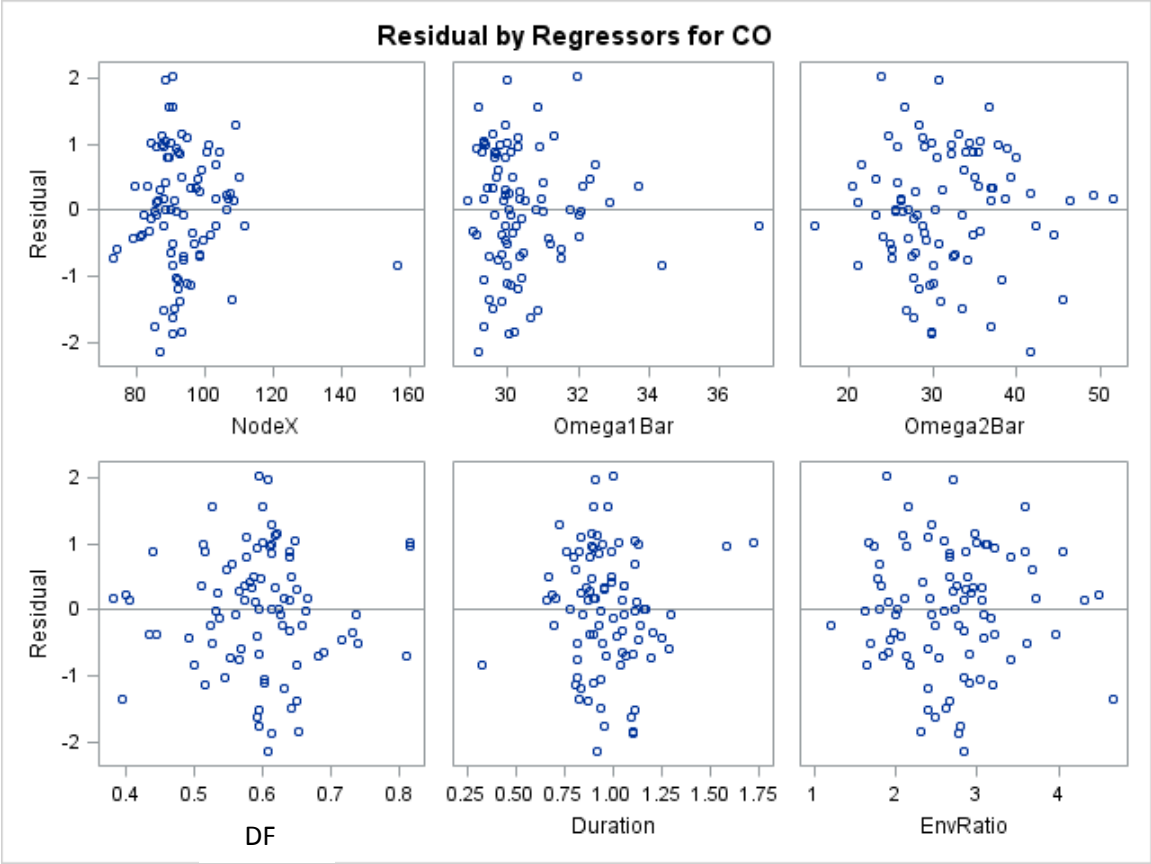

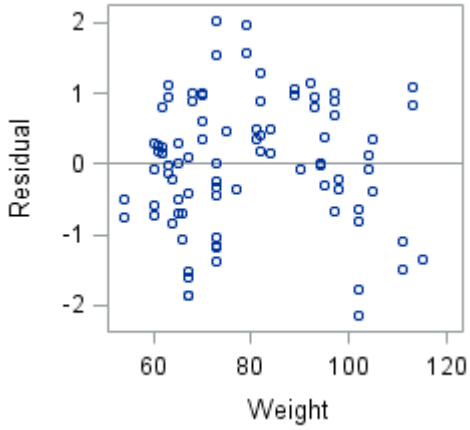

When we include both Weight and a combination of IFs variables, the correlation increases considerably in value (R=0.68, Rsquare=0.47, p<0.0001) as per table 12. All residual plots show random distributions. The QQ plot as well as the proportion less plot

are more adequate (figure 33). This model seems better. When we apply Bland Altman analysis on this model, we obtain the below results:

Mean of the Diff.	0
Std Dev of the Diff	0.9104411
+/- 1.96.SD	+/- 1.78
N	87
PE	35%

Bias = 0 L.A = +/- 1.78 L/min

PE = (1.96SD/Meanref * 100) = (1.8)/ 4.95) * 100 = 36%.

r=0.68

Figure 34: Bland Altman Analysis of CO-Model 4

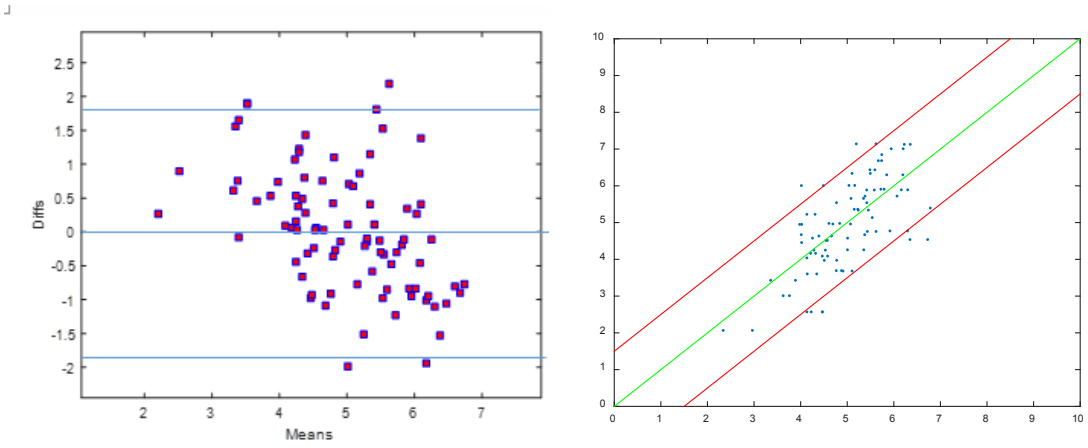

As per the above results, PE improves as well, even though it remains slightly above the 30% threshold value for the interchangeability purpose. It is interesting to know that a combination of IFs variables and weight can greatly improve CO estimations. We try to simplify our model by reducing the number of predictors. We target Omega2Bar, the variable that has the lowest p-value after weight. We obtain the following minimalistic model (table 13):

Model 5: CO= Omega2Bar Weight:

Table 13: CO-Model 5

Analysis of Variance – Obs=87					
Source	**DF**	**Sum of Squares**	**Mean Square**	**F Value**	**Pr > F**
Model	2	55.39144	27.69572	29.84	<.0001
Error	84	77.97349	0.92826		
Corrected Total	86	133.36493			

Root MSE	0.96346	**R-Square**	0.4153
Dependent Mean	4.94801	**Adj R-Sq**	0.4014
Coeff Var	19.47166		

Parameter Estimates							
Variable	**Label**	**DF**	**Parameter Estimate**	**Standard Error**	**t Value**	**Pr > |t|**	**Variance Inflation**
Intercept	Intercept	**1**	-0.11494	0.67285	-0.17	0.8648	0
Omega2Bar	Omega2Bar	**1**	0.09404	0.01573	5.98	<.0001	1.01372
Weight	Weight	**1**	0.02651	0.00637	4.16	<.0001	1.01372

Figure 35: Graphs combination related to CO-Model 5

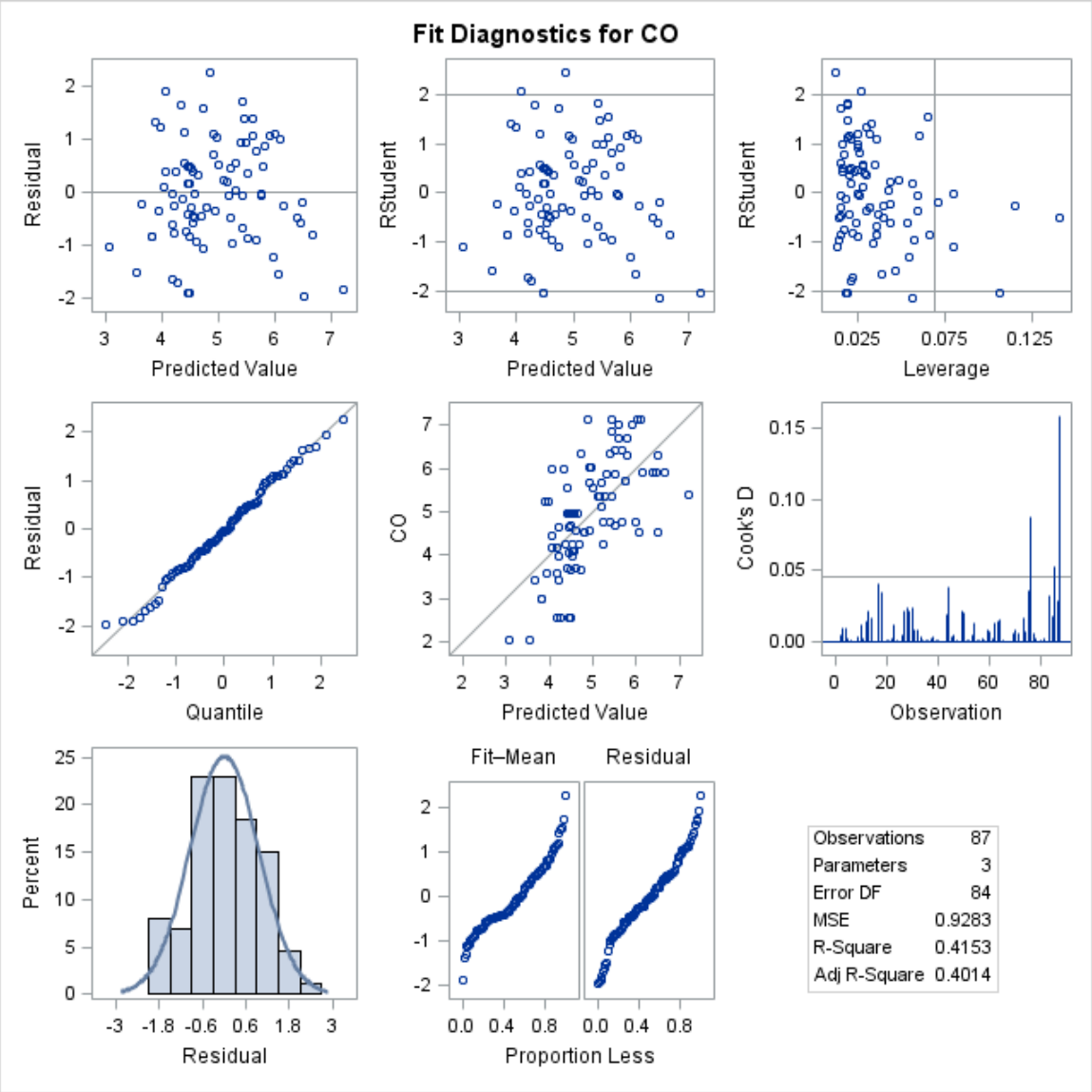

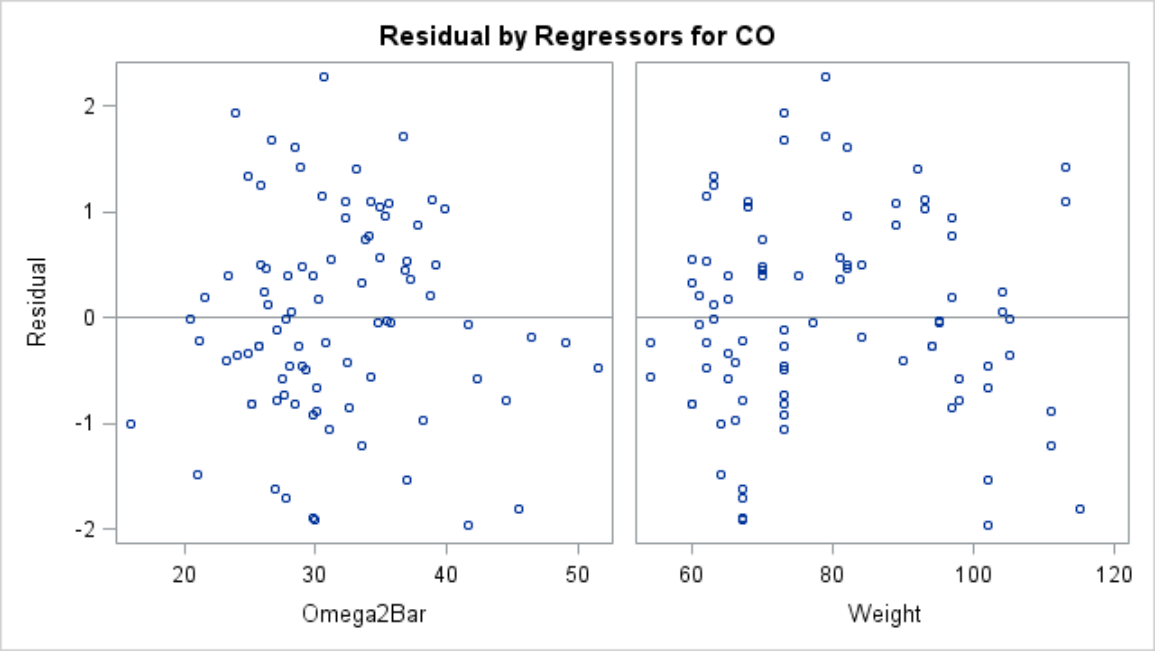

We notice that Adjrq has a very slight decrease but RMSE is almost the same. In this reduced model Omega2Bar becomes significant alongside Weight (table 13). The fit diagnostics plots are adequate (figure 35). We generate the related Bland Altman results:

Mean Bias	-2.04e-17
Std Dev of Diff	0.9521914
+/- 1.96 SD	+/- 1.86
PE	37.57%

PE = 1.86/5.12 = 37.57%

R=0.64

Therefore including a physiological variable such as weight can be useful in the conception of a new method for CO evaluation. Future studies are needed though to further explore this statement. Moreover, the addition of Height or Body Surface Area as a predictor, can improve the above results. Indeed as mentioned earlier in the literature

review section, and according to Jegier et. Al, both CO and stroke volume are related closely to the size of the individual[131].

4.1.3 Data analysis: estimating PWV with IFs methodology

Aortic stiffness is a powerful indicator of present and possible future cardiovascular risk. The non-invasive methods currently in use assess aortic pulse wave velocity (PWV), which is known to be a key indicator of aortic stiffness. Monitoring and obtaining accurate measurement for this parameter is crucial. In this study, we compare IFs estimations of PWV with the gold standard tonometry measurements. First, we use FHS_400 as our training dataset to explore the best fit model. This file is composed of 400 observations, from which 279 data points are useable (because of a few missing values and the filtering process). Then, we use FHS_6500 to test our trained models and evaluate their respective percentage error.

4.1.3.1 Training - Modeling the relationship between PWV_IFs and PWV_Tonometry

Prior running a regression analysis and training our data, we generate a scatterplot matrix (figure 36) in order to study correlations among variables and also to have an overall understanding of the existing relationships. The actual PWV values are from Tonometry.

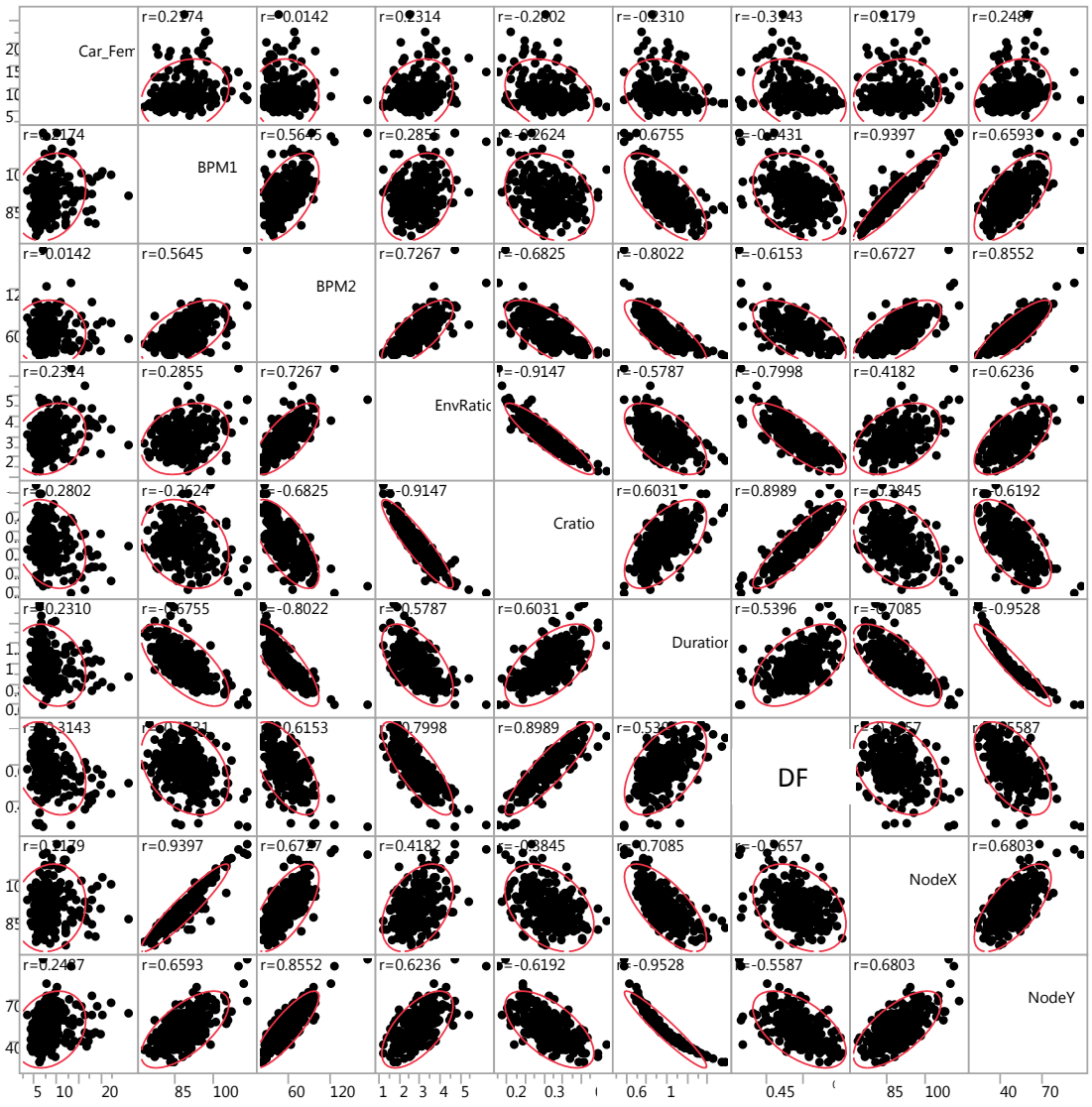

Figure 36: Scatterplot Matrix for PWV

We notice that most of the above explanatory variables can contribute to some extent to our regression relationship. We also observe that some of these variables are highly correlated, such as BPM1 and NodeX, or NodeY and Duration. Consequently, we decide to base the model selection process on the VIF criterion.

To find the best fit model, we perform a preliminary regression analysis including "all" the above variables, which we call "Core" variables. The Core variables consist of: BPM1, BPM2, NodeX, NodeY, Duration, DF, Envratio and Cratio. We obtain the following results:

Model 1: Predicted Car_FemPWV = f (Core variables)

Figure 37: Model 1- PWV predicted versus PWV actual values and the related QQ plot

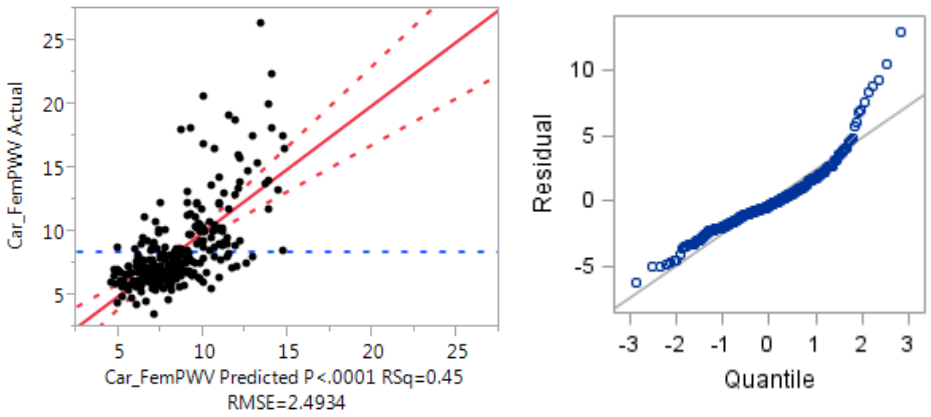

Table 14: PWV_Model 1

Analysis of Variance – Obs= 279					
Source	**DF**	**Sum of Squares**	**Mean Square**	**F Value**	**Pr > F**
Model	8	1368.81203	171.10150	27.52	<.0001
Error	270	1678.57639	6.21695		
Corrected Total	278	3047.38842			

Root MSE	2.49338	**R-Square**	0.4492
Dependent Mean	8.45123	**Adj R-Sq**	0.4329
Coeff Var	29.50319		

Parameter Estimates							
Variable	**Label**	**DF**	**Parameter Estimate**	**Standard Error**	**t Value**	**Pr > |t|**	**Variance Inflation**
Intercept	Intercept	**1**	-3.48108	6.86652	-0.51	0.6126	0
BPM1	BPM1	**1**	0.34314	0.10804	3.18	0.0017	24.35979
BPM2	BPM2	**1**	-0.18979	0.02035	-9.33	<.0001	6.93601
NodeX	NodeX	**1**	-0.24101	0.10773	-2.24	0.0261	24.10918
NodeY	NodeY	**1**	0.26689	0.05780	4.62	<.0001	18.96582
Cratio	Cratio	**1**	-25.54652	13.43738	-1.90	0.0583	19.25093
EnvRatio	EnvRatio	**1**	1.27039	0.57305	2.22	0.0275	7.58140
Duration	Duration	**1**	5.28218	3.28442	1.61	0.1089	13.19637
DF	DF	**1**	-0.49486	6.28947	-0.08	0.9373	10.41600

As per the above table, the value for Adjrq is moderately high (0.43), which is good, however many of the independent variables have VIF values above the threshold of 10, highlighting multicollinearity issues. Moreover, QQ plot of the residuals reveals that the points deviate from the identity line. Therefore, the normality of the residuals might be of concern. In order to minimize multicollinearity, and produce better plots, we run a regression analysis targeting variables that have VIF values under 10. We first eliminate Nodex, followed by Nodey and Cratio, which are the variables that disclosed the highest values for VIF. We obtain the following model:

Model 2 : Car_FemPWV predicted= f(BPM1 BPM2 EnvRatio Duration DF)

Figure 38: Model 2- PWV predicted versus PWV actual values and the related QQ plot

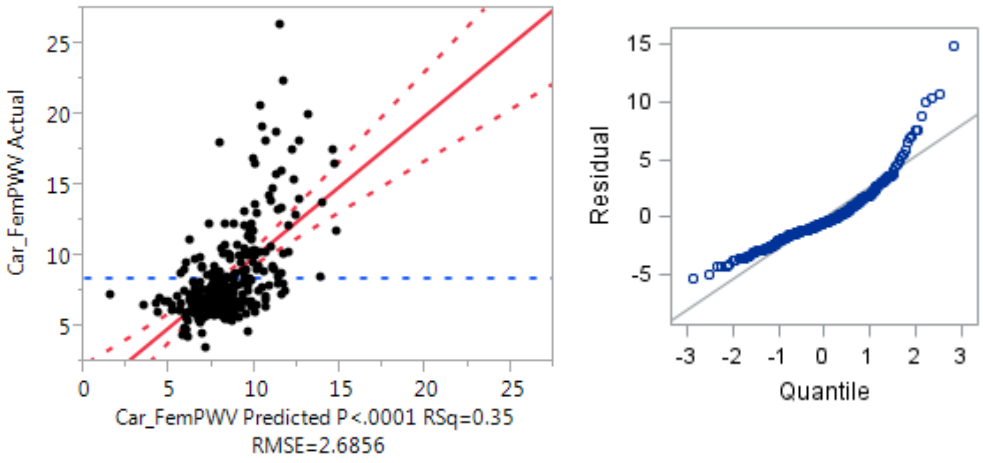

Table 15: PWV-Model 2

Analysis of Variance – Observations = 279					
Source	**DF**	**Sum of Squares**	**Mean Square**	**F Value**	**Pr > F**
Model	5	1078.35872	215.67174	29.90	<.0001
Error	273	1969.02969	7.21256		
Corrected Total	278	3047.38842			

Root MSE	2.68562	**R-Square**	0.3539
Dependent Mean	8.45123	**Adj R-Sq**	0.3420
Coeff Var	31.77789		

Parameter Estimates							
Variable	**Label**	**DF**	**Parameter Estimate**	**Standard Error**	**t Value**	**Pr > |t|**	**Variance Inflation**
Intercept	Intercept	**1**	19.43927	5.51308	3.53	0.0005	0

Parameter Estimates							
Variable	**Label**	**DF**	**Parameter Estimate**	**Standard Error**	**t Value**	**Pr > |t|**	**Variance Inflation**
BPM1	BPM1	**1**	0.11543	0.03331	3.47	0.0006	1.99616
BPM2	BPM2	**1**	-0.16952	0.01683	-10.07	<.0001	4.09355
EnvRatio	EnvRatio	**1**	1.74057	0.44885	3.88	0.0001	4.00921
Duration	Duration	**1**	-10.02438	1.84109	-5.44	<.0001	3.57415
DF	DF	**1**	-11.65532	3.57705	-3.26	0.0013	2.90409

We notice that Adjrq drops to 0.34 but in this model all VIF values are below the threshold of 10, making the coefficients of the equation more stable. Nevertheless, the results are inadequate. We conclude that an improved model is required to address the nonlinearity and non-normality issues shown in figure 38 and to produce a better fit for our data. According to Montgomery et al., to correct the non-normality, it can be helpful to apply a Box Cox transformation on the response variable. We run SAS automated Box Cox transformation feature, which suggests a lambda of -0.75, corresponding to inverse square root transformation of the response variable (table 16):

Table 16: Box Cox transformation on Model 2-PWV

Box-Cox Transformation Information for Car_FemPWV		
Lambda	**R-Square**	**Log Like**
-3.00	0.21	-289.426
-2.75	0.23	-266.522
-2.50	0.25	-246.008
-2.25	0.27	-228.008
-2.00	0.29	-212.643
-1.75	0.31	-200.034
-1.50	0.33	-190.301

Box-Cox Transformation Information for Car_FemPWV

Lambda		R-Square		Log Like	
-1.25		0.34		-183.567	
-1.00	+	0.35		-179.953	*
-0.75		0.36		-179.580	<
-0.50		0.37		-182.566	
-0.25		0.38		-189.019	
0.00		0.38		-199.032	
0.25		0.38		-212.676	
0.50		0.37		-229.993	
0.75		0.36		-250.987	
1.00		0.35		-275.627	
1.25		0.34		-303.846	
1.50		0.33		-335.539	
1.75		0.31		-370.576	
2.00		0.29		-408.802	
2.25		0.28		-450.052	
2.50		0.26		-494.150	
2.75		0.24		-540.919	
3.00		0.22		-590.182	

< - Best Lambda
*** - 95% Confidence Interval**
+ - Convenient Lambda

After applying the inverse square root transformation on the response variable of Model 2, we obtain the following results:

Model 3:

1/Square root (Car_FemPWV predicted) = f(BPM1 BPM2 EnvRatio Duration DF)

Figure 39: Graphs combination related to PWV-Model 3

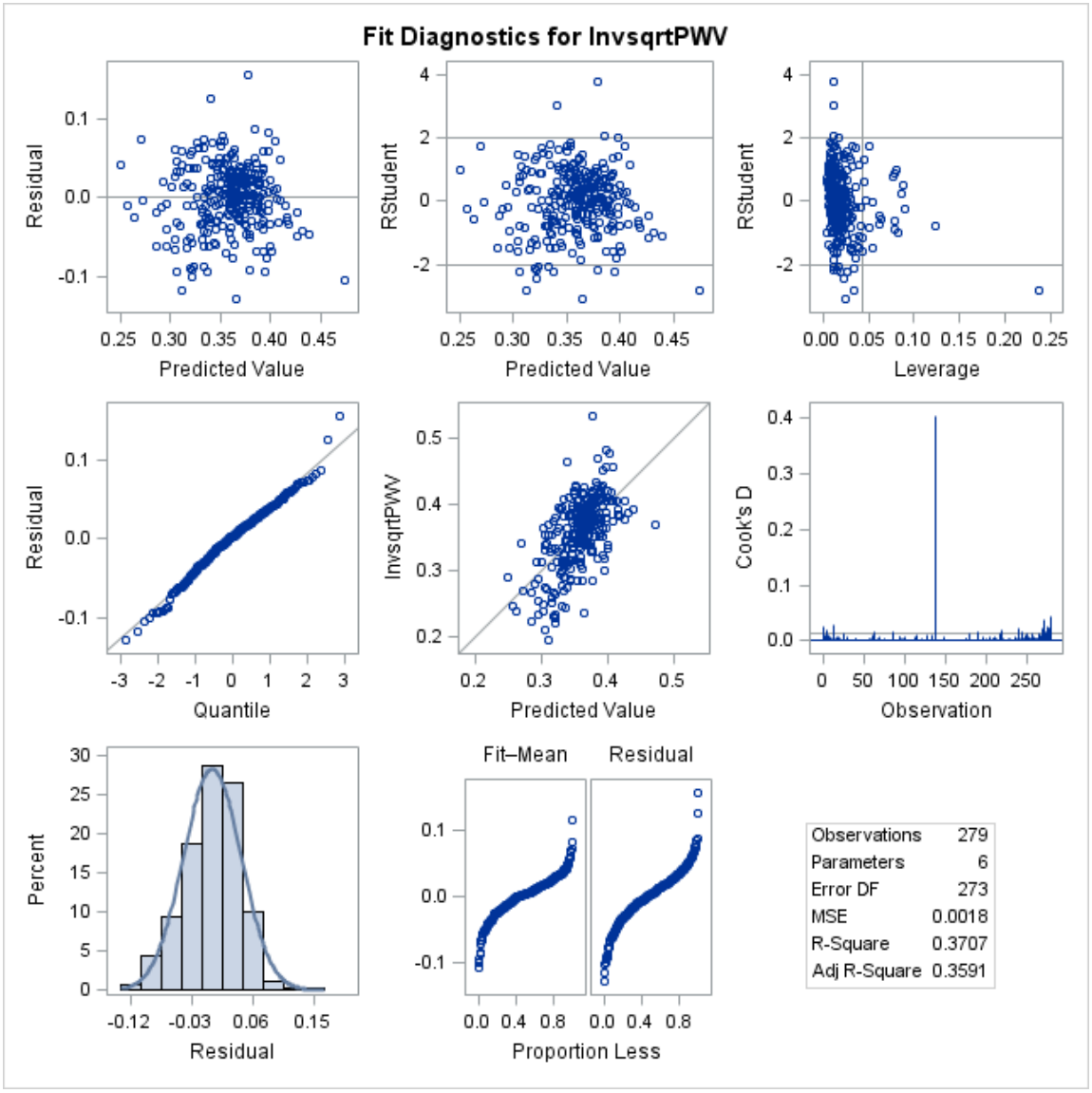

Figure 40:
PWV-Model 4

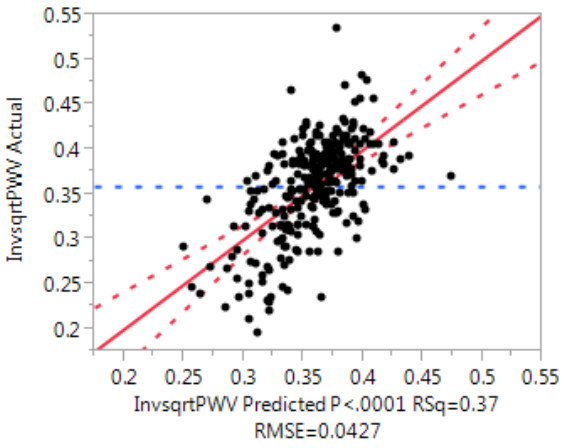

According to these plots, Adjrq value slightly increases from 0.34 to 0.36 and QQ plot becomes more adequate, showing an improved normality of the residual data. This model seems better, however, the coefficient of determination is still small. We thus decide to try a transformation on the predictors instead of the response. We use Parseal Wilson and continue to emphasize our selection on VIF and Adjrq. We set the polynomial power feature to 2 and the mix to 4. The below equation is consequently produced:

Model 4

Car_FemPWV predicted = 2.12352 - 1.22624 * ((BPM1^2) / (EnvRatio * Cratio^2 * NodeX^2)) - 2922.83499 * ((BPM2 * Cratio * Duration) / (NodeX^2)) + 0.02589 * ((DF * NodeY^2) / (BPM2 * Cratio^2)) + 0.00276 * ((BPM2^2 * Cratio^2 * NodeX^2) / (NodeY^2)) - 0.00425 * ((NodeX^2) /(DF^2 * Duration^2 * BPM2))+ 0.01753 * ((NodeX * NodeY^2) /(BPM2^2 * Duration^2)) + 4.08007 * ((BPM2^2 * Duration^2) / (NodeX * NodeY)) + 8266.96783 * ((NodeY) / (NodeX * DF^2 * BPM2^2))

This model includes 8 predictors:

Var1 = ((BPM1^2) / (EnvRatio * Cratio^2 * NodeX^2))

Var2 = ((BPM2 * Cratio * Duration) / (NodeX^2))

Var3 = ((DF * NodeY^2) / (BPM2 * Cratio^2))

Var4 = ((BPM2^2 * Cratio^2 * NodeX^2) / (NodeY^2))

Var5 = ((NodeX^2) /(DF^2 * Duration^2 * BPM2))

Var6 = ((NodeX * NodeY^2) /(BPM2^2 * Duration^2))

Var7 = ((BPM2^2 * Duration^2) / (NodeX * NodeY))

Var8 = ((NodeY) / (NodeX * DF^2 * BPM2^2))

The following results are generated in order to analyze the Model's adequacy (table 17):

Table 17: PWV-Model 4

Model- Wilson Mix 4 Power 2 – 8-31-15

Analysis of Variance – Observations = 279

Source	DF	Sum of Squares	Mean Square	F Value	Pr > F
Model	8	1658.18792	207.27349	40.28	<.0001
Error	270	1389.20049	5.14519		
Corrected Total	278	3047.38842			

Root MSE	2.26830	**R-Square**	0.5441
Dependent Mean	8.45123	**Adj R-Sq**	0.5306
Coeff Var	26.83990		

Parameter Estimates

Variable	Label	DF	Parameter Estimate	Standard Error	t Value	Pr > |t|	Variance Inflation
Intercept	Intercept	**1**	2.12352	2.59943	0.82	0.4147	0
Var1	Var1	**1**	-1.22624	0.39232	-3.13	0.0020	2.91725
Var2	Var2	**1**	-2922.83499	783.63490	-3.73	0.0002	5.13028
Var3	Var3	**1**	0.02589	0.00355	7.30	<.0001	7.11899
Var4	Var4	**1**	0.00276	0.00083496	3.31	0.0011	4.99986
Var5	Var5	**1**	-0.00425	0.00145	-2.93	0.0037	6.66576
Var6	Var6	**1**	0.01753	0.01023	1.71	0.0878	7.41955
Var7	Var7	**1**	4.08007	1.63530	2.49	0.0132	7.83728
Var8	Var8	**1**	8266.96783	941.50288	8.78	<.0001	4.62778

Figure 41: Graphs combination related to PWV – Model 4

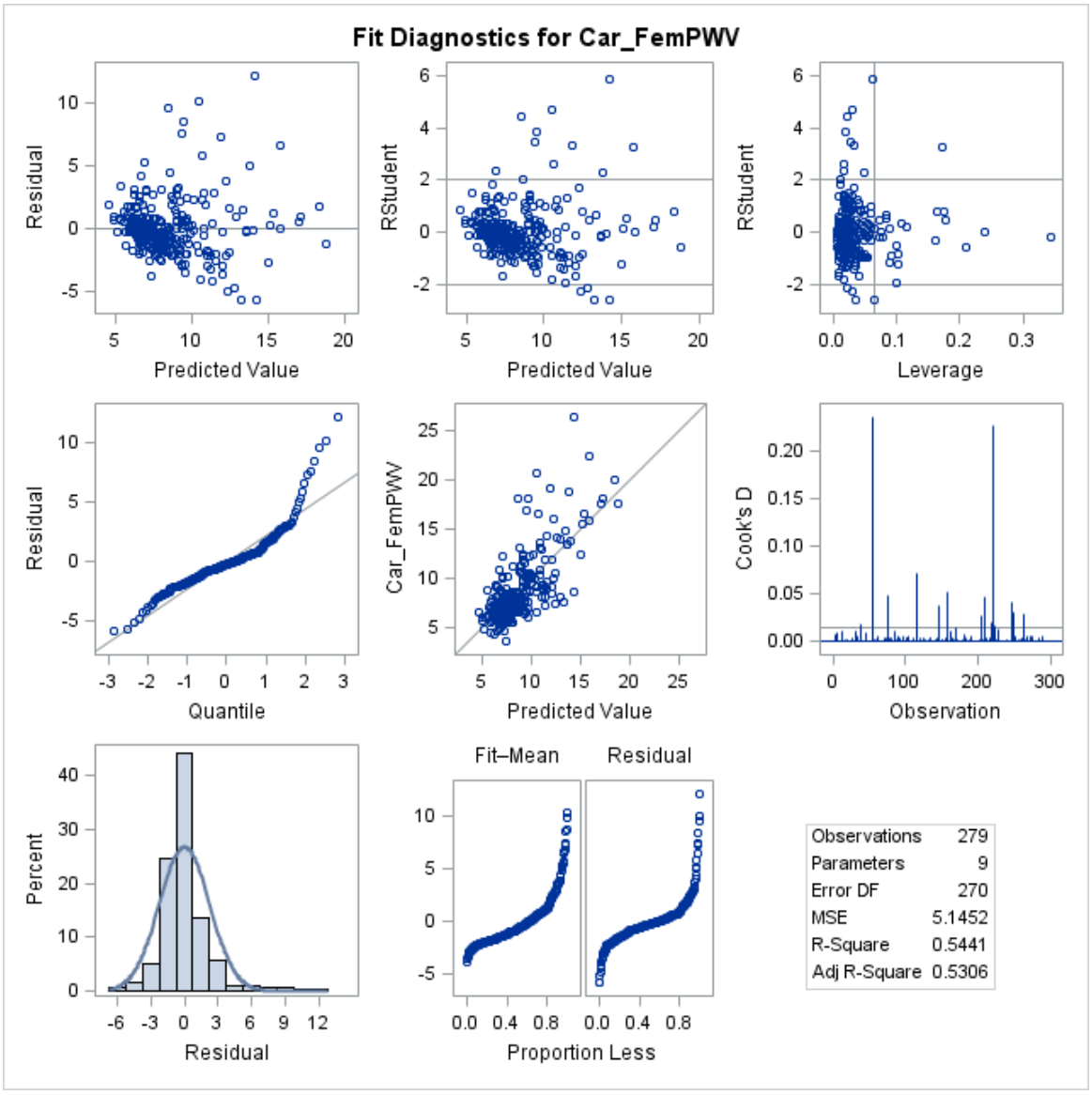

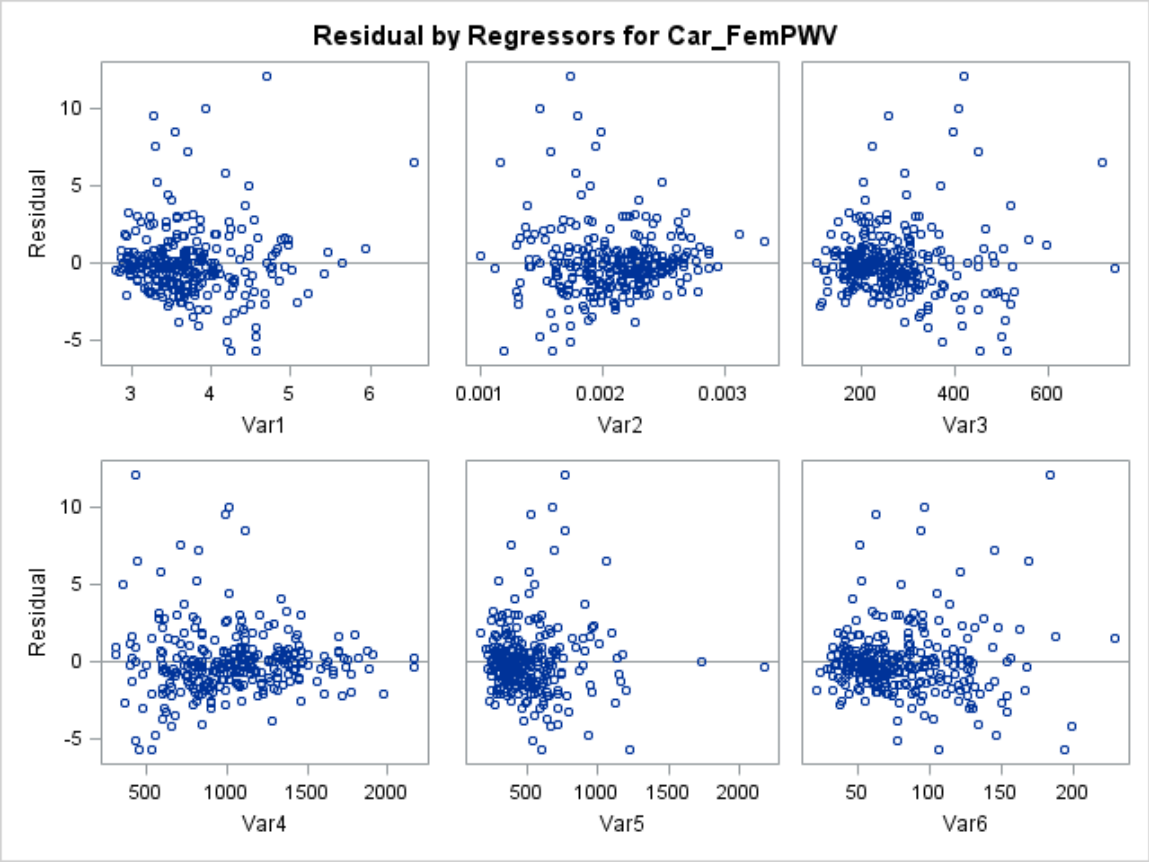

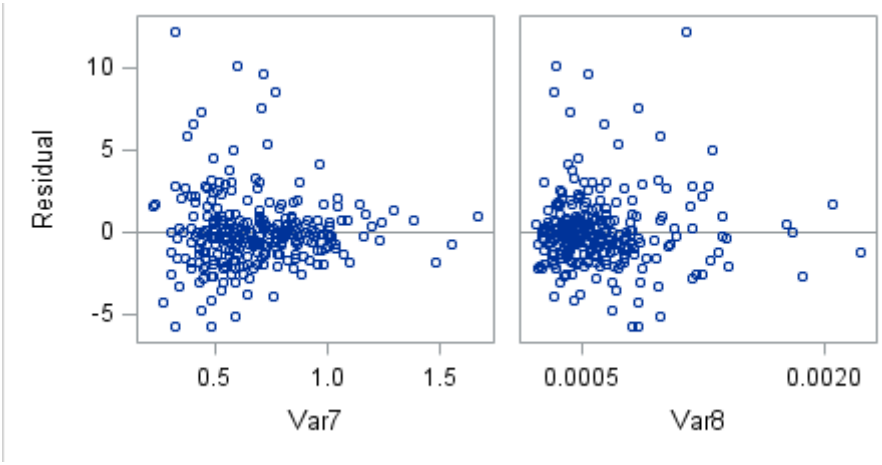

The REG Procedure

Figure 42: Details of CooksD plot for Model 4

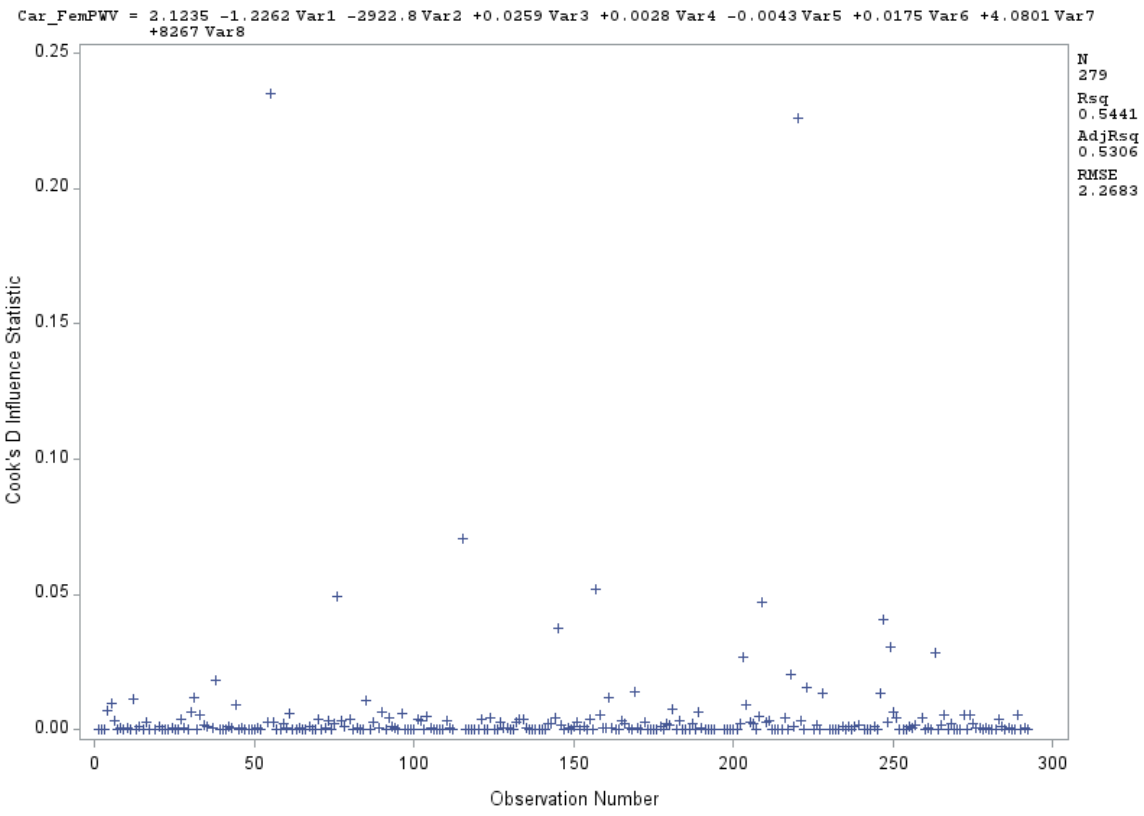

This model is not perfect and needs some work since QQ plot shows a deviation from the normality assumption (figure 41). Also, the residual plots for variable 4 and 7 show a slight funnel shape distribution, revealing a small heteroscedasticity. There are 2 outliers (figure 42), but their related Cooks' D is negligible (below the benchmark) and they are also both legitimate points. We need to improve this regression equation, but since it produces somewhat good results, like an Adjrq that jumps to 0.53 (Rsquare=0.54, $p<0.0001$), we decide to explore the model's agreement with the reference method. The Bland Altman statistical analysis is thus applied. We obtain the following results:

Mean Bias = 0 and L.A = +/-4.38 m/s; PE= 52%.

Figure 43: Bland Altman PWV-Model 4 –training set

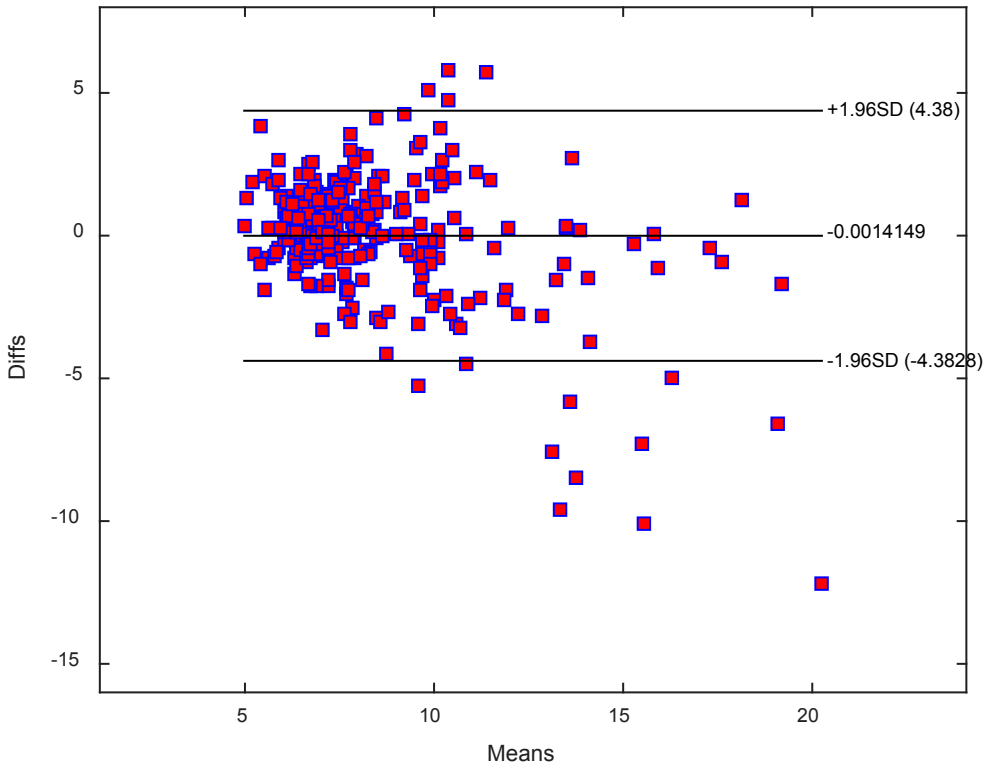

We notice that the limits of agreement are wide, leading to a percentage error of 52% (figure 43). Moreover, as mentioned previously QQ plot shows points that deviate from the top end of the diagonal line (figure 41). The plot of Predicted versus actual PWV highlights non linearity. These observations direct us to consider a new predictor as an explanatory variable: “Age”. As per the study lead by the European Heart Journal, PWV values increase with age. Thus, it may be helpful to establish values based on the distribution of PWV with age to address the deviation from linearity observed earlier in our plots. Before deciding to use Age as a predictor in our model, we need to ensure that

its effect on PWV is real within our own dataset. To explore this concept, we first perform a pairwise analysis between PWV and Age, then a regression analysis between Age (response variable) and IFs variables (explanatory).

1- Pairwise analysis between Age and PWV:

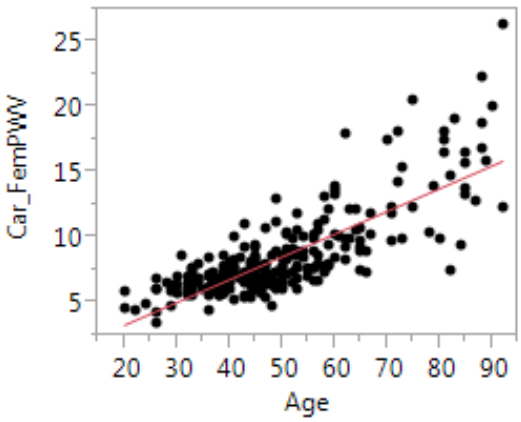

Figure 44: Scatterplot of Age versus PWV

We generate a Pearson correlation (r=0.79, p<00001) which is strong. Moreover the plot shows that PWV and Age display a linear relationship for the age category that targets the interval "60 years old and below" (figure 44). This information is important for our upcoming analysis.

2- We run a multivariable regression between Age (response variable) and IFs core variables and obtain the following results: Adjrq is reasonable (0.53) and the correlation is significant and high (r=0.74, p<0.0001).

Consequently we decide to add Age as a predictor. We also choose to use a segmented regression plot with the following intervals: individuals 60 years old or less

and individuals older than 60 years old. Thus, initially we add Age as an explanatory variable (Model 5), then we target the interval 60 years old and less (Model 6).

Model 5 Predicted PWV = var1 var2 var3 var4 var5 var6 var7 var8 Age

Table 18: PWV-Model 5

Analysis of Variance – Obs = 279					
Source	**DF**	**Sum of Squares**	**Mean Square**	**F Value**	**Pr > F**
Model	9	2213.27945	245.91994	79.31	<.0001
Error	269	834.10896	3.10078		
Corrected Total	278	3047.38842			

Root MSE	1.76090	**R-Square**	0.7263
Dependent Mean	8.45123	**Adj R-Sq**	0.7171
Coeff Var	20.83606		

Parameter Estimates							
Variable	**Label**	**DF**	**Parameter Estimate**	**Standard Error**	**t Value**	**Pr > |t|**	**Variance Inflation**
Intercept	Intercept	**1**	-3.03714	2.05450	-1.48	0.1405	0
Var1	Var1	**1**	-0.66547	0.30743	-2.16	0.0313	2.97249
Var2	Var2	**1**	-2458.14443	609.33351	-4.03	<.0001	5.14700
Var3	Var3	**1**	0.01025	0.00299	3.43	0.0007	8.40058
Var4	Var4	**1**	0.00253	0.00064842	3.90	0.0001	5.00350
Var5	Var5	**1**	-0.00215	0.00114	-1.89	0.0601	6.79493
Var6	Var6	**1**	0.02257	0.00795	2.84	0.0049	7.43624
Var7	Var7	**1**	5.06498	1.27163	3.98	<.0001	7.86363
Var8	Var8	**1**	3813.08124	803.13270	4.75	<.0001	5.58772
Age	Age	**1**	0.14579	0.01090	13.38	<.0001	2.40753

Figure 45: Graphs combination related to PWV-Model 5

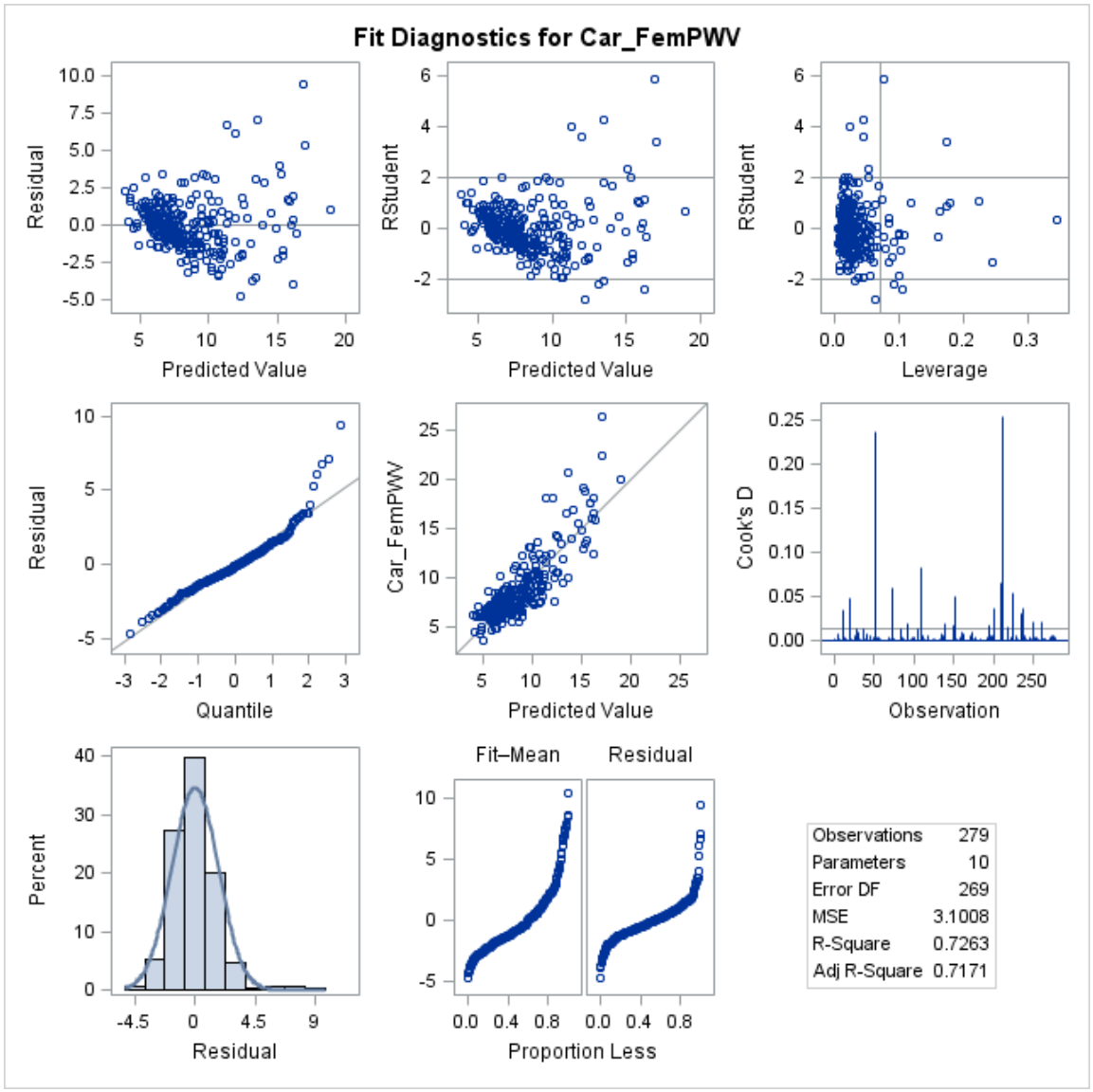

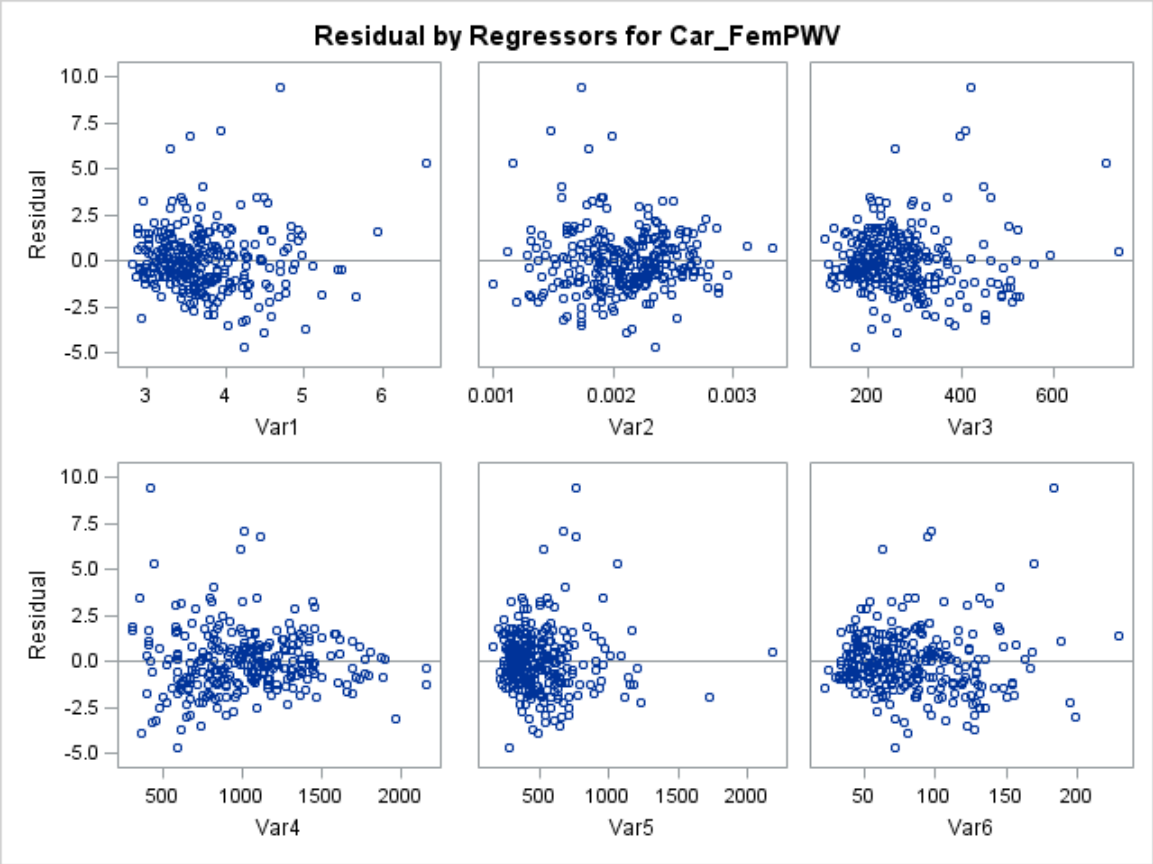

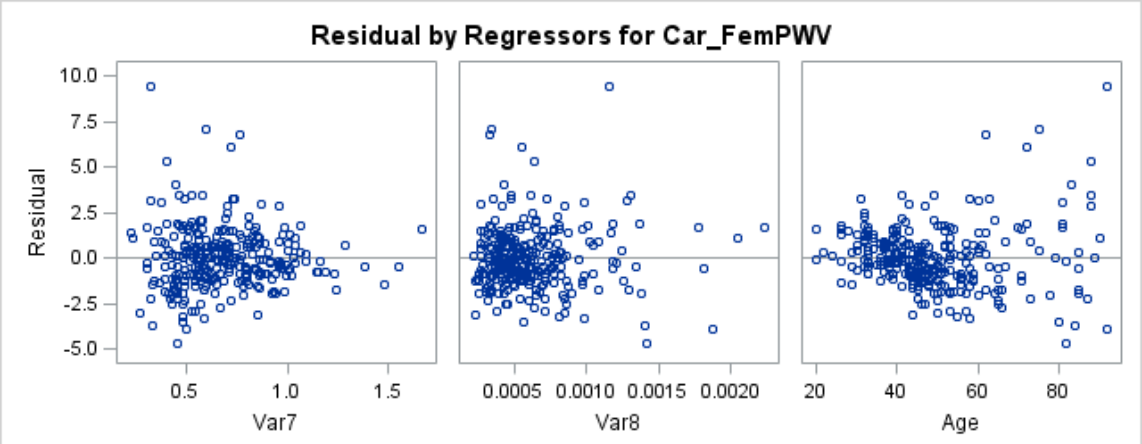

As per the above results, we have a strong relationship now, with a multiple correlation coefficient R=0.86, however QQ plot needs further improvement. The limits

of agreement remain wide, nevertheless they are slightly improved. Bland Altman analysis generates the following results:

Bias=0 LA = +/-(1.96*1.73)=3.39 m/s PE=3.39/8.45=40%

Model 6

Car_FemPWV = f(var1 var2 var3 var4 var5 var6 var7 var8 +Age) and Age<=60 as a criterion

Table 19 : PWV – Model 6

Number of Observations Read	279
Number of Observations Used	229

Analysis of Variance

Source	DF	Sum of Squares	Mean Square	F Value	Pr > F
Model	9	349.79748	38.86639	27.59	<.0001
Error	219	308.45706	1.40848		
Corrected Total	228	658.25454			

Root MSE	1.18679	**R-Square**	0.5314
Dependent Mean	7.37341	**Adj R-Sq**	0.5121
Coeff Var	16.09560		

Parameter Estimates

Variable	Label	DF	Parameter Estimate	Standard Error	t Value	Pr > |t|	Variance Inflation
Intercept	Intercept	**1**	2.96861	1.87569	1.58	0.1149	0
Var1	Var1	**1**	-0.37706	0.24667	-1.53	0.1278	3.00876
Var2	Var2	**1**	-1414.44226	455.49672	-3.11	0.0022	4.77956

Parameter Estimates							
Variable	**Label**	**DF**	**Parameter Estimate**	**Standard Error**	**t Value**	**Pr > |t|**	**Variance Inflation**
Var3	Var3	**1**	0.00220	0.00278	0.79	0.4295	10.39351
Var4	Var4	**1**	0.00090064	0.00057525	1.57	0.1189	6.07776
Var5	Var5	**1**	0.00013290	0.00086477	0.15	0.8780	6.98261
Var6	Var6	**1**	0.01542	0.00626	2.47	0.0145	7.66113
Var7	Var7	**1**	1.89490	0.96011	1.97	0.0497	8.23791
Var8	Var8	**1**	1178.56728	950.81430	1.24	0.2165	6.64881
Age	Age	**1**	0.09159	0.01138	8.05	<.0001	1.67329

Figure 46: Graphs combination related to PWV – Model 6

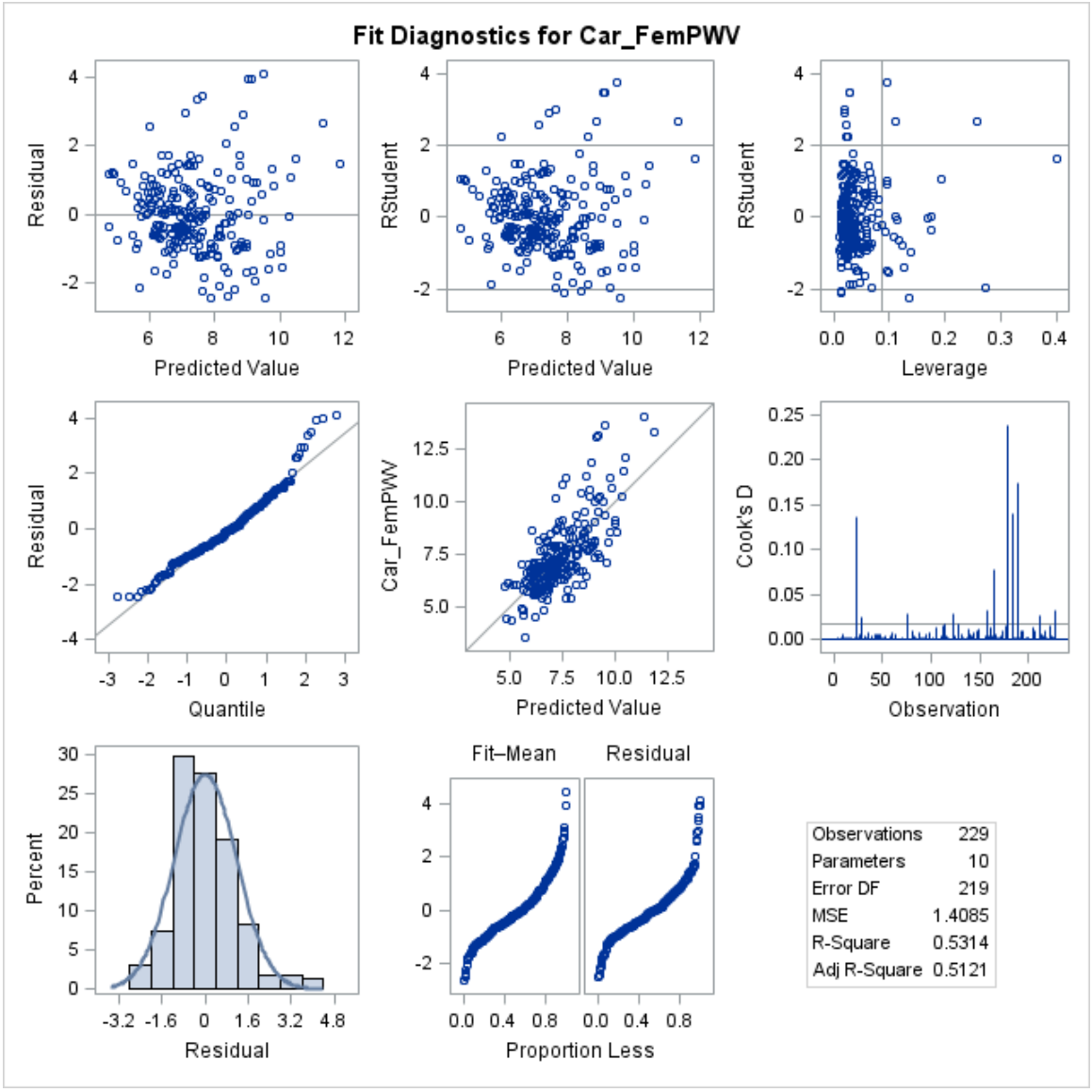

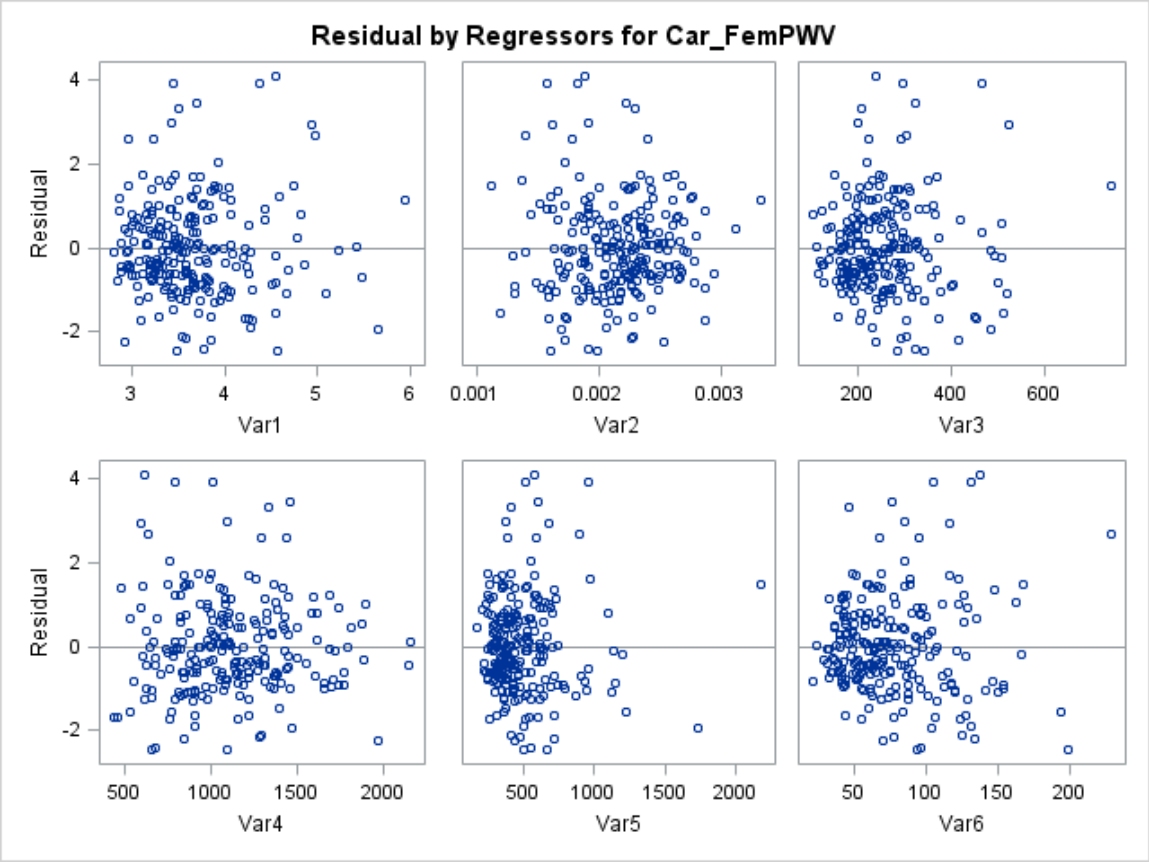

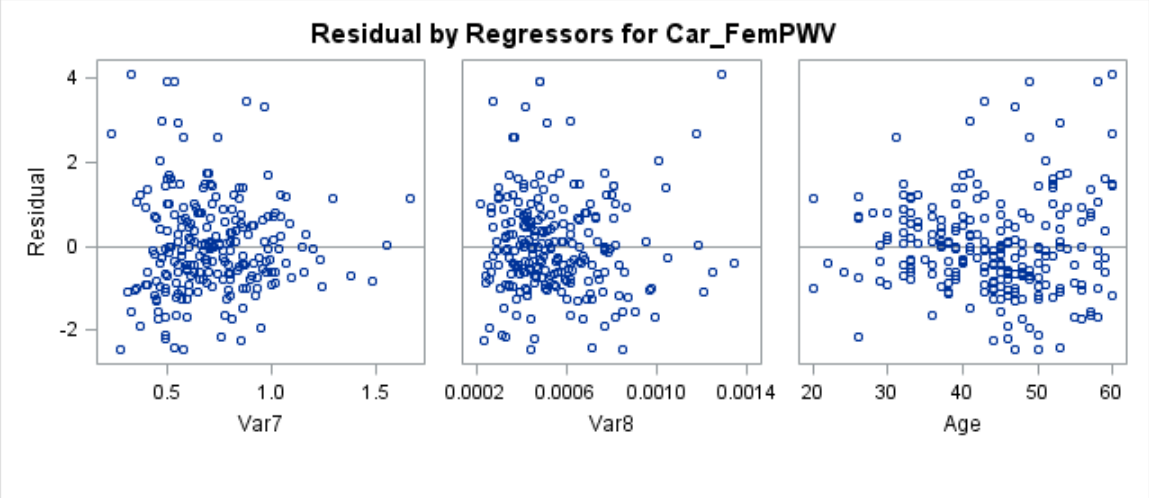

We produce a moderately high Adjrsq (0.51) and a greatly improved RMSE of 1.19. This model's overall plots seem better, however, the value of VIF for variable 3 is borderline (table 19). Also the coefficients of variables 5 and 8 display a moderately high

p-values and thus they do not contribute much to the overall relationship. Therefore, we to try to explore the effect of a dimension reduction and consequently eliminate 3 variables from the regression equation. This procedure leads us to Model 7.

Model 7: Car_FemPWV = f (var1 var2 var4 var6 var7 Age), for Ages<=60

Table 20: PWV = Model 7

Analysis of Variance – Observations = 229					
Source	**DF**	**Sum of Squares**	**Mean Square**	**F Value**	**Pr > F**
Model	6	347.14329	57.85722	41.29	<.0001
Error	222	311.11125	1.40140		
Corrected Total	228	658.25454			

Root MSE	1.18381	**R-Square**	0.5274
Dependent Mean	7.37341	**Adj R-Sq**	0.5146
Coeff Var	16.05511		

Parameter Estimates							
Variable	**Label**	**DF**	**Parameter Estimate**	**Standard Error**	**t Value**	**Pr > |t|**	**Variance Inflation**
Intercept	Intercept	**1**	4.39901	1.46238	3.01	0.0029	0
Var1	Var1	**1**	-0.22938	0.21809	-1.05	0.2941	2.36376
Var2	Var2	**1**	-1535.39877	338.56241	-4.54	<.0001	2.65389
Var4	Var4	**1**	0.00041252	0.00032413	1.27	0.2045	1.93936
Var6	Var6	**1**	0.01653	0.00461	3.59	0.0004	4.17848
Var7	Var7	**1**	1.77019	0.71088	2.49	0.0135	4.53896
Age	Age	**1**	0.09413	0.01109	8.49	<.0001	1.59959

Figure 47: Graphs combination related to PWV – Model 7

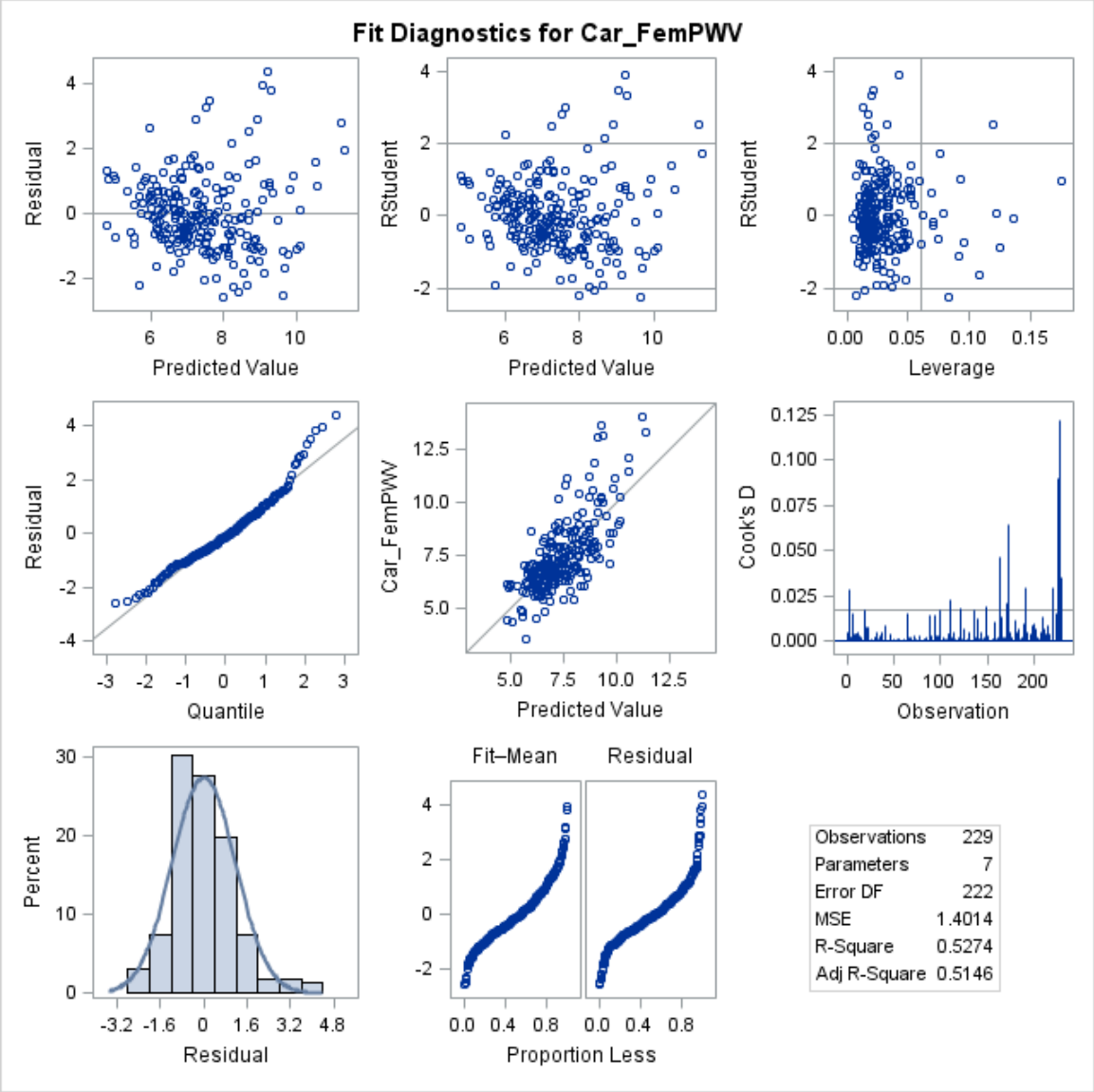

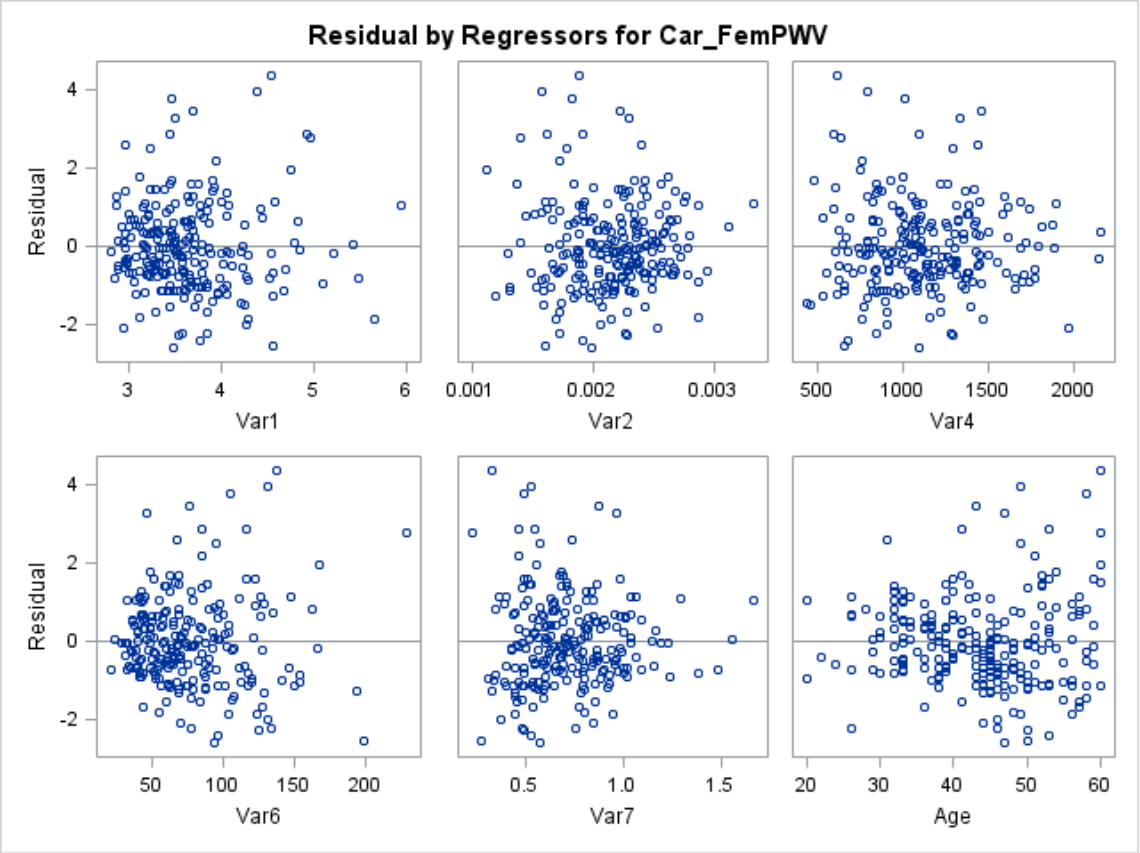

As per table 20, we observe that the coefficients' standard errors improve and become more stable. Moreover, Var2's coefficient becomes significant. The plots of residuals show a random pattern and QQ plot improves (graphs combination). RMSE value becomes smaller and Adjrq slightly increases to 0.5146 (R=73%). To further analyze this model we examine if it agrees with the established method. We apply Bland Altman analysis on this Model and generate the following results (figure 48):

Bias=0 LA=1.96*1.168128 = +/- 2.3

PE = 2.3/7.37 = 0.31

Figure 48: Bland Altman for PWV-Model 7

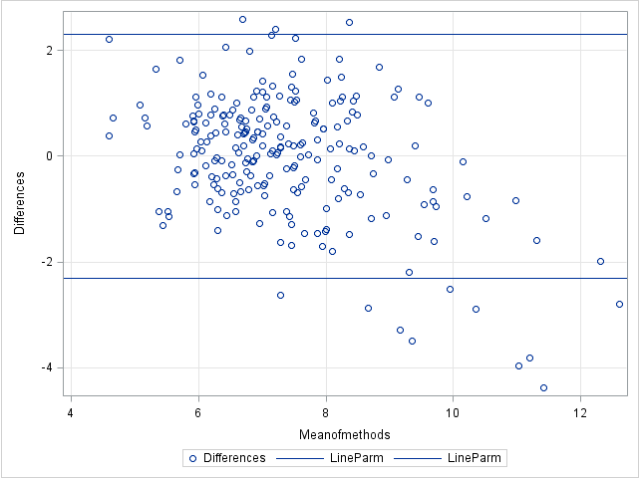

We observe that the limits of agreement are narrower than the previous models (explored earlier) for PWV. We also observe that if we keep only Var 2 and Age in the equation, we generate a similar result but with a "simpler" model:

Model 8

Car_FemPWV = f (Var2 Age) , **for Ages<=60**

Despite being very simple and minimalistic, this Model manages to generate a relatively fair result with an Adjrq of 0.49 and the following output:

Bias=0 LA=1.96*1.2191 = +/- 2.4 PE = 2.4/7.37 = 0.33 R=70% RMSE=1.22

This last model displays the importance of variable 2 and its significant contribution to the relationship, especially when combined with Age. Further investigation is needed though as the contribution of the other predictor may be necessary to the overall relationship.

The above methods show that overall there is a moderately good relationship between IFs method and the reference method of evaluating PWV. Since we generated many models targeting individuals 60 years old or less, we also need a model targeting individuals older than 60 years old. However, our training database (FHS_400) does not include enough observations to run such regression analysis without over-fitting our data. We would need approximately 20 datapoints per predictor, which we currently don't have within the training set (we only have 49 subjects above 60). Also, since the data points for subjects above 60 showed a non-linear pattern, we should follow the recommendations of the European Heart Journal that we reviewed earlier in the literature search section: develop a model according to age and blood pressure category in order to produce better result and include the interval 60 and over.

Nevertheless, since our results for subjects 60 years old or less were adequate, we decide to further validate them by testing a few of the above models on FHS_6500 dataset.

4.1.3.2 Testing process

We apply some of the learned algorithms previously obtained with FHS_400 database on FHS_6500, our testing database, which contains 5,684 useable observations (after filtering and eliminating the missing values). It also includes FHS_400 training set that we previously used. We could not exclude this training set from the new set as the SUBID numbers have been modified. Pearson Correlation and Bland Altman results are displayed:

Model 4:

Car_FemPWV = f (var1 var2 var3 var4 var5 var6 var7 var8) – Obs=5684

Model 4 : Bias = 0.07m/s LA(unbiased) = +/- 5.986m/s r=0.52 p<0.0001

PE=(5.986/8.44) * 100 = 70.9%

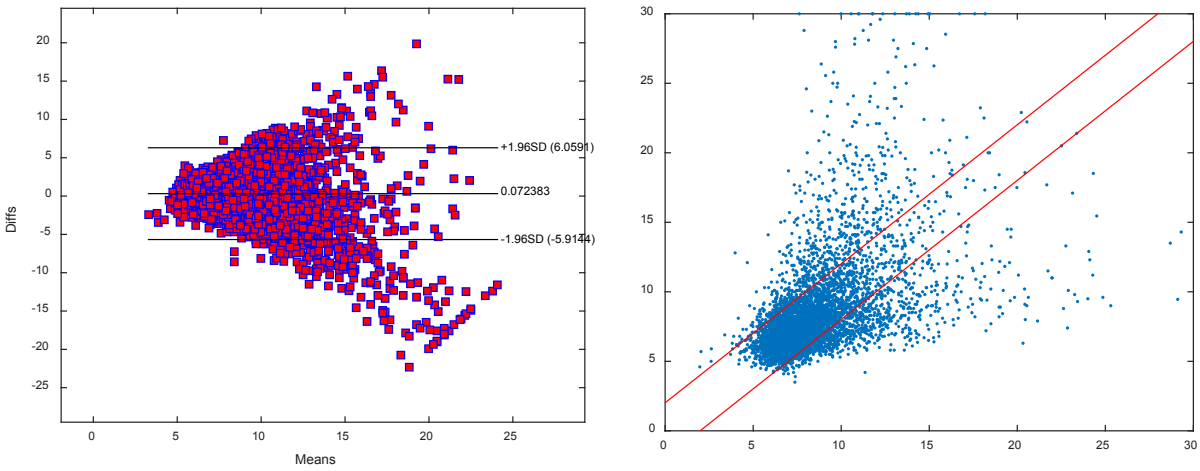

Figure 49: Bland Altman and identity line– FHS-6500-testing Model 4 – All ages

Model 4 but with Age categorization: Age<= 60 Obs= 4437

Car_FemPWV = f (var1 var2 var3 var4 var5 var6 var7 var8) with Age<=60

Bias = 0.56m/s LA = +/- 3.68m/s r=0.43 p<0.0001 PE=(3.68/7.26) * 100 = 50.68%

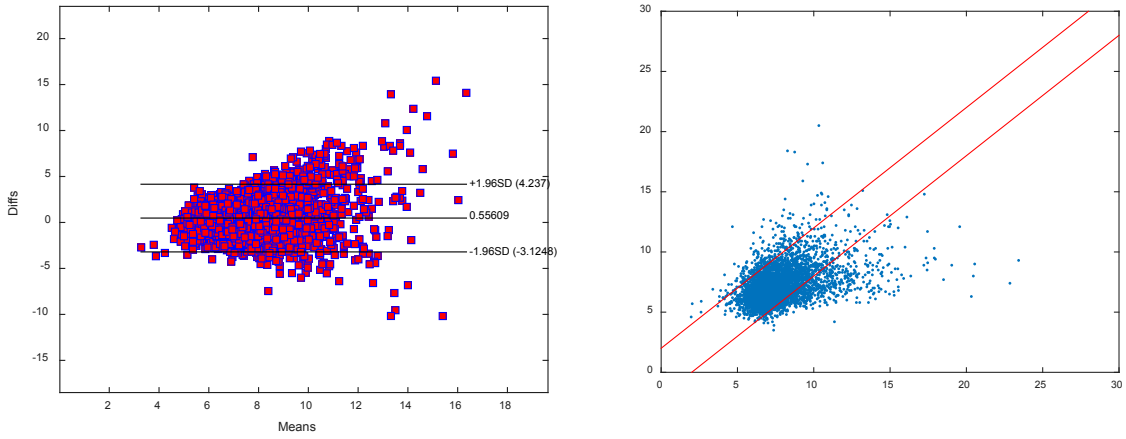

Figure 50: Bland Altman and identity line– FHS-6500-testing Model 4-Age<=60

Model 6:

Car_FemPWV = f (var1 var2 var3 var4 var5 var6 var7 var8 Age) Ages<=60 ; Obs=4437

Bias = 0.59m/s LA = +/- 2.84m/ r=0.62 p<0.0001 PE=2.84/7.26 = 39%

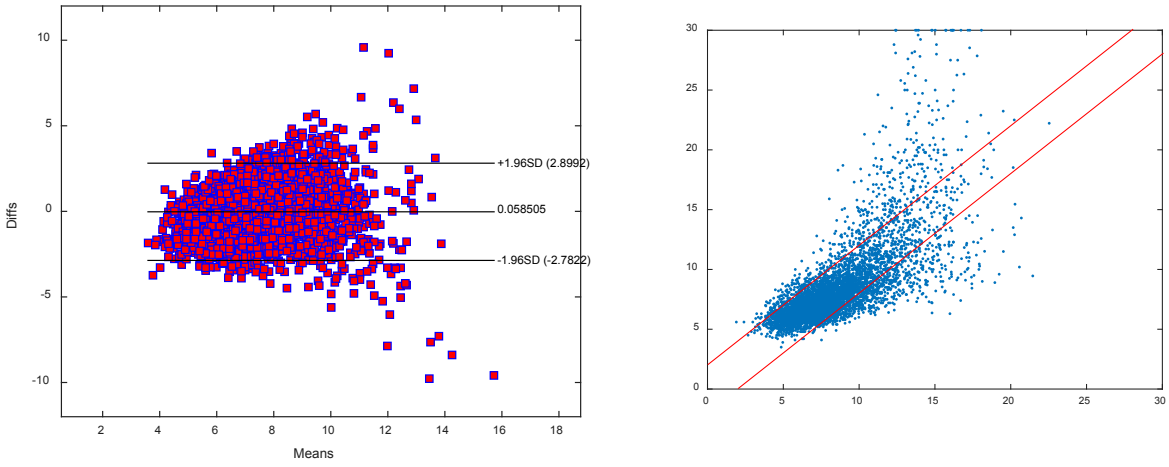

Figure 51: Bland Altman and identity line– FHS-6500-testing Model 6

Model 7

Car_FemPWV = f (var1 var2 var4 var6 var7 Age), for Ages<=60 ; Obs=4437

Bias = -0.021m/s LA = +/- 2.37m/s; r=0.64 p<0.0001 PE = 2.37/7.26=32.64%;

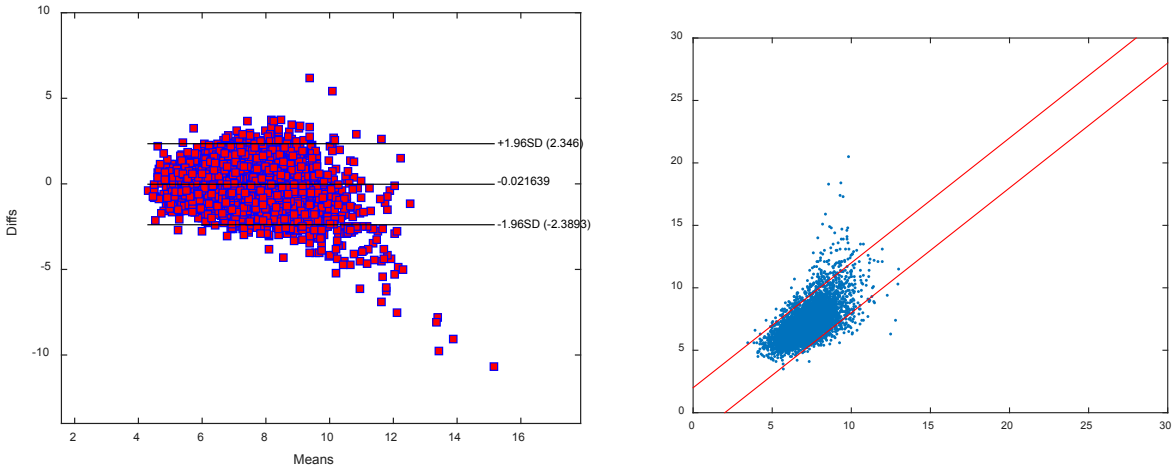

Figure 52: Bland Altman and identity line– FHS-6500-testing Model 7 – Age<=60

Model 7 but with Age<=70 ; Obs=5054

Car_FemPWV = f (var1 var2 var4 var6 var7 Age), for Ages<=70

Bias = -0.15m/s LA = +/-3.1m/s r=0.67 p<0.0001 PE = (3.1/7.67)*100= 40%

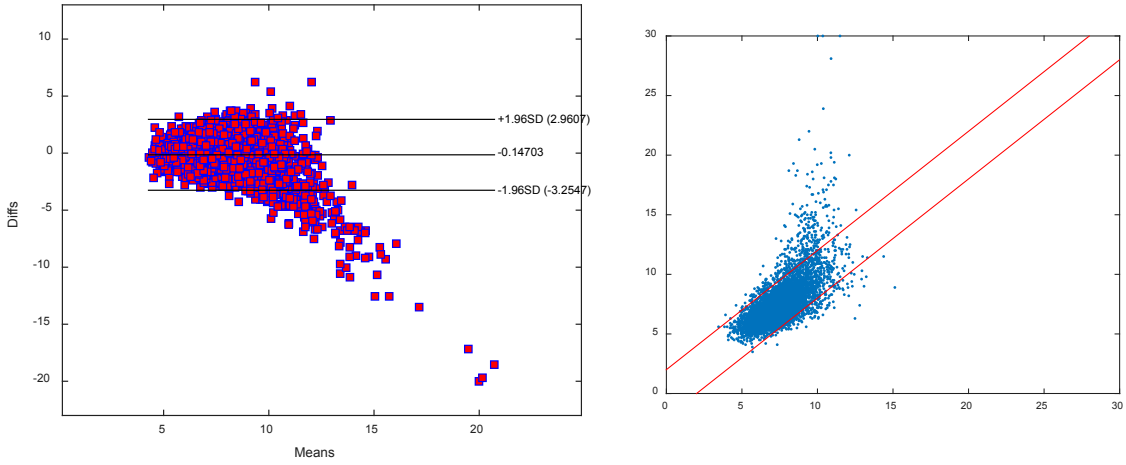

Figure 53: Bland Altman and identity line– FHS-6500-testing Model 7 – Age<=70

4.2 Discussion

Heart disease is a leading cause of death in America. It also implicates disability and excessive medical costs. New monitoring technologies are imperative to reduce the burden of CVDs. The principal aim of our research was to statistically evaluate a new non-invasive methodology that could potentially offer an inexpensive, safe and practical solution to the epidemic of heart disease. This novel approach, based on IFs technique (which includes a combination of IFs indices and heart shape factors), could generate estimates of the major cardiovascular parameters, such as LVEF, CO and PWV. Ideally, any new assessment technique should be able to provide measurements close to the values produced by an established method. Consequently, we statistically compared IFs

results to the values generated by the established technologies (which we used as reference methods). We applied "Supervised Machine Learning" and used Regression to develop "trained" models that would best represent the relationship between IFs technique and conventional methods. These trained algorithms were subsequently applied on testing datasets to evaluate their prediction strength and percentage error. Bland Altman analysis was applied to the selected models in order to highlight the "clinical agreement" between the IFs technique and the established monitoring methods since, according to published studies, the Pearson correlation "per se" is not sufficient to validate measurements produced by a new device compared to a conventional technology.

IFs methodology produced promising results, which we discuss throughout this chapter. These results bring us one step closer to the use of a safe, practical and cost-efficient cardiovascular monitoring technology, which can be performed anyplace and anytime. Indeed, the IFs algorithm can be inserted in any light-weight sensor type device (such as an iPhone) rendering the entire monitoring procedure handy and inexpensive. This ease of usage is mainly due to the fact that the IFs indices rely exclusively on the "shape" of the subject's arterial pressure-wave and not the magnitude. This aspect of this method is very valuable since unlike many current heart assessment technologies where bulky devices and wires are involved, IFs technique does not require sophisticated machines. This new method can go mobile and render the overall cardiovascular monitoring procedure stress-free and inexpensive. In the following sections, we discuss

and interpret the results generated by the IFs methodology and compare them to the outputs produced by conventional devices currently in use.

4.2.1 Estimating LVEF values by IFs

We performed an observational study to validate the use of IFs methodology for estimating LVEF measurements. We used both HMRI and FHS databases. In order to produce an optimal algorithm, we applied the regression technique and trained our model, by pairing the input with the expected output. We then checked for the adequacy of the selected model by diagnosing the fit and the residual plots. Next, to assess the accuracy and precision of the learned (fitted) function or algorithm, we applied Bland Altman analysis. Lastly, the performance of the learned function was measured on a test set that was separate from the training set.

The results of this study showed that the calculated LVEF values derived from IFs_Tonometry displayed a weak correlation with the LVEF measurements produced by Echocardiography, even though the limits of agreement were adequate. This discrepancy could be related to the different "range" of LVEF values used in the training and testing databases. The training database (HMRI) had a wider range of observations, including a few low LVEF values (as seen in figure 15, graphs combination related to LVEF-Model 4), adding linearity to the shape of the related scatterplot and thus, producing a better correlation ($R=0.79$, $Rsquare=0.62$, Adjusted $Rsquare=0.61$, $p<0.0001$). The testing database (FHS) did not include any low LVEF values and therefore the range of the data-points was narrower, leading to a weak correlation coefficient ($r=0.2$) and datapoints forming a sphere shape. In conclusion, the results of LVEF estimations from

IFs_Tonometry were not conclusive and may need further evaluation by considering a database that includes a reasonable number of low LVEF values.

The results of the calculated LVEF values generated from IFs_iPhone models revealed a strong and significant correlation with LVEF measurements from MRI ($r=0.79$, $p<0.0001$, testing set related to Model 2). Moreover, the corresponding outputs generated from Bland Altman analysis were adequate and consistent: the calculated LVEF measurements from IFs_iPhone and the LVEF values from MRI were closely in agreement, displaying a low percentage error. We can state that our IFs_iPhone results were promising. They revealed that IFs method and established technique of LVEF assessment are in good agreement.

A summary of the LVEF analysis is featured below (the LA values are unbiased):

- **LVEF_IFs measures from tonometry derived waveforms:**

Training Model 4 (HMRI database with **MRI** as reference method):

Predicted EF = f(Var1 Var2 Var3 Var4)

Adjrq = 0.61 RMSE = 7.51 R=0.79 p<0.0001

Bias= -0.04% LA=+/- 14.48% P.E= 25%

Testing Model 4 (FHS_400 database with **Echo** as reference):

Predicted EF = f(Var1 Var2 Var3 Var4)

Bias= 1.8595% LA=+/- 10.17% P.E= 16% r=19%

Testing Model 4 (FHS_6500 database with **Echo** as reference):

Predicted EF = f(Var1 Var2 Var3 Var4)

Bias=1.62% LA= +/-10.71% PE = 16.8% r=20% p<0.0001

- **LVEF_IFs measures from iPhone derived waveforms:**

Training of Model 2 (HMRI-ref = **MRI**):

Predicted LVEF = f(BPM1 Omega1Bar Omega2Bar NodeY DF Duration Envratio)

Adjrq = 0.46 RMSE = 8.89 R=71% p<0.0001

Testing model 2 (ref=**MRI**):

Bias= 1.763% LA=+/- 17.44% r= 79% p<0.0001 P.E= 31.2%

Training Model 3 (HMRI-ref=**MRI**):

LVEF = f(BPM1 Omega1Bar DF Envratio)

Adjrq = 0.42 RMSE = 9.17 R=67% p<0.0001

Testing model 3 (HMRI-ref=**MRI**):

Bias= 1.138% LA=+/- 18.53% r=76% p<0.0001 P.E= 33%

To further explore if these results for the assessment of LVEF were satisfactory, we compared them to the outcome of popular devices. We observed that the above numbers were approximately as suitable as the numbers generated in the study performed by Greupner et al, during which they assessed LVEF with 64-Row CT, CVG and 3D echo in comparison with MRI[86]:

CT:	Bias=0	LA=14.2%	PE=14.2/55.6=25.5%	r=0.89
CVG:	Bias=5 %	LA= +/-20.2%	PE= 20.2/55.6= 36.3%	r=0.77
3DEcho:	Bias=-2%	LA=+/-21.2%	PE= 21.2/55.6= 38.1%	r=0.79

Thus, our results suggest that the proposed IFs_iPhone models allow a reasonably good evaluation of LVEF. Indeed, this non-invasive technique can perform close to the established reference methods. Furthermore, since the related algorithm can be embedded in a simple sensor type device, this novel non-invasive technique can be easily used by the patient within a clinical as well as a non-clinical environment, such as home or office.

4.2.2 Estimating CO values by IFs

Various methods of CO measurement are being currently in use, but most of them are invasive, unsafe and expensive. Moreover, they require a clinical setting which is not always available. Throughout this study, we showed that IFs estimations of CO significantly correlated ($p<0.0001$) with CO measurements produced by the established technique (MRI). We used the HMRI setting to statistically analysis this relationship. The actual CO measurements were performed via MRI and the IFs indices were extracted from the subjects' carotid waveform, captured through tonometry. In a study regarding CO measurements, Critchley et al, stated that if the PE of a new method is less than 30%, the two methods could be used interchangeably[118]. Thus, with respect to this argument, we produced PE values for IFs methodology, while performing a comprehensive Bland Altman analysis of the "learned" models that we previously obtained through regression. The equation related to Model 2 included IFs core variables only and it led to a PE of 41%. We noticed that if we include "Weight" as an explanatory variable, our results improve. According to Jegier et al., CO is closely related to the size of the individual[131]. We observed this trend within our own study with Model 4, when we included Weight:

the value of the multiple correlation coefficient (between CO measures from MRI and CO values from IFs) jumped from 0.52 to 0.68 and PE decreased from 41% to 36%. Below is a highlight of the different trained models (Bias and LA are expressed in L/min):

Model-2 (ref=**MRI**)

Calculated CO = f(Omega1Bar Omega2Bar NodeX DF Duration Envratio)

Adjrq = 0.23	RMSE = 1.06	R=52%	p<0.0001
Bias =0	LA=+/- 2.04	PE=41%	

Model-4 (ref=**MRI**)

Calculated CO = f(Omega1Bar Omega2Bar NodeX DF Duration Envratio Weight)

Adjrq = 0.42	RMSE = 0.95	R=68%	p<0.0001
Bias = 0	LA=+/- 1.78	PE=36%	

Model-5 (ref=**MRI**)

Calculated CO = f(Omega2Bar Weight)

Adjrq = 0.4	RMSE = 0.92	R=65%	p<0.0001
Bias = 0	LA=+/- 1.86	PE=38%	

The above models generated percentage errors slightly above the targeted threshold, however Model 4's PE was very close to the benchmark of 30%. To have an acceptable PE for CO, the limits of agreement in our study should not be wider than +/- 1.5 L/min (4.95*0.3). We can pursue that even though there is a moderately good correlation between IFs and MRI methods of CO assessment, the precision of Model 4 needs to be slightly improved. We can perhaps achieve this objective by adding

parameters that are related to BSA, since the strategy of transforming variables did not produce suitable results. We decided to further evaluate the performance of IFs technique, by comparing our best model to the minimally invasive methods currently in use, such as PICCO, VolumeView as well as to a non-invasive technique like Nexfin. The following results were generated for these devices through various recent studies (Bias and LA are expressed in L/min):

Nexfin (ref=TPTD)[101]	Bias = 0.4	LA=2.32	PE=36%	r=0.82
Nexfin (ref=PCA)[101]	Bias=0.2	LA=2.32	PE=37%	r=0.84
CCO VolumeView (ref=TPTD)[129]	Bias=-0.07	LA=2	PE=29%	r=0.83
CCO PICCO (ref=TPTD)[129]	Bias=0.03	LA=2.48	PE=37%	r=0.76

These methods are all based on arterial pulse contour analysis for continuous CO measurements. We notice that although these techniques are currently in use within the clinical practice, most of them do not meet the alleged Critchley criteria of an acceptable PE. Thus, despite the fact that the results obtained for IFs with Model 4 need improvement, the related PE (36%) is close to the PE value obtained for Nexfin or PICCO, showing therefore a relatively good precision and accuracy. We should also emphasize that this routinely used PE error threshold has been questioned by Peyton and colleagues: they showed that "no group" of the minimally invasive hemodynamic monitoring tools, such as Doppler, met the set PE threshold and thus it has been discussed that for medical applications, a larger value for PE needed to be considered ("based on the limitations of all CO" measurement methods)[128]. The performance of IFs

method is nevertheless as reliable as the above devices. However, a testing dataset is required to further validate this statement.

4.2.3 Estimating PWV values by IFs

Arterial stiffness, assessed by PWV is a crucial biomarker of heart diseases. The efficient monitoring of this parameter can greatly decrease the mortality rate. Throughout this study, we used FHS database and showed that IFs method was suitable for PWV estimation. Indeed, there was a significant correlation between this new method and the standard technique, which consisted of the simultaneous use of two-tonometers. We applied different statistical analysis to examine this relationship. In this section, in order to further discuss our results, we compare them to those obtained with similar non-invasive reference technologies, such as Pulse Trace, Complior and PulsePen. In a study led by Salvi et al. in 2008 on a population of 50 individuals (male and female between the ages of 20 and 84 years), these 3 methods were compared to the established 2-tonometers method (which is the same as our reference method) and the following results were published (Bias and LA are expressed in m/s):

Pulse Trace:	Bias = -1.12	LA=+/- 4.92	PE=61%	r=0.73
Complior:	Bias = 2.09	LA = +/- 2.68	PE=33.2%	r=0.83
PulsePen:	Bias = -0.15	LA=+/- 0.62	PE=7.6%	r=0.99

In order to compare our results to the above calculations and to efficiently evaluate IFs method of estimation, we developed several models. Our selection process was mainly based on the following 2 criteria: Adjusted Rsquare and VIF, for which we set a threshold

of 10 to address multicollinearity. Numerous models were obtained. Most of them displayed a good accuracy with the reference method, but some revealed a low precision. We tried to increase the precision level by narrowing the limits of agreement. The results are featured below:

Model 4: Predicted Car_FemPWV = f(Var1 Var2 Var3 Var4 Var5 Var6 Var7 Var8)

Training:

Adjrq = 0.53 R=0.73 p<0.0001 RMSE = 2.27

Bias = 0 LA=+/- 4.38 PE=52%

Testing:

- No Age categorization:

Bias = 0.07 LA=+/- 5.986 PE=71% r=0.52

- Age <= 60:

Bias = 0.56 LA = +/- 3.68 PE= 51% r=0.43

Model 6:

Predicted Car_FemPWV = f(Var1 Var2 Var3 Var4 Var5 Var6 Var7 Var8 Age) with Age<=60

Training:

Adjrq = 0.51 R=0.73 p<0.0001 RMSE = 1.19

Testing:

Bias = 0.059 LA = +/- 2.84 PE = 39% r=0.62

Model 7: Predicted Car_FemPWV = f(Var1 Var2 Var4 Var6 Var7 Age)

- With Age<=60

Training:

Adjrq = 0.51 R=0.73 p<0.0001 RMSE = 1.18

Bias=0	LA=+/- 2.3	PE=31%	
Testing:			
Bias = -0.022	LA = +/- 2.37	PE = 33%	r=0.64

- With Age<=70

Testing:			
Bias = 0.15	LA = +/- 3.1	PE = 40%	r=0.67

The above results show that there is a reasonable association between IFs method and the more established method of PWV measurement (2-Tonometers). IFs method shows a good accuracy. The precision of the method increases when we include Age as an explanatory variable, in conjunction with "age categorization". Indeed, the limits of agreement become narrower and the PE decreases with Model 7, which includes Age in the equation and at the same time targets individuals that are 60 years old or younger. This model thus reveals an increased precision and shows that the overall performance of IFs method is significantly better than Pulse-Trace technique, where the limits of agreement are wider and the precision smaller. The results that we produced are closer to Complior's results. However, Pulsepen performance remains superior. According to Salvi et al, the existing strong relationship between Pulsepen and the 2-tonometers (reference technique) is mainly due to the fact that both methods use a nearly similar algorithm. Indeed, "the algorithm used by PulsePen software to determine the foot of the pressure wave closely follows the method used by the two operators to detect the waveform foot printed on the paper"[126]. Thus, the performance of Pulsepen needs to be further reviewed. Moreover, both Complior and PulsePen methods profoundly depend

on the adeptness of the operator to produce reliable results. These devices can be expensive to use too. In contrast, IFs method does not involve trained health professionals. It can be performed within a non-clinical setting such as home or office and therefore reduce medical costs considerably.

CHAPTER V CONCLUSION AND RECOMMENDATIONS

IFs method becomes one step closer to a safe, practical and inexpensive solution to the epidemic of heart diseases. The present study revealed that the estimations of LVEF, CO and PWV by the IFs technique are close to the values produced by the established devices. There is indeed a moderately strong and significant correlation between this novel technique and the conventional methods of cardiovascular monitoring and the limits of agreement are acceptable. In future studies, we recommend to strengthen this relationship and agreement by addressing the limitations that we encountered during this investigation. In the below sections, we highlight some of the measures that we could implement in regards to LVEF, CO and PWV estimations, in order to enhance the overall performance of the IFs method.

5.1 Agreement between IFs and established devices to assess LVEF

The overall results showed that IFs can effectively estimate LVEF and that the measurements are in clinical agreement with the values produced by the established devices. Indeed, IFs (Model 2-iPhone) and MRI displayed a strong correlation ($r=0.79$, $p<0.0001$) and the clinical agreement was acceptable: bias = 1.76% and the unbiased LA=+/- 17.44%. However, IFs_iPhone study produced better results than IFs_Tonometry study. Indeed, there was a divergence of correlation results between the training and testing sets for LVEF values derived from IFs_Tonometry and LVEF

measurements produced from the conventional devices. Moreover, as per figure 16 and 19, some of the low LVEF values were unreasonably calculated by our regression algorithm. This is due to the fact that we had a limited number of observations with low LVEF values. We need additional low LVEF values in our training set to better "train our data" and ensure that the produced algorithm estimates low LVEF measurements adequately in a new dataset. We also need low LVEF values in our testing sets, especially in FHS_400 (which had none). This is the underlying reason for the small correlation coefficient obtained between the estimated and actual LVEF values in our FHS_400 testing set (r=0.19). The correlation coefficient in the training set (HMRI) was larger (R=0.79) because it contained more low LVEF values and thus the "range" of LVEF values in the training database was wider, making the shape of the estimates closer to a linear form (figure 16). However, the range of values was narrower in the FHS400 testing set as it lacked low LVEF measurements (figure 18). Therefore, in future studies we strongly recommend to use a database that includes a reasonable number of low LVEF values to explore a revised and improved model that addresses the above issue.

In future studies, we also recommend to further investigate the impact of measures produced with different devices. Indeed, for LVEF_tonometry estimations, we used a training database that had MRI as the reference technology and then we tested the related learned algorithm on a database that had Echo as the reference method. Additional studies are needed to investigate possible discrepancies between the results obtained with the use of various reference devices.

5.2 Agreement between IFs and established devices to assess CO

Within our study we demonstrated that there is a moderately strong relationship between CO measures produced by MRI and CO values generated via IFs method: R=0.68, p<0.0001, bias = 0 and LA (unbiased)=+/- 1.78 L/min. We observed that IFs estimations of CO improved when we included Weight as a predictor and did not vary much when we used Age. Indeed, according to Jegier et al., Cardiac Output varies depending on the size of the subject[131]. In future studies, we could ultimately use "Cardiac Index" as a response variable instead of Cardiac Output since Cardiac Index is a function of the cardiac output and square meter of BSA. If we continue using cardiac output as a response variable, we can target Height instead of BSA in our training equation to improve our model. Our training database (HMRI) was limited as we did not have values related to Height or BSA of the subjects. We recommend to include these important parameters and also split the data into male and female since BSA differs accordingly, generating different outputs. We also recommend to use a new dataset to test the trained algorithms. Our testing dataset (FHS_400) was limited at the time of study since it did not include Weight. Moreover, it would be more effective to statistically compare IFs method with a reference method such as, Thermodilution, the gold standard for CO measurements, which has been used for over 20 years[129,138]. All these measures could greatly refine the results obtained for IFs methodology.

5.3 Agreement between IFs and established devices to assess PWV

IFs estimation of PWV were promising and IFs displayed a moderately strong and significant correlation with Tonometry (r=0.64, p<0.0001). The clinical agreement

between IFs and Tonometry was reasonable: bias = -0.022 m/s and the unbiased LA = +/- 2.37 m/s. In the future, we can further improve the results if we implement a more segmented Age grouping in conjunction with "Blood Pressure" (BP) categorization. Indeed, as we pointed out in the literature review section, in a study published by European heart journal in 2010, scientists demonstrated that PWV increases with both age and BP category and Reference values were established after PWV values "were categorized by age "decade" and subdivided according to BP categories"[130]. We observed within our own study and model analysis that a slight age grouping helped improve results. The data points are approximately linear up to the age of 60, but they become dispersed afterward. Thus, we recommend a new trained algorithm (formula) that would specifically target individuals older than 60 years old. Our training database (FHS_400) did not include enough observations to run such regression analysis without over-fitting our data. We needed approximately 15 to 20 points per predictor (to avoid overfitting and type 2 errors), which were not available at the time of the study as we only had 49 subjects above 60. In order to enhance the results that we found earlier, we also recommend to filter the data between male and female subjects. Indeed according to a previous study that we performed a few months ago with the same database (FHS_400), which included 142 male and 156 female subjects of 60 years old or less, male subjects displayed a higher correlation for PWV ($r=0.72$, $p<0.0001$), compared to females of same age group ($r= 0.52$, $p<0.0001$), when we used IFs core variables. However, it seems that this divergence diminishes when we include other predictors in our equation, such as age. Thus, further examination on this finding is recommended.

In future studies, we can greatly improve the performance of IFs method for estimating PWV by considering all the above measures and also by categorizing our database according to both age and blood pressure. Implementation of this plan requires a larger database. We can consequently use the new FHS_6500 as both a training and testing sets, since it includes over 5,000 data points. We can randomly partition the data set into two groups, for example 70% for training and 30% for testing. By including more data points in the training set, we can also produce stronger equations since our parameter estimates would have smaller variances.

References

1 - Murphy SL, Xu JQ, Kochanek KD. Deaths: Final data for 2010. National Vital Statistics Report, 2013;61(4)

2 - Centers for Disease Control and Prevention. http://www.cdc.gov/dhdsp/data_statistics/fact_sheets/fs_heart_disease.htm. Accessed February 10, 2015.

3 - What is coronary Heart Disease, NIH, National Heart, Lung and Blood Institute http://www.nhlbi.nih.gov/health/health-topics/topics/cad. Accessed February 10, 2015.

4 - Hypertension explained: How to Understand Blood Pressure Readings http://www.healthline.com/health/high-blood-pressure-hypertension/blood-pressure-reading-explained. Accessed March 4, 2016.

5 - Blood Pressure https://en.wikipedia.org/wiki/Blood_pressure. Accessed February 11, 2015.

6 - Centers for Disease Control and Prevention. http://www.cdc.gov/heartdisease/cardiomyopathy.htm. Accessed February 7, 2015.

7 - Maron BJ, Doerer JJ, Haas TS, et al. Sudden Deaths in young competitive athletes: analysis of 1866 deaths in the United States, 1980-2006. *Circulation.*2009;119(8):1085-1092.

8 - Maron BJ, McKenna WJ, Danielson GK, et al. American College of Cardiology/European Society of Cardiology clinical expert consensus document on hypertrophic cardiomyopathy. *Journal of the American College of Cardiology*. 2003;42(9):1687-1713.

9 - Zaret BL. What can go wrong. In: *Yale University School Of Medicine Heart Book*. New York: William Morrow and Co.; 1992:11-20

10 - Elwardt HA. Let's Stop the #1 Killer of Americans Today, A Natural Approach to Preventing & Reversing Heart Disease. AuthorHouse; 2006:10

11 - Life After Sudden Death. *Life After Sudden Death*. Available at: http://www.cedars-sinai.edu/patients/programs-and-services/heart-institute/centers-and-programs/clinical-electrophysiology/life-after-sudden-death.aspx. Accessed January 21, 2015.

12 - Cardiac Arrest: MedlinePlus. *U.S National Library of Medicine*. http://www.nlm.nih.gov/medlineplus/cardiacarrest.html. Accessed January 21,2015.

13 - Chronic disease prevention and health promotion, http://www.cdc.gov/chronicdisease/resources/publications/AAG/dhdsp.htm. Accessed January 22, 2015.

14 - Morgan B. Critical Care Concept: Hemodynamic Waveform Interpretation. 2005. http://www.caccn.ca/en/pdfs/4a hemodyn_waves (b morgan).pdf. Accessed September 18, 2015.

15 - Dulak S. PA catheters: What the waveforms reveal. *Modern medicine*. http://www.modernmedicine.com/modern-medicine/content/pa-catheters-what-waveforms-reveal?page=full. Accessed February 8, 2015.

16 - Foucha B. The ABCs of A to V: Right Atrial/ Left Atrial (PCW) Pressures. *Cath Lab Digest* 2009. http://www.cathlabdigest.com/articles/the-abcs-a-v-right-atrial-left-atrial-pcw-pressures. Accessed September 24, 2015.

17 - Cardiovascular Disorders (Adult Care Nursing) Part 4. *whatwhenhow RSS*. http://what-when-how.com/nursing/cardiovascular-disorders-adult-care-nursing-part-4/. Accessed February 2, 2015

18 - The cardiac cycle. *YouTube*. https://www.youtube.com/watch?v=5tuwof6wenk. Accessed February 25, 2015.

19 - Khurana I. *Textbook Of Medical Physiology*. New Delhi: Elsevier; 2006: 279.

20 - The Sinoatrial Node: The Body's Natural Pacemaker. http://hyperphysics.phy-astr.gsu.edu/hbase/biology/sanode.html. Accessed February 15, 2015.

21 - The electrical and mechanical sequence of a heartbeat, http://www.csun.edu/~vcpsy00i/dissfa01/xECG_Lesson.html. Accessed February 26, 2015

22 - Reinking L. Cardiopulmonary physiology, Pumping action of the heart. *millersville.edu*. Accessed January 8, 2015

23 - Hemodynamics, http://www.merriam-webster.com/dictionary/hemodynamics, Accessed December 27, 2014.

24 - What Is Atrial Fibrillation? - *NHLBI, NIH*. http://www.nhlbi.nih.gov/health/health-topics/topics/af. Accessed January 27, 2015

25 - Mukkamala R, Kuiper J, Sala-mercado JA, et al. Continuous left ventricular ejection fraction monitoring by central aortic pressure waveform analysis. Conf Proc IEEE Eng Med Biol Soc. 2006;1:620-3.

26 - Parragh S, Hametner B, Bachler M, Weber T, Eber B, Wassertheurer S. Non-invasive wave reflection quantification in patients with reduced ejection fraction. Physiol Meas. 2015;36(2):179-90.

27 - Gulanick M, Myers JL. Nursing Care Plans - Pageburst E-Book on VitalSource (Retail Access Card), Diagnoses, Interventions, and Outcomes. Mosby Incorporated; 2013.

28 - Pahlevan N, Tavallali P, inventors; California institute of technology, assignee. Intrinsic Frequency Hemodynamic Waveform Analysis. US patent 20130184573 A1, July 18, 2013

29 - Pahlevan N, Tavallali P, Rinderknecht DG, et al. Intrinsic frequency for a systems approach to haemodynamic waveform analysis with clinical applications. *Journal of The Royal Society Interface* 2014:20140617–20140617.

30 - Tavallali P, Hou TY, Shi Z. Extraction of Intrawave Signals Using the Sparse Time-Frequency Representation Method. *Multiscale Modeling & Simulation Multiscale Model. Simul.*:1458–1493.

31 - What is a waveform? http://www.techopedia.com/definition/269/waveform. Accessed March 10, 2015

32 - Kani AN. *Signals And Systems*. New Delhi, India: Tata McGraw Hill Education; 2010.

33 - Forouzan BA, Fegan SC. *Data Communications and Networking*. 4th ed. New York: McGraw-Hill Higher Education; 2007:57.

34 – Myocardial Infarction. https://simple.wikipedia.org/wiki/Myocardial_infarction Accessed February 5, 2015.

35 - Marzullo P, Parodi O, Marcassa C, Neglia D, L'abbate A. When the electrocardiogram fails to define site and extent of myocardial ischemia. Can J Cardiol. 1986;Suppl A:85A-90A.

36 - What is an electrocardiogram? http://www.patient.co.uk/health/electrocardiogram-ecg. Accessed February 5, 2015.

37 - Electro-cardiogram library, http://www.ecglibrary.com/ecghome.php. Accessed February 5, 2015.

38 - Jain PK, Tiwari AK. Heart monitoring systems--a review. Comput Biol Med. 2014;54:1-13.

39 - Galeotti L, Johannesen L, Vincente J, Strauss DG. Measurement of noise in ECG signals to improve automatic delineation. http://www.researchgate.net/publication/261036824_measurement_of_noise_in_ecg_signals_to_improve_automatic_delineation. Accessed March 1, 2015.

40 - Cardiac catheterization, http://www.heartpoint.com/cathtell.html. Accessed March 1, 2015

41 - NIH Study Shows MRI Provides Faster, More Accurate Way To Diagnose Heart Attacks http://www.nih.gov/news/pr/jan2003/nhlbi-29.htm, Accessed on January 2, 2015.

42 - Why Does an MRI Cost So Darn Much? http://time.com/money/2995166/why-does-mri-cost-so-much. Accessed February 5, 2015

43 - Waves and Complexes, http://meds.queensu.ca/central/assets/modules/ECG/waves_and_complexes.html. Accessed February 19,2015.

44 - U-wave, http://lifeinthefastlane.com/ecg-library/basics/u-wave/ Accessed February 3, 2015

45 - Magnetic Resonance Imaging (MRI) - Cardiac (Heart), http://www.radiologyinfo.org/en/info.cfm?pg=cardiacmr, Accessed February 3, 2015.

46 - Heart MRI: MedlinePlus Medical Encyclopedia. *US National Library of Medicine*. Available at: http://www.nlm.nih.gov/medlineplus/ency/article/003795.htm. Accessed February 9, 2015.

47 - Masoudi FA, Magid DJ, Vinson DR, et al. Implications of the failure to identify high-risk electrocardiogram findings for the quality of care of patients with acute myocardial infarction: results of the Emergency Department Quality in Myocardial Infarction (EDQMI) study. Circulation. 2006;114(15):1565-71.

48 - Cardiac Catheterization/Angioplasty, http://www.caccllc.com/page/tests/cardiac-catheterization, Accessed February 3, 2015

49 - Cardiac catheterization, http://www.heartpoint.com/cathtell.html Accessed February 3, 2015

50 - Heart Catheterization, http://www.womens-health-advice.com/heart-disease/cardiac-catheterization.html, Accessed February 4, 2015

51 – Wiggers Diagram, https://commons.wikimedia.org/wiki/File:Wiggers_Diagram.svg Accessed February 4, 2015

52 - Tan I, Butlin M, Liu YY, Ng K, Avolio AP. Heart rate dependence of aortic pulse wave velocity at different arterial pressures in rats. Hypertension. 2012;60(2):528-33.

53 - Pulsewave velocity, http://www.datasci.com/solutions/cardiovascular/pulse-wave-velocity. Accessed March 1, 2005

54 - Salvi P, Palombo C, Salvi GM, Labat C, Parati G, Benetos A. Left ventricular ejection time, not heart rate, is an independent correlate of aortic pulse wave velocity. *Journal of Applied Physiology* 2013:1610–1617.

55 - Martini F, Bartholomew EF. The cardio vascular system: the heart. In: *Essentials of Anatomy &Amp; Physiology*. 6th ed. Boston: Pearson; 2013.

56 - The Electrical and Mechanical Sequence of a Heartbeat, http://www.csun.edu/~vcpsy00i/dissfa01/xECG_Lesson.html. Accessed February 10, 2015.

57 - MIT algorithm measures your pulse by looking at your face, http://www.wired.co.uk/news/archive/2012-07/25/mit-algorithm, Accessed March 5, 2015.

58 - MIT releases open-source software that reveals invisible motion and detail in video. *http://www.extremetech.com/extreme/149623-mit-releases-open-source-software-that-reveals invisible-motion-and-detail-in-video. Accessed March 5, 2015.*

59 - Eulerian Video Magnification, http://www.extremetech.com/wpcontent/uploads/2013/02/eulerian-video-magnification-diagram.jpg. Accessed March 5, 2015.

60 – Bland Altman Plot, https://en.wikipedia.org/wiki/Bland%E2%80%93Altman_plot. Accessed March 5, 2015.

61 - Myles PS, Cui J. I. Using the Bland Altman method to measure agreement with repeated measures. *British Journal of Anaesthesia* 2007:309–311.

62 - Syed Z, Stultz CM, Scirica BM, Guttag JV. Computationally generated cardiac biomarkers for risk stratification after acute coronary syndrome. Sci Transl Med. 2011;3(102):102ra95.

63 - Ejection Fraction, https://en.wikipedia.org/wiki/Ejection_fraction Accessed September 9, 2015.

64 - Ejection fraction: What does it measure? - *Mayo Clinic*. http://www.mayoclinic.org/ejection-fraction/expert-answers/faq-20058286. Accessed September 9, 2015.

65 - Safar ME, Henry O, Meaume S. Aortic Pulse Wave Velocity: An Independent Marker of Cardiovascular Risk. *The American Journal of Geriatric Cardiology*:295–304

66 - Mattace-Raso, FU. Arterial Stiffness and Risk of Coronary Heart Disease and Stroke: The Rotterdam Study. *Circulation*. 2006:657–663.

67- Semba, RD, Najjar, SS, Sun, K, Lakatta, EG, Ferrucci, L. Serum Carboxymethyl-Lysine, an Advanced Glycation End Product, Is Associated With Increased Aortic Pulse Wave Velocity in Adults. *American Journal of Hypertension*. 2009:74–79.

68 - Hofmann, B, Riemer, M, Erbs, C, et al. Carotid to Femoral Pulse Wave Velocity Reflects the Extent of Coronary Artery Disease. *J Clin Hypertens The Journal of Clinical Hypertension*. 2014:629–633.

69 - Calabia, J, Torguet, P, Garcia, M, et al. Doppler ultrasound in the measurement of pulse wave velocity: agreement with the Complior method. *Cardiovasc Ultrasound Cardiovascular Ultrasound*.:13–13.

70 - Cardiac output. *Mosby's Medical Dictionary, 8th edition*. (2009). http://medical-dictionary.thefreedictionary.com/cardiac+output Accessed September 11 2015

71 - Stroke volume. *The American Heritage® Medical Dictionary*. (2007). http://medical-dictionary.thefreedictionary.com/stroke+volume Accessed September 11 2015

72 - Cardiac Output . http://medical-dictionary.thefreedictionary.com/cardiac+output Accessed 9/11/2015

73 - Foley, TA, Mankad, SV, Anavekar, NS, et al. Measuring Left Ventricular Ejection Fraction – Techniques and Potential Pitfalls. *European Cardiology Review*.:108–108.

74 - Otto, CM. *The practice of clinical echocardiography*. 4th ed. Philadelphia, PA: Elsevier/Saunders; 2012:67.

75 - Nosir, YF, Fioretti, PM, Vletter, WB, et al. Accurate Measurement of Left Ventricular Ejection Fraction by Three-dimensional Echocardiography: A Comparison With Radionuclide Angiography. Circulation. 1996:460–466.

76 - Cwajg E, Cwajg J, He Z-X, et al. Gated myocardial perfusion tomography for the assessment of left ventricular function and volumes: comparison with echocardiography. J Nucl Med. 1999;40:1857–1865

77 - White HD, Cross DB, Elliot JM, Norris RM, Yee TW. Long-term prognostic importance of patency of the infarct-related coronary artery after thrombolytic therapy for acute myocardial infarction. Circulation. 1994;89:61–67

78 - Ritchie JL, Bateman TM, Bonow RO. Guidelines for clinical use of cardiac radionuclide imaging. Report of the American College of Cardiology/Heart Association Task Force on the Assessment of Diagnostic and Therapeutic Cardiovascular Procedures. J Am Coll Cardiol. 1995;25:521–547

79 - Sharir T, Germano G, Kang X, et al. Prediction of myocardial infarction versus cardiac death by gated myocardial perfusion SPECT: risk stratification by the amount of stress-induced ischemia and the poststress ejection fraction. J Nucl Med. 2001;42:831–837

80 Shokawa, T, Imazu, M, Yamamoto, H, et al. Pulse Wave Velocity Predicts Cardiovascular Mortality. *Circulation Journal Circ J*.:259–264.

81- 64-Slice CT Scanner. *64-Slice CT Scanner*. Available at: http://www.wellmont.org/medical-services/radiology/64-slice-ct-scanner.aspx. Accessed September 28, 2015

82 - Cardiac CT Angiography. - *The University of Chicago Medicine*. Available at: http://www.uchospitals.edu/specialties/heart/services/imaging/ct-angiography.html. Accessed September 28, 2015

83 - Yang, Y, Yam, Y, Chen, L, et al. Assessment of left ventricular ejection fraction using low radiation dose computed tomography. *Journal of Nuclear Cardiology J Nucl Cardiol*. 2015.

84 - Weighing the Costs of a CT Scan's Look Inside the Heart http://www.nytimes.com/2008/06/29/business/29scan.html?pagewanted=all&_r=0 Accessed September 28, 2015.

85 - Ventriculogram. https://www.cardiosmart.org/Healthwise/tu61/25ab/c/tu6125abc Accessed September 28,2015 9/28/2015

86 - Greupner, J, Zimmermann, E, Grohmann, A, et al. Head-to-Head Comparison of Left Ventricular Function Assessment with 64-Row Computed Tomography, Biplane Left Cineventriculography, and Both 2- and 3-Dimensional Transthoracic Echocardiography. *Journal of the American College of Cardiology*.:1897–1907.

87 - Nissen, SE. Limitations of Computed Tomography Coronary Angiography. . *Journal of the American College of Cardiology*. 2008;52(25).

88- CT Angiography Screening in Asymptomatic Patients Leads to More Medicines, Tests and Procedures, Without Clear Benefit http://www.hopkinsmedicine.org/news/media/releases/ct_angiography_screening_in_asymptomatic_patients_leads_to_more_medicines_tests_and_procedures_without_clear_benefit Accessed September 30, 2015

89 - Ostchega Y, Zhang G, Sorlie P, et al. Blood pressure randomized methodology study comparing automatic oscillometric and mercury sphygmomanometer devices: National Health and Nutrition Examination Survey, 2009-2010. Natl Health Stat Report. 2012;(59):1-15.

90 - Bonnafoux P. Auscultatory and oscillometric methods of ambulatory blood pressure monitoring, advantages and limits: a technical point of view. Blood Press Monit. 1996;1(3):181-185.

91- Remmen, JJ, Aengevaeren, WRM, Verheugt, FWA, et al. Finapres arterial pulse wave analysis with Modelflow is not a reliable non-invasive method for assessment of cardiac output. *Clinical Science*. 2002:143–143.

92 - Geerts BF, Aarts LP, Jansen JR. Methods in pharmacology: measurement of cardiac output. Br J Clin Pharmacol. 2011;71(3):316-30.

93- Frese EM, Fick A, Sadowsky HS. Blood Pressure Measurement Guidelines for Physical Therapists. *Cardiopulmonary Physical Therapy Journal*. 2011;22(2):5-12.

94 - Finapres Nova technology. http://www.finapres.com/Products/Finpares-NOVA-Technology, Accessed October 10, 2015

95 - Van der does Y, Van loon LM, Alsma J, et al. Non-invasive blood pressure and cardiac index measurements using the Finapres Portapres in an emergency department triage setting. Am J Emerg Med. 2013;31(7):1012-6.

96- Langewouters, GJ, Settels, JJ, Roelandt, R, Wesseling, KH. Why use Finapres or Portapres rather than intraarterial or intermittent non-invasive techniques of blood pressure measurement? *J Med Eng Technol Journal of Medical Engineering & Technology*.:37–43.

97- Model of Aortic Blood Flow Using the Windkessel Model
www.isn.ucsd.edu Accessed October 10, 2015

98 - Continuous noninvasive arterial pressure,
https://en.wikipedia.org/wiki/Continuous_noninvasive_arterial_pressure
Accessed October 2, 2015

99 - Wheeler, DS. *Pediatric critical care medicine: basic science and clinical evidence*. London: Springer; 2007:603.

100 - Lee AJ, Cohn JH, Ranasinghe JS. Cardiac Output Assessed by Invasive and Minimally Invasive Techniques. *Anesthesiology Research and Practice*. 2011;2011:475151. doi:10.1155/2011/475151.

101- Ameloot, K, Vijver, KVD, Broch, O, et al. Nexfin Noninvasive Continuous Hemodynamic Monitoring: Validation against Continuous Pulse Contour and Intermittent Transpulmonary Thermodilution Derived Cardiac Output in Critically Ill Patients. *The Scientific World Journal*.:1–11.

102 - Porhomayon J, Zadeii G, Congello S, Nader ND. Applications of minimally invasive cardiac output monitors. *International Journal of Emergency Medicine*. 2012;5:18. doi:10.1186/1865-1380-5-18.

103 - Critchley LA, Lee A, Ho AM. A critical review of the ability of continuous cardiac output monitors to measure trends in cardiac output. Anesth Analg. 2010 Nov;111(5):1180-92. doi: 10.1213/ANE.0b013e3181f08a5b.

104 - Fischer MO, Fellahi JL. Noninvasive cardiac output monitoring with Nexfin: we really need impact studies. Anesth Analg. 2014;118(1):238-9.

105 - Critchley, LAH, Huang, L, Zhang, J. Continuous Cardiac Output Monitoring: What Do Validation Studies Tell Us? *Current Anesthesiology Reports Curr Anesthesiol Rep*. 2014:242–250.

106 - Broch O, Renner J, Gruenewald M, et al. A comparison of the Nexfin® and transcardiopulmonary thermodilution to estimate cardiac output during coronary artery surgery. Anaesthesia. 2012;67(4):377-83.

107- Ghasemzadeh N, Zafari AM. A brief journey into the history of the arterial pulse. Cardiol Res Pract. 2011;2011:164832.

108 - Antorio Santorio (1561-1636) http://www.sportsci.org/news/history/santorio.html Accessed on October 9th, 2015

109 - McArdle, WD, Katch, FI. *Essentials of exercise physiology*. 2nd ed. Philadelphia: Lippincott Williams & Wilkins; 2000.

110 - Perret-Guillaume, C, Joly, L, Benetos, A. Heart Rate as a Risk Factor for Cardiovascular Disease. *Progress in Cardiovascular Diseases*.:6–10.

111- Grogan, What does the term "ejection fraction" mean? What does it measure? www.mayoclinic.org Accessed October 10, 2015

112 - Nexfin http://promolding.nl/project.php?lan=uk&c=59, Accessed October 10, 2015

113 - Mahmood SS, Levy D, Vasan RS, Wang TJ. *The Framingham Heart Study and the epidemiology of cardiovascular disease: a historical perspective.* Lancet. 2014;383(9921):999-1008.

114 - Supervised learning http://www.mathworks.com/discovery/supervised-learning.html , Accessed October 13, 2015

115 - Tarca, AL, Carey, VJ, Chen, X-W, Romero, R, Drăghici, S. Machine Learning and Its Applications to Biology. *PLoS Comput Biol PLoS Computational Biology*.

116 - Montgomery, DC, Peck, EA. *Introduction to linear regression analysis*. New York: Wiley; 2006.

117 - Bland, JM, Altman, D. Statistical Methods For Assessing Agreement Between Two Methods Of Clinical Measurement. *The Lancet*.:307–310.

118 - Continuous Cardiac Output Monitoring, https://www.infona.pl/resource/bwmeta1.element.springer-b6389f4a-7139-3776-ada9-471bdd8b1847 Accessed October 15, 2015

119 - Comparing two measurement devices, http://www.jerrydallal.com/lhsp/compare.htm. Accessed October 15, 2015

120 - Bland Altman Plot, https://www.medcalc.org/manual/blandaltman.php. Accessed October 16, 2015

121 - Simple linear regression and correlation http://www.stat.ucla.edu/~hqxu/stat105. Accessed October 16, 2015

122 - Interactions in Multiple Linear Regression http://www.medicine.mcgill.ca/epidemiology/joseph/courses/EPIB-621/interaction.pdf, Accessed October 17, 2015

123- Brazdzionyte J, Macas A. Bland-Altman analysis as an alternative approach for statistical evaluation of agreement between two methods for measuring hemodynamics during acute myocardial infarction. Medicina (Kaunas). 2007;43(3):208-14.

124 –Bland-Altman plot http://imaging.mrc-cbu.cam.ac.uk/statswiki/FAQ/balt?action=AttachFile&do=get&target=balt.pdf, Accessed October 17, 2015

125 - Elliott, AC, Woodward, WA. *SAS® essentials: mastering SAS for data analytics*. Second. Hoboken, New Jersey: John Wiley and Sons, Inc; 2015:295.

126 - Salvi, P, Magnani, E, Valbusa, F, et al. Comparative study of methodologies for pulse wave velocity estimation. J Hum Hypertens Journal of Human Hypertension. 2008:669–677.

127 - White, L, Haines, H, Adams, T. *Cardiac output related to body weight in small mammals.* Comparative Biochemistry and Physiology.*:559–565.*

128 - Peyton PJ, Chong SW. Minimally invasive measurement of cardiac output during surgery *and critical cre: a meta-analysis of accuracy and precision. Anesthesiology 2010; 113: 1220-35*

129 - Bendjelid, K, Marx, G, Kiefer, N, et al. Performance of a new pulse contour method for continuous cardiac output monitoring: validation in critically ill patients. *British Journal of Anaesthesia*. 2013:573–579.

130 - The Reference Values for Arterial Stiffness' Collaboration. "Determinants of Pulse Wave Velocity in Healthy People and in the Presence of Cardiovascular Risk Factors: 'establishing Normal and Reference Values.'" *European Heart Journal* 31.19 (2010): 2338–2350.

131 - Jegier, W. et al. "The relation between cardiac output and body size." *British Heart Journal* 25.4 (1963): 425–430.

132 - Dilated and Restrictive Cardiomyopathie http://www.clevelandclinicmeded.com/medicalpubs/diseasemanagement/cardiology/dilated-restrictive-cardiomyopathy/ Accessed November 6, 2015

133 - Najjar SS, Scuteri A, Shetty V, et al. Pulse Wave Velocity Is an Independent Predictor of the Longitudinal Increase in Systolic Blood Pressure and of Incident Hypertension in the Baltimore Longitudinal Study of Aging. *J Am Coll Cardiol.* 2008;51(14):1377-1383. doi:10.1016/j.jacc.2007.10.065.

134 Ejection Fraction, what does it measure? http://www.mayoclinic.org/ejection-fraction/expert-answers/faq-20058286 Accessed November 6, 2015

135 – Putler, DS, Krider, RE. *Customer and business analytics: applied data mining for business decision making using R*. Boca Raton, FL: CRC Press; 2012:97.

136 - Making Data Normal Using Box-Cox Power Transformations http://www.isixsigma.com/tools-templates/normality/making-data-normal-using-box-cox-power-transformation Accessed November 12, 2015

137 - Williams, LR. Reference Values for Total Blood Volume and Cardiac Output in humans. 1994. http://web.ornl.gov/info/reports/1994/3445606042010.pdf. Accessed October 2015.

138 - Chakravarthy M. Cardiac output--have we found the 'gold standard'? *Annals of Cardiac Anaesthesia Ann Card Anaesth*.:2008;11(1):1-2.

139 - Cardiovascular physiology http://www.kumc.edu/AMA-MSS/Study/phys2.htm Accessed November 1, 2015

APPENDIX

MEASURES OF CENTRAL TENDENCY FOR LVEF, CO AND PWV DISTRIBUTIONS

1) LVEF_MRI – HMRI training database for IFs_Tonometry study

Quantiles

100.0%	maximum	73.2
99.5%		73.2
97.5%		71.1
90.0%		69.75
75.0%	quartile	64.7
50.0%	median	59.95
25.0%	quartile	54.3
10.0%		41.65
2.5%		25.2
0.5%		7.8
0.0%	minimum	7.8

Summary Statistics

Mean	57.450806
Std Dev	12.055262
Std Err Mean	1.0825945
Upper 95% Mean	59.593736
Lower 95% Mean	55.307877
N	124

2) LVEF_ECHO - FHS400 Testing Database for IFs_Tonometry study

Quantiles

100.0%	maximum	72.63
99.5%		72.63
97.5%		69.2753
90.0%		67.609

75.0%	quartile	65.87
50.0%	median	63.995
25.0%	quartile	60.9025
10.0%		58.698
2.5%		55.5038
0.5%		46.79
0.0%	minimum	46.79

Summary Statistics

Mean	63.385882
Std Dev	3.6740724
Std Err Mean	0.2817885
Upper 95% Mean	63.942161
Lower 95% Mean	62.829604
N	170

3) LVEF_ECHO – FHS6500 testing database for IFs_Tonometry study

Quantiles

100.0%	maximum	80.15
99.5%		73.8686
97.5%		71.0608
90.0%		68.31
75.0%	quartile	66.0675
50.0%	median	63.82
25.0%	quartile	61.51
10.0%		59.157
2.5%		56.2278
0.5%		50.8834
0.0%	minimum	32.77

Summary Statistics

Mean	63.725051
Std Dev	3.8523095
Std Err Mean	0.0646012
Upper 95% Mean	63.85171
Lower 95% Mean	63.598392
N	3556

4) LVEF_MRI – HMRI training database for IFs_iPhone study

Quantiles

100.0%	maximum	73.2
99.5%		73.2
97.5%		73.0425
90.0%		69.6
75.0%	quartile	64.7
50.0%	median	60.35
25.0%	quartile	55.775
10.0%		47.12
2.5%		24.7
0.5%		7.8
0.0%	minimum	7.8

Summary Statistics

Mean	57.840244
Std Dev	12.047651
Std Err Mean	1.3304405
Upper 95% Mean	60.487403
Lower 95% Mean	55.193085
N	82

5) LVEF_MRI – HMRI testing database for IFs_iPhone study

Quantiles

100.0%	maximum	73.2
99.5%		73.2
97.5%		71.8875
90.0%		69.75
75.0%	quartile	64.625
50.0%	median	59.65
25.0%	quartile	52.3
10.0%		32.9
2.5%		9.9875
0.5%		7.8
0.0%	minimum	7.8

Summary Statistics

Mean	55.834375
Std Dev	14.344472
Std Err Mean	1.793059

Upper 95% Mean	59.417518
Lower 95% Mean	52.251232
N	64

6) CO_MRI – HMRI training database for IFs_CO study

Quantiles

100.0%	maximum	7.14101
99.5%		7.14101
97.5%		7.12761
90.0%		6.68399
75.0%	quartile	5.904
50.0%	median	4.95044
25.0%	quartile	4.18454
10.0%		3.4008
2.5%		2.57059
0.5%		2.0678
0.0%	minimum	2.0678

Summary Statistics

Mean	4.987612
Std Dev	1.2199683
Std Err Mean	0.1095564
Upper 95% Mean	5.2044722
Lower 95% Mean	4.7707519
N	124

7) PWV_Tonometry – FHS400 training database

Quantiles

100.0%	maximum	26.3333
99.5%		24.7412
97.5%		18.1
90.0%		12.8333
75.0%	quartile	9.3
50.0%	median	7.4
25.0%	quartile	6.5
10.0%		5.8
2.5%		4.8

0.5%		3.82
0.0%	minimum	3.5

Summary Statistics

Mean	8.4512264
Std Dev	3.3108653
Std Err Mean	0.1982163
Upper 95% Mean	8.841422
Lower 95% Mean	8.0610308
N	279

8) PWV_Tonometry – FHS6500 training database

Quantiles

100.0%	maximum	30
99.5%		27.8382
97.5%		18.4901
90.0%		12.1
75.0%	quartile	9.1
50.0%	median	7.4
25.0%	quartile	6.4
10.0%		5.8
2.5%		5.2
0.5%		4.7
0.0%	minimum	3.5

Summary Statistics

Mean	8.4446039
Std Dev	3.4397369
Std Err Mean	0.0456245
Upper 95% Mean	8.5340453
Lower 95% Mean	8.3551624
N	5684